Report of Investigations No. 127

Ground-water hydraulics and hydrochemical facies in Eocene aquifers of the East Texas Basin

Graham E. Fogg and Charles W. Kreitler

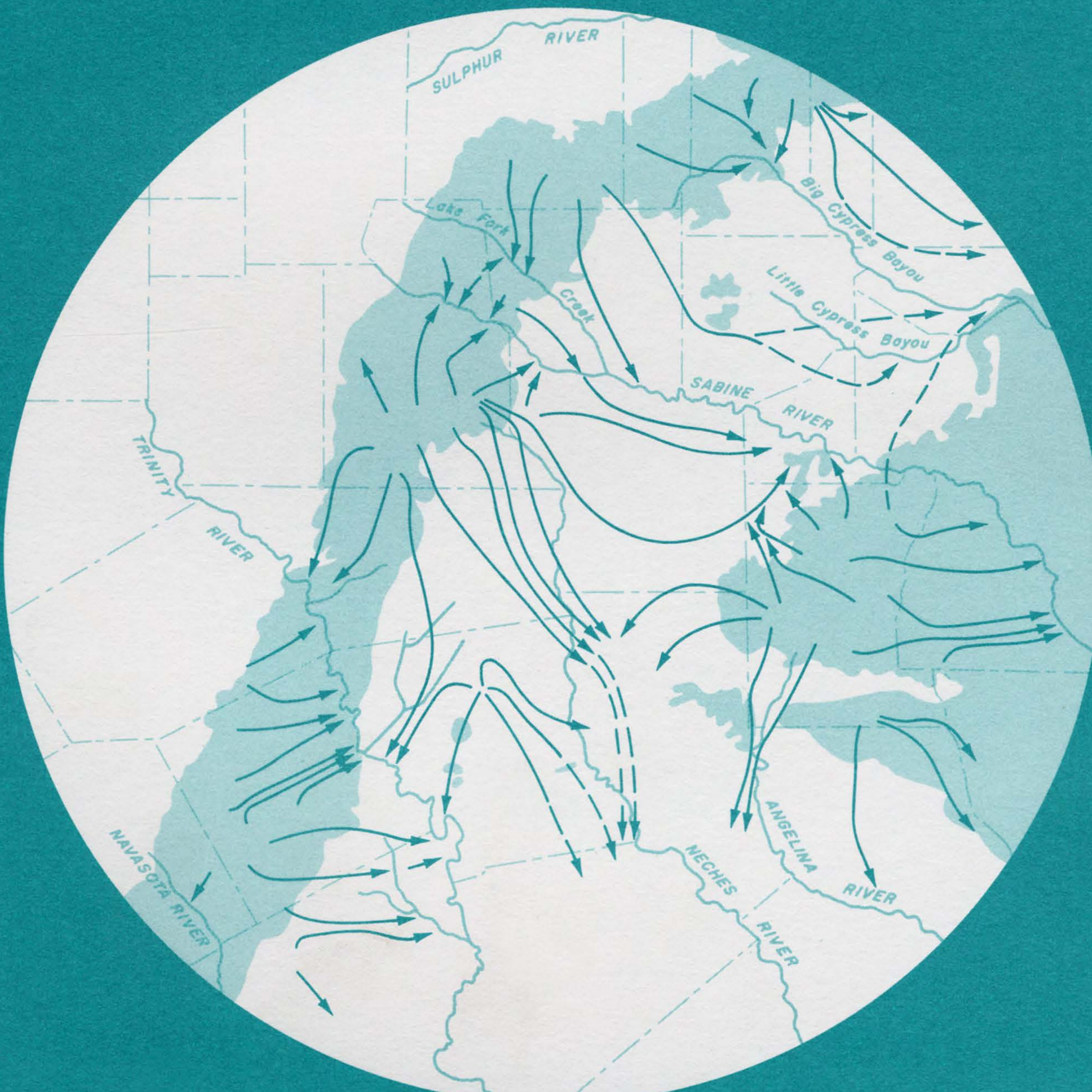

Bureau of Economic Geology • W. L. Fisher, Director

The University of Texas at Austin • Austin, Texas 78712 • 1982

Report of Investigations No. 127

Ground-water hydraulics and hydrochemical facies in Eocene aquifers of the East Texas Basin

Graham E. Fogg and Charles W. Kreitler

Research funded by the U.S. Department of Energy
Contract No. DE-AC97-80ET46617

Bureau of Economic Geology • W. L. Fisher, Director

The University of Texas at Austin • Austin, Texas 78712 • 1982

CONTENTS

FIGURES

TABLES

ABSTRACT

Eocene stratigraphic units in the East Texas Basin are composed of a thick sedimentary sequence (approximately 2,000 ft [600 m]) of fresh-water aquifers and aquitards covering an area of approximately 15,000 mi^2 (51,000 km^2). Analysis of abundant data on hydraulic head, pressure, and water chemistry from water wells tapping the Wilcox, Carrizo, and Queen City aquifers reveals the regional ground-water circulation patterns, locations and mechanisms of major recharge and discharge areas, and evolution of ground-water chemistry.

The Queen City aquifer is primarily a water-table (unconfined) system in which effects of topography create a series of local ground-water basins. The Wilcox-Carrizo aquifer system includes (1) an artesian (confined) section that is separated from the Queen City by the Reklaw Formation, a leaky aquitard, and (2) a water-table (unconfined) system where the Wilcox-Carrizo crops out along the west, north, and east margins of the basin. Structure and topography are major controls on ground-water circulation in the Wilcox-Carrizo. A structural ridge in the Wilcox-Carrizo corresponds roughly to a ground-water divide that separates a southward component of flow from one that is directed northeastward toward the Texas-Louisiana border. Topographically controlled vertical leakage between the Queen City and Wilcox-Carrizo aquifer systems affects circulation in the Wilcox-Carrizo. The vertical head differentials and the distribution of flowing wells indicate downward leakage over most of the basin and upward leakage only beneath the Trinity and Sabine Rivers. Similarly, pressure-versus-depth data from the Wilcox-Carrizo indicate a predominantly downward component of vertical flow that intensifies toward topographically higher areas and reverses direction beneath the Trinity River.

As ground water flows from outcrop down the hydraulic gradient into the artesian part of the Wilcox-Carrizo aquifer, it is consistently altered chemically from an acidic oxidized calcium-magnesium-bicarbonate-sulfate water to a basic reduced sodium bicarbonate water. This change in the water chemistry is predominantly controlled by two reactions: calcite dissolution and cation exchange with montmorillonitic clays. Water samples with anomalous chemical composition (compared with regional chemistry) indicate salt dome dissolution or anomalous hydrologic conditions, such as relatively high rates of recharge to the artesian part of the Wilcox-Carrizo through leaky aquitards.

INTRODUCTION

This study addresses the regional hydrogeology of fresh-water Eocene aquifers in the East Texas Basin. The data base for these aquifers includes abundant hydraulic head measurements and water-chemistry analyses and provides a comprehensive picture of the hydrogeologic system. Our methodology included mapping horizontal and vertical components of flow using the head data and mapping the chemical evolution of the ground water using results of chemical analyses of major anions and cations. The hydraulic head and chemistry data are complementary: The former provide details about apparent circulation patterns, and the latter can be used as a natural tracer to verify regional flow patterns. The study examines the system's behavior and the hydrologic factors that primarily affect the system. Results include information that can serve both as a framework for site-specific studies in the East Texas Basin and as a reference on regional ground-water systems.

The East Texas Basin covers approximately 15,000 mi^2 (51,000 km^2) of the Gulf Coast Interior Basin, which crosses East Texas, Louisiana, and Mississippi. The East Texas Basin is bounded approximately by the Elkhart Graben-Mount Enterprise fault system to the south, the Mexia-Talco fault zone to the west and north, and the Sabine Uplift to the east (fig. 1). Fresh-water aquifers occur under both confined and artesian conditions in a sedimentary sequence of Eocene age that is greater than 2,000 ft (910 m) thick. From oldest to youngest, the Eocene units are the Wilcox Group and the Carrizo, Reklaw, Queen City, Weches, and Sparta Formations (fig. 2). All formations but the Reklaw and Weches are aquifers, and of these, the Wilcox and Carrizo are the most productive. The subhumid climate and annual precipitation of 38 to 50 inches (97 to 127 cm) sustain a shallow water table and perennially flowing streams.

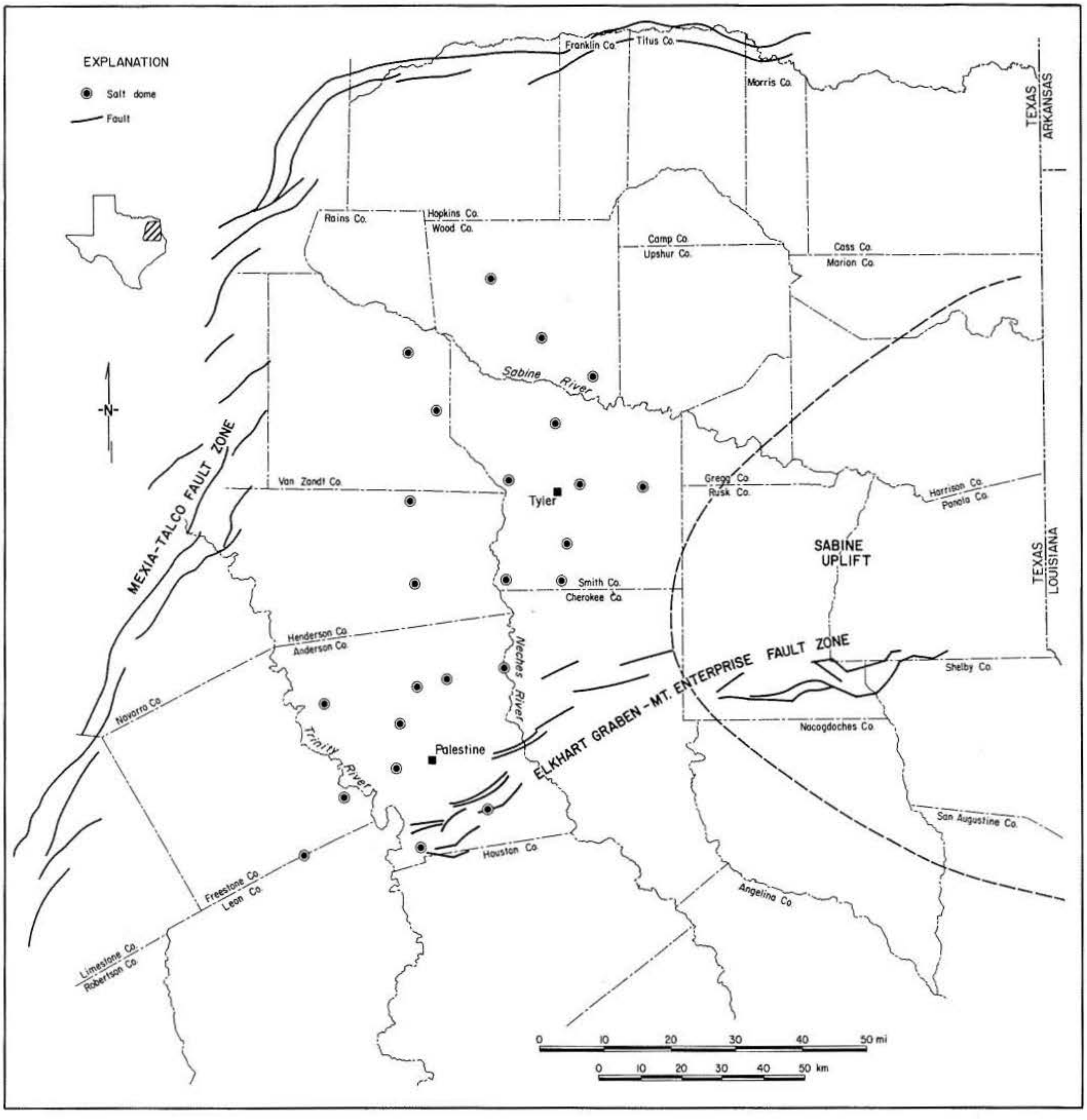

Figure 1. Location and structural features of the East Texas Basin.

This study stems from a research program addressing the hydrologic and geologic suitability of East Texas salt domes for isolation of high-level nuclear wastes. Primary goals of the hydrologic research are (1) to determine whether salt dome dissolution by circulating ground water would jeopardize a repository in a dome and (2) to predict the probable destinations of radionuclides should they escape from such a repository. Of the 30 domes in the basin, 15 are shallower than 3,000 ft (915 m). Most domes in the basin have uplifted the fresh-water aquifers and pierced or disrupted the aquitards. Five domes are less than 250 ft (76 m) deep and show evidence of salt dissolution and discharge of saline waters at the surface (Fogg, in preparation). Although it is thought that dissolution of salt domes would alter the ground-water composition, minimal dissolution of the East Texas domes has been detected.

The Wilcox and Carrizo aquifers are the only fresh-water aquifers in contact with the salt domes; thus, they significantly influence the hydrologic suitability of the domes. Deeper saline aquifers such as the Cretaceous Woodbine Formation also contact the domes, but these saline aquifers have limited capacity for dissolution and transport of contaminants because of higher saturation with respect to halite and because of much slower rates of ground-water flow.

The regional hydrologic analysis presented in this report will provide the basis for subsequent site-specific investigations. A site-specific analysis may be more pertinent to a given hydrologic problem, but frequently such an analysis (1) represents only a facet of a larger system and (2) lacks the data needed to understand hydrogeology on the site-specific scale. Regional analysis, on the other hand, often permits delineation of a coherent system using limited data. It is not always advisable to extrapolate the regional hydrology directly to site hydrology because local complexities are often missed in the regional hydrology. However, properly applied knowledge of the regional system generally enhances the site-specific interpretation.

PREVIOUS WORK

Regional ground-water investigations for water resource planning in the East Texas Basin were conducted for the Texas Water Commission (presently part of the Texas Department of Water Resources) by Baker and others (1963a, 1963b) and Peckham and others (1963). They reported the general ground-water conditions in each major river basin (the Sabine, Neches, and Trinity Rivers, respectively) and discussed regional aquifer geometries, ground-water chemical quality, potential ground-water resources, and ground-water use. As a preliminary investigation of the hydrologic suitability of salt domes in the basin for nuclear waste storage, Smith (1976) constructed a potentiometric surface map for the Wilcox aquifer in Anderson, Henderson, Van Zandt, Smith, and Wood Counties. Relatively detailed ground-water resource surveys were conducted by the Texas Water Commission and Texas Water Development Board in most counties of the study area: Anderson, Cherokee, Freestone, and Henderson (Guyton and Associates, 1972); Angelina and Nacogdoches (Guyton and Associates, 1970); Camp, Franklin, Morris, and Titus (Broom and others, 1965); Gregg and Upshur (Broom, 1969); Houston (Tarver, 1966); Leon (Peckham, 1965); Rains and Van Zandt (White,

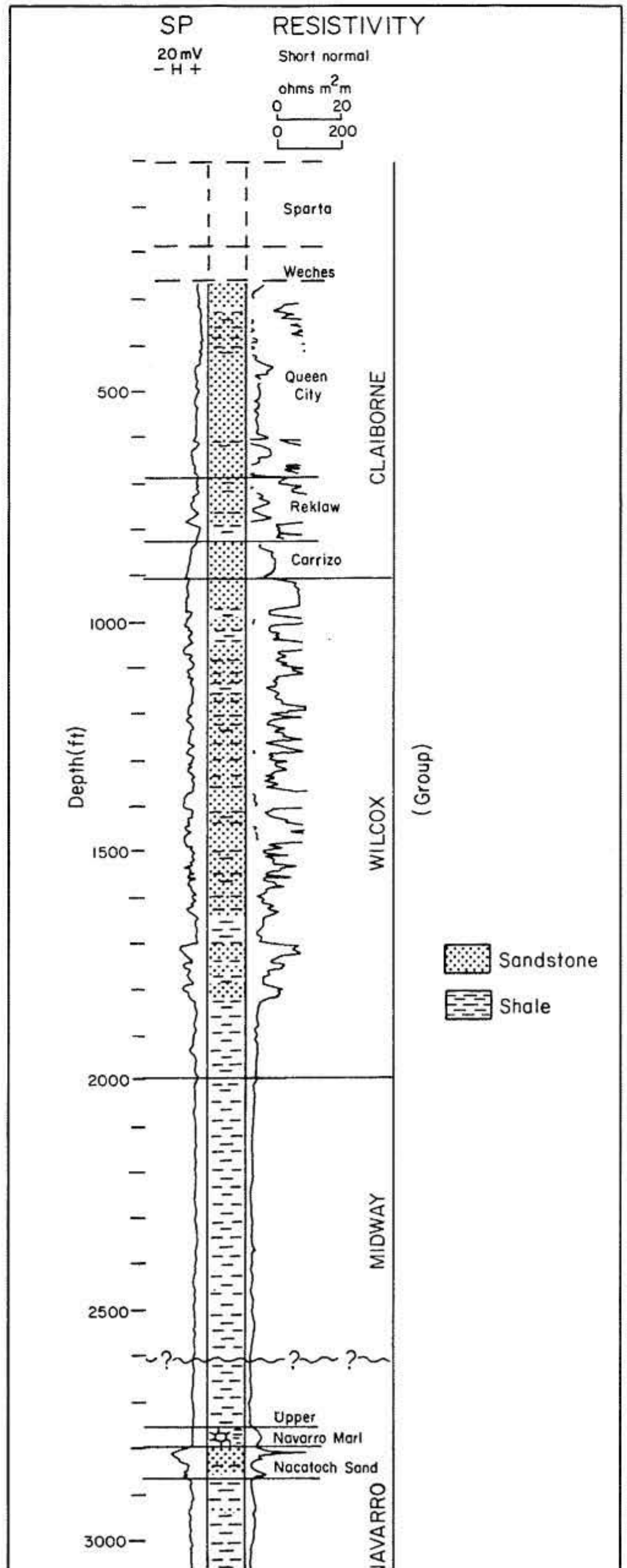

Figure 2. Stratigraphic column and composite log of Tertiary and Upper Cretaceous formations, Smith County, East Texas Basin. The Wilcox, Carrizo, Queen City, and Sparta are fresh-water aquifers, and the Midway, Reklaw, and Weches are aquitards.

1973); Sabine and San Augustine (Anders, 1967); Smith (Dillard, 1963); and Wood (Broom, 1968).

These reports provide abundant raw data on water levels in wells, well completion depths, and water-quality distributions for many of the existing wells. Most of the reports include hydrologic maps, geologic structure maps, and cross sections. Additional data are available from computer files of the Texas Natural Resources Information System.

SCOPE

The study area is confined to that part of the basin containing salt domes and comprises the Trinity, Neches, and Sabine watersheds (fig. 1). Certain parts of the basin outside this area are included on maps to support regional interpretations. The study was restricted principally to the Wilcox, Carrizo, and Queen City aquifers and the Reklaw aquitard. The Weches and Sparta Formations cover a relatively small part of the basin and are consequently less important regional flow systems; accordingly, these units are briefly discussed. Rates of ground-water movement, recharge, and discharge are not provided for any of the aquifers, except where a possible range of ground-water flow rates in the Wilcox-Carrizo is estimated using Darcy's equation.

HYDROGEOLOGIC SETTING

PHYSIOGRAPHY AND CLIMATE

The East Texas Basin is characterized by a southeastward-sloping rolling to hilly surface that ranges from about 775 ft (236 m) to slightly less than 200 ft (61 m) above mean sea level (fig. 3). Maximum elevations are near the middle of the basin in Anderson and Cherokee Counties, where the highest hills are capped by resistant ironstone in the Weches Formation (Fisher, 1965).

The climate is subhumid; average winter and summer temperatures near the center of the basin are 47°F (8°C) and 83°F (28°C), respectively. Mean annual precipitation increases from about 38 inches (97 cm) along the western edge of the basin to about 50 inches (127 cm) along the eastern edge. Precipitation is evenly distributed during the year; maximum monthly rainfall is 4 to 6 inches per month (10 to 15 cm) and generally occurs in April and May. Mean annual potential evapotranspiration, as calculated by the Thornthwaite (1948) method, is 41 inches (104 cm).

Vegetation correlates well with surface geologic units and precipitation. Along the northwest basin margin, precipitation is low, outcropping Cretaceous and Paleocene strata support clay-rich soils, and prairies predominate. To the east and southeast, where Eocene units form sandy soils and precipitation is high, vegetation grades from an oak-dominated savannah to well-developed pine forests.

SURFACE WATER

The major streams draining the salt dome areas are the Trinity, Neches, Angelina, and Sabine Rivers (fig. 3); table 1 lists stream-flow statistics. Additionally, Big and Little Cypress Creeks and the Sulphur River drain the extreme northeastern end of the basin.

Naturally impounded water occurs only in very small lakes and ponds, and dams create several large reservoirs (fig. 3).

GEOLOGY RELATED TO GROUND WATER

The East Texas Basin formed by Triassic block faulting and sediment accumulation during the rest of the Mesozoic and the Tertiary (Nichols and others, 1968). More than 20,000 ft (6,100 m) of sediments were deposited, the bulk of which is Jurassic and Cretaceous marine evaporite, carbonate, and clastic facies. The evaporites include thick halite beds (the Louann Salt) from which the salt domes have grown. Dome growth has deformed and faulted overlying sediments, and in several cases domes have pierced and uplifted the Eocene formations that are exposed throughout the basin and that form the fresh-water aquifers.

The Eocene formations were deposited by regressive fluvial-deltaic and transgressive marine environments (Fisher, 1964). Sandy fluvial and fluvial-deltaic sediments of the Wilcox Group, Carrizo Formation, Queen City Formation, and Sparta Formation are the principal fresh-water aquifers. Marine sediments of the Midway Group (Paleocene), Reklaw Formation, and Weches Formation are relatively muddy (silt- or clay-rich) and constitute intervening aquitards. Outcrops and regional stratigraphic relations of these units are

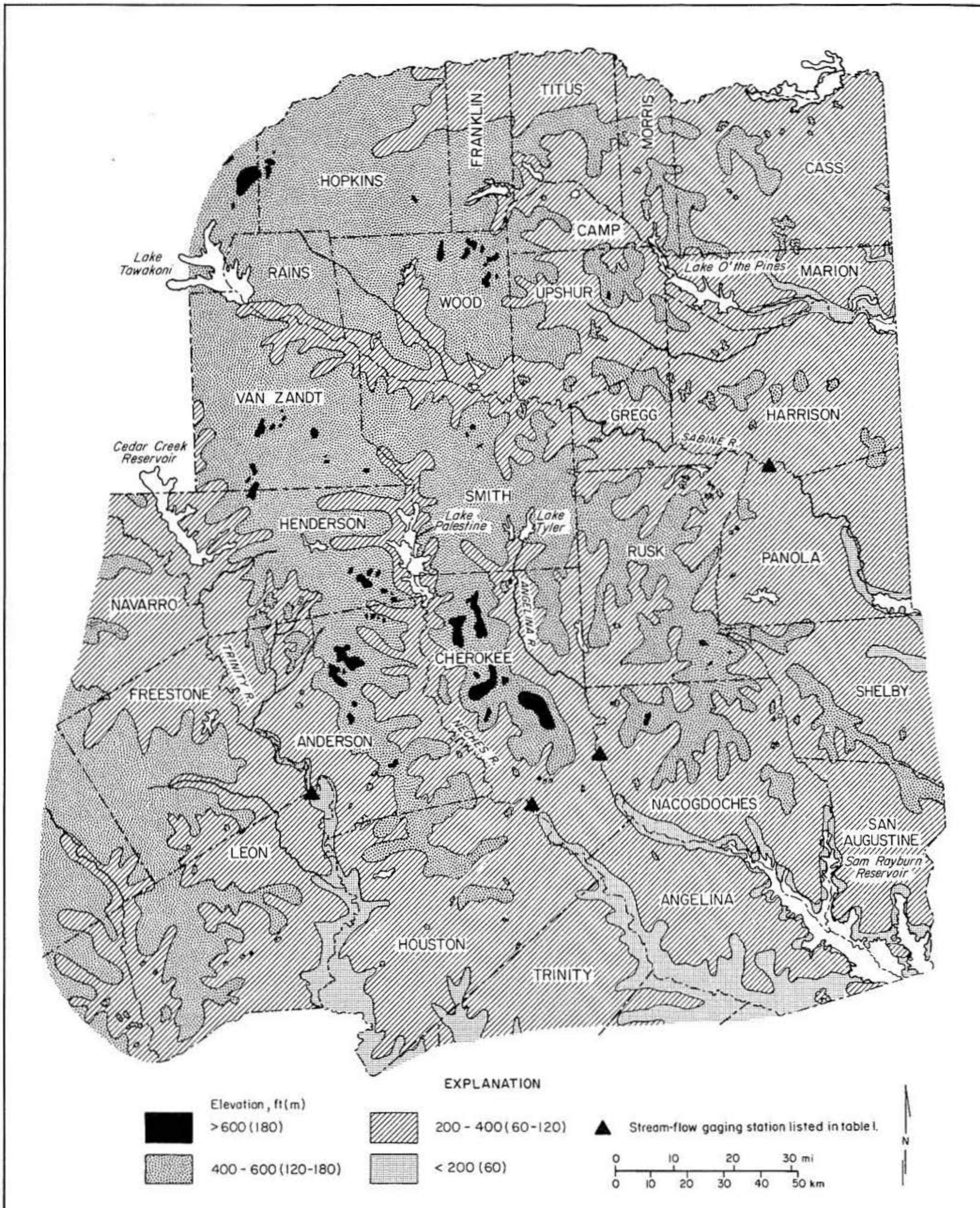

Figure 3. Topographic map showing major reservoirs and locations of stream-flow gaging stations referenced in table 1. Some of the highest elevations are in the middle of the basin in Anderson and Cherokee Counties.

Table 1. Flow characteristics of major rivers in the East Texas Basin.*

Watershed	Gage location*	Discharge (ft^3/sec [m^3/sec]) Mean	Maximum	Year	Minimum	Year	Period of record
Trinity	near Oakwood, Leon Co.	4,762.0 (135.0)	153,000.0 (4,333.0)	1942	28.0 (0.8)	1925	1923-70
Neches	near Alto, Cherokee Co.	1,165.0 (33.0)	42,800.0 (1,212.0)	1945	0.1 (0.003)	1954	1944-70
Angelina	near Alto, Cherokee Co.	752.0 (21.0)	30,600.0 (867.0)	1966	2.0 (0.06)	1964	1938-70
Sabine	near Tatum, Panola Co.	2,463.0 (70.0)	123,000.0 (3,483.0)	1945	2.4 (0.07)	1964	1940-42 1944-49 1959-70

Source: U.S. Geological Survey, 1975.
*Locations of stream gages are shown in figure 3.

illustrated on a map of surface geology (fig. 4) and cross sections (figs. 5a, b, and c).

Midway and Upper Cretaceous strata

The Midway Group is a thick calcareous to noncalcareous clay containing some sand (Barnes, 1970, 1972; Nichols and others, 1968). Precise thickness of the Midway is difficult to measure because it generally cannot be differentiated from the underlying upper Navarro Group (Upper Cretaceous) using electric logs. Therefore, the Midway, upper Navarro Clay (also called Kemp Clay), and the Navarro Marl are undifferentiated on cross sections (fig. 5). These formations compose one low-permeability hydrologic unit in the study area from about 700 to 1,100 ft (210 to 340 m) thick. The Midway-Navarro section is an aquiclude, isolating the Eocene aquifers from deeper flow systems except, perhaps, in fault zones and along flanks of salt domes where vertical avenues for flow may exist.

The most significant pre-Eocene aquifer is composed of sands of the Cretaceous Woodbine Group. One of the most prolific hydrocarbon reservoirs in the United States, the Woodbine contains up to 600 ft (180 m) of sand. It is separated from the overlying Eocene aquifers by about 2,000 to 3,400 ft (600 to 1,370 m) of relatively impermeable limestone, clay, and discontinuous sands.

Wilcox Group

The marine clays of the Midway Group grade upward into the deltaic and fluvial sediments of the Wilcox aquifer, which is composed of up to 2,700 ft (830 m) of interbedded lenticular sand, mud (any mixture of sediment in the silt or clay size ranges), and lignite. The sands, which constitute about 50 percent of the total Wilcox, occur in beds from a few feet to about 200 ft (60 m) thick and consist of very fine grained to coarse-grained quartz sand containing various amounts of silt and clay. Thickness of lignite beds reaches about 25 ft (8 m) (W. R. Kaiser, personal communication, 1981).

Barnes (1970) subdivided the Wilcox Group south of the Trinity River (fig. 4) into three formations, from youngest to oldest: Calvert Bluff, Simsboro, and Hooper. Of the three formations, the Simsboro typically contains the most massive, coarsest sands. The Simsboro occurs only south of the Trinity River, and thus north of the river, the Wilcox is not divided (Barnes, 1967, 1970).

The lateral extent of individual beds within the Wilcox Group is extremely variable. Some beds, primarily lignites, can be correlated over distances of a few miles, whereas others appear to pinch out or lose character within 1,000 ft (305 m) or less. Fisher and McGowen (1967) recognized a "vertical persistence or stacking" of Wilcox sand bodies. Using electric logs, they mapped a dendritic pattern of high net sand (channels) converging from north to south.

More recently, Kaiser and others (1978) used additional data (approximately 900 logs) to construct detailed net-sand and sand-percent maps for the Calvert Bluff and the undivided Wilcox Group. Their maps for the undivided Wilcox section (figs. 6 and 7) clearly illustrate the dendritic pattern of stacked sand bodies typical of fluvial systems and provide information regarding apparent variations in aquifer transmissivity (aquifer thickness times hydraulic conductivity). The most transmissive sections of the Wilcox should generally correspond to areas of high percentage sand (fig. 7), where the major streams during Wilcox time tended to locate and to deposit the thickest, coarsest grained sand bodies. Both sand maps indicate a gradual north to south increase in transmissivity.

Detailed mapping of the environmental geology of the Wilcox outcrop belt (located along the western basin margin) has been conducted by Henry and Basciano (1979). Using geomorphic and substrate characteristics, they mapped various environmental geologic units that are pertinent to land use, hydrology, and material resources such as lignite, clay, sand, and gravel. They found that hills were generally formed by sands that are relatively resistant to erosion; therefore, the "sand hills" were considered important recharge areas. Henry and Basciano also found that many of the high-sand-

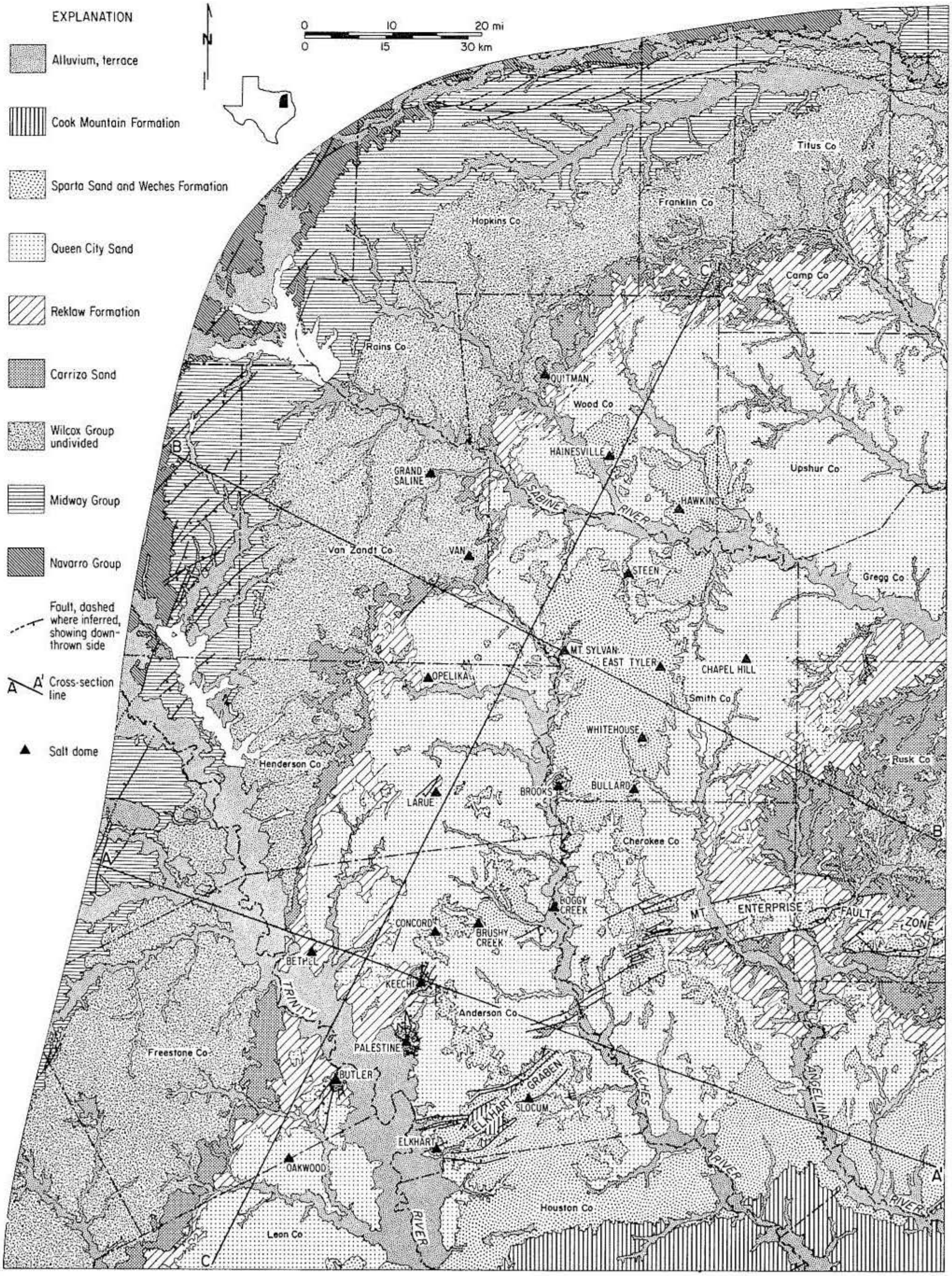

Figure 4. Surface geology, East Texas Basin (compiled from Barnes, 1965, 1966, 1968, 1970, and 1972).

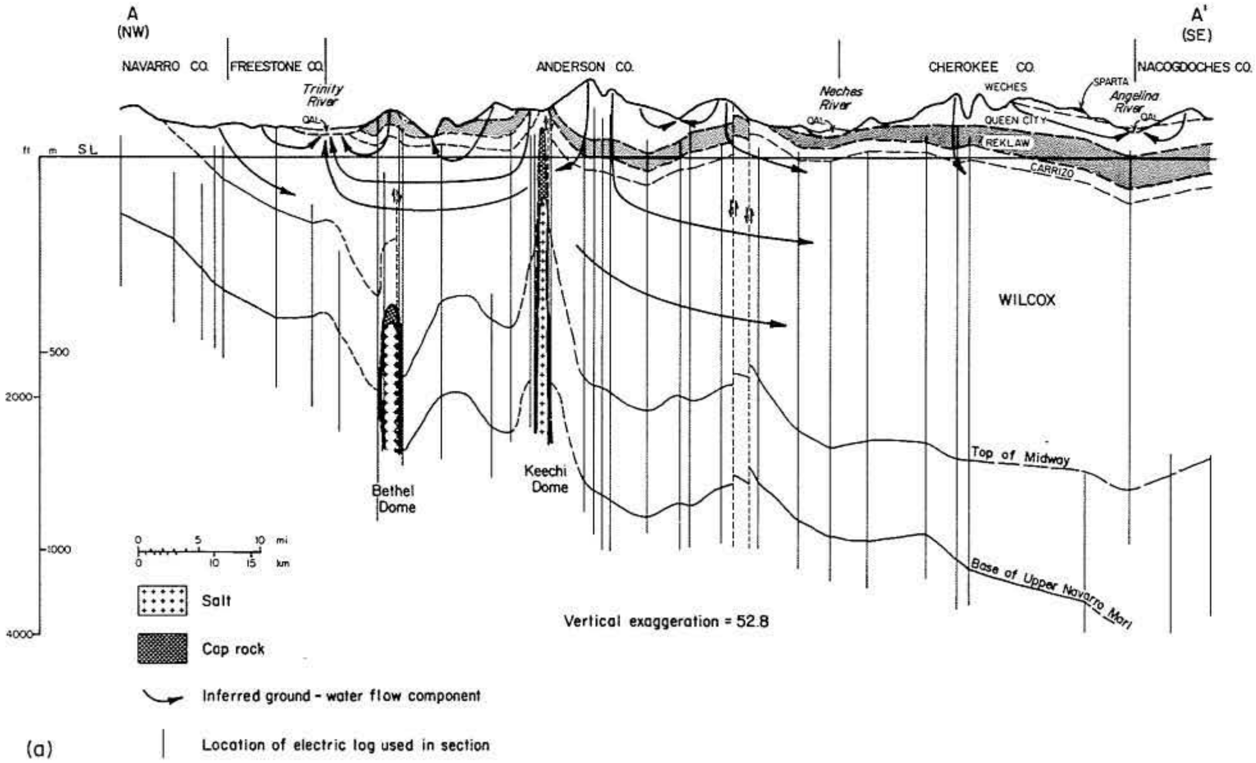

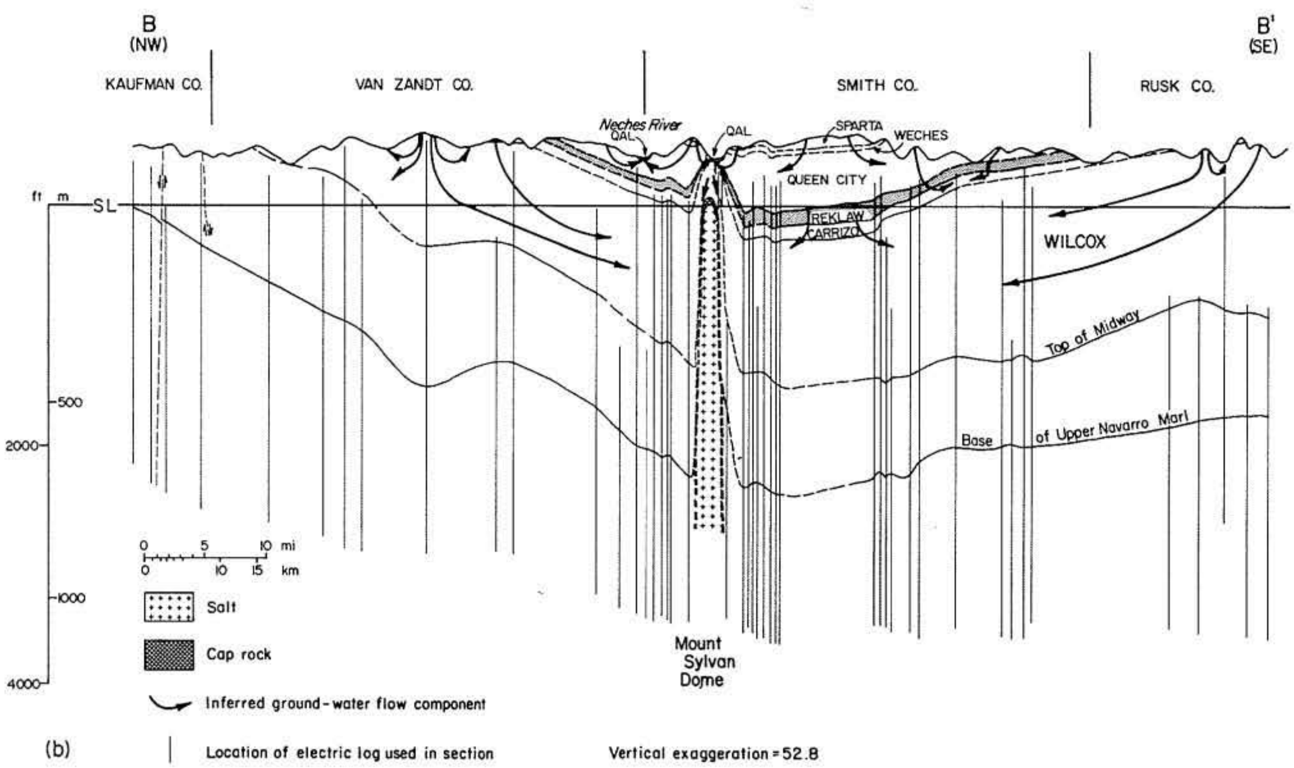

Figure 5. Structural cross sections (a) A-A', (b) B-B', and (c) C-C', showing Tertiary and Upper Cretaceous formations, East Texas Basin (adapted from Wood and Guevara, 1981). See figure 4 for location of sections. Ground-water flow lines are inferred from hydraulic head data as discussed in section entitled "Aquifer Hydraulics."

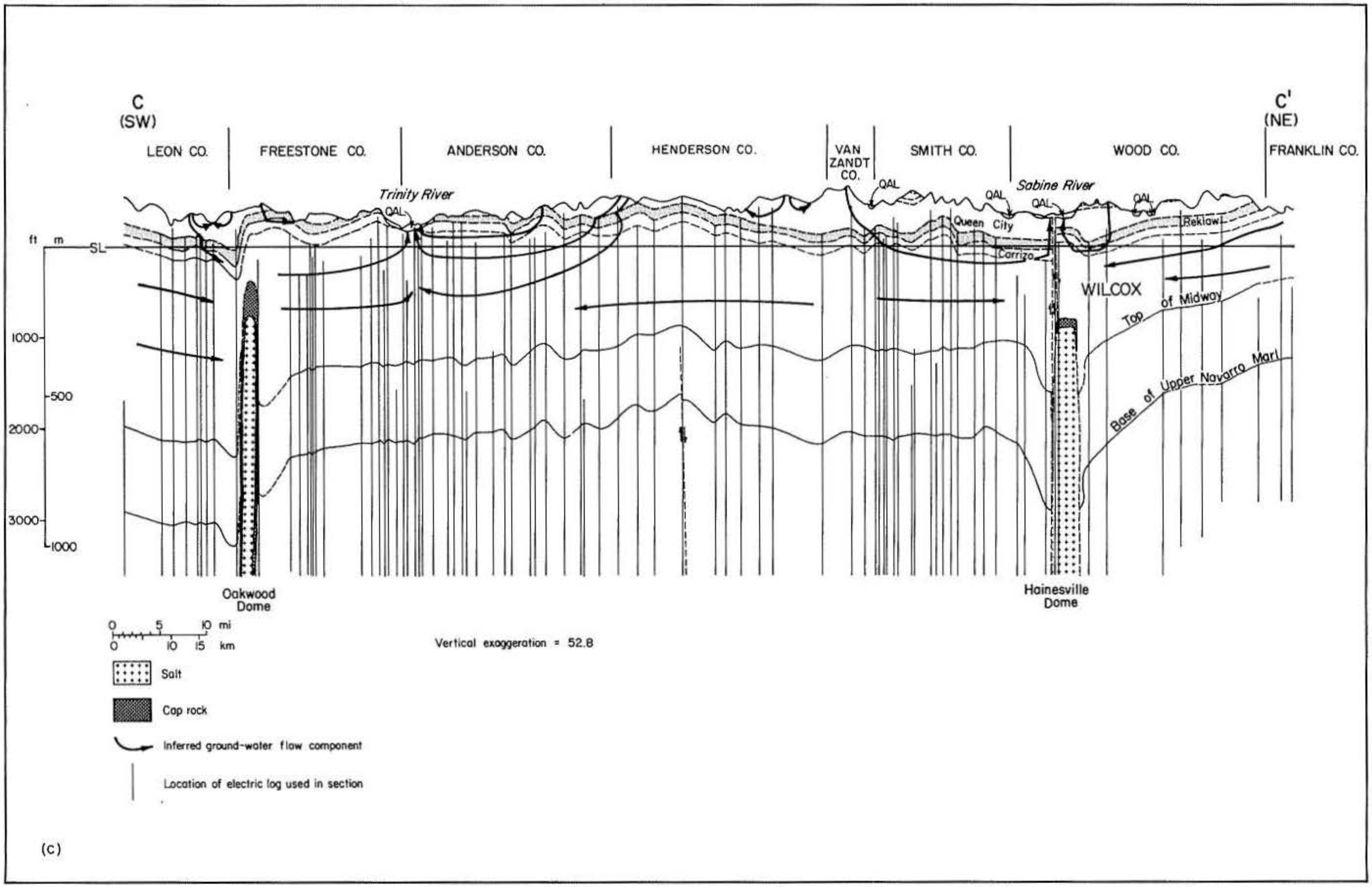

Figure 5 (continued).

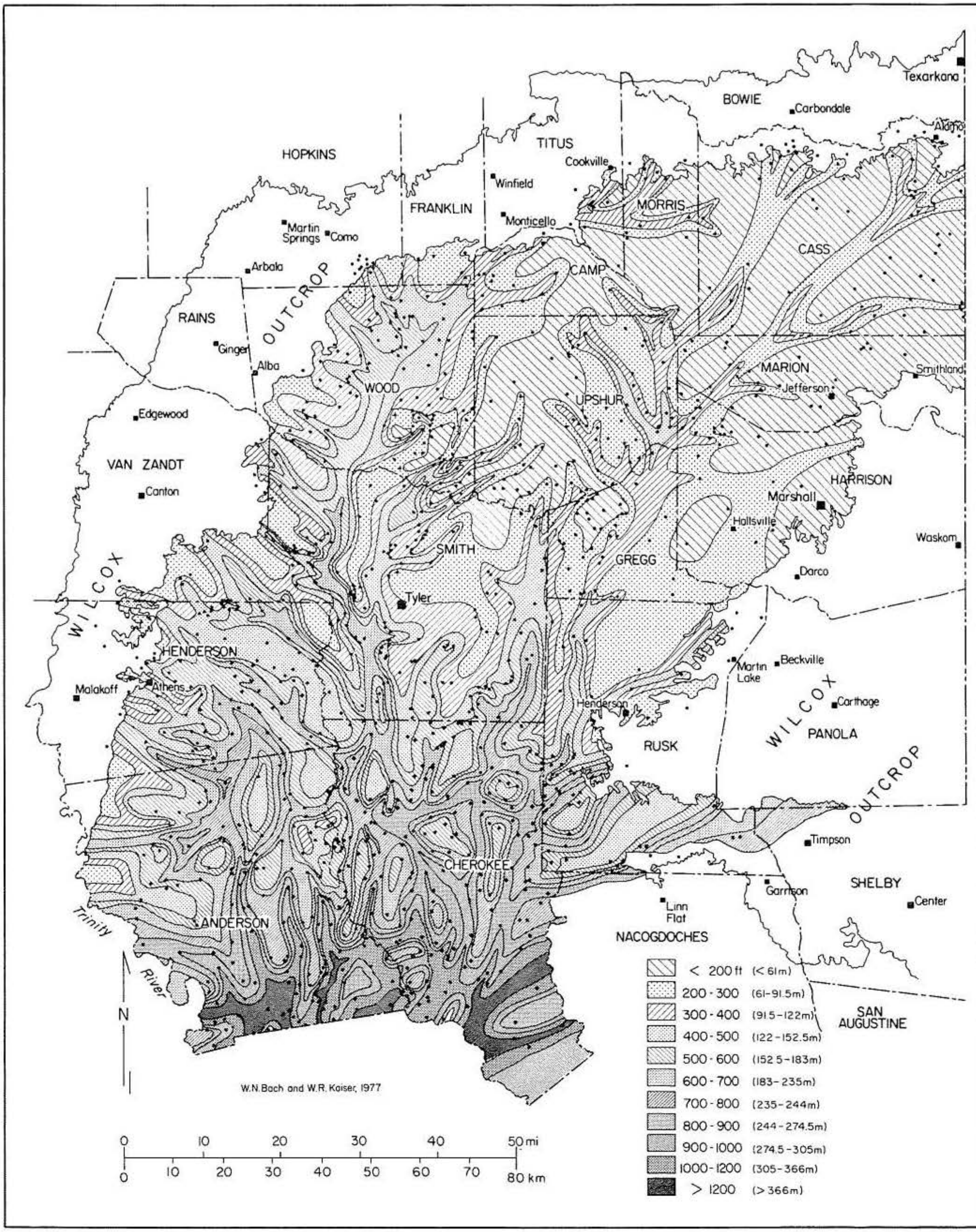

Figure 6. Net-sand-thickness map, Wilcox Group (from Kaiser and others, 1978).

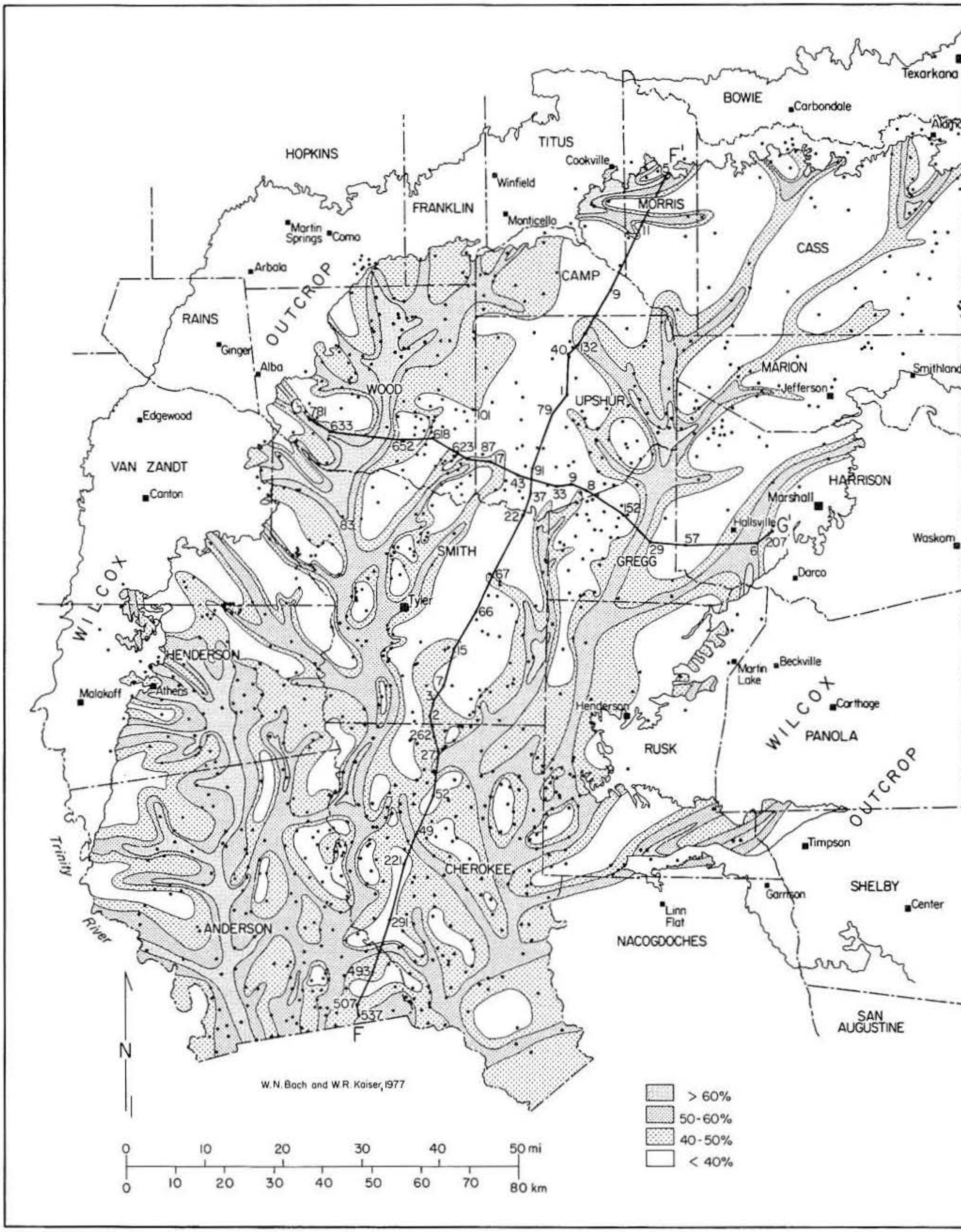

Figure 7. Percent-sand-thickness map, Wilcox Group (from Kaiser and others, 1978). Dendritic pattern of sand thickness reflects fluvial systems that deposited the Wilcox. Values of transmissivity and hydraulic conductivity should increase from areas of low sand thickness to areas of high sand thickness.

percent channels of Kaiser and others (1978) (fig. 7) project updip to the sand outcrops, suggesting that the channels are zones of relatively rapid recharge in outcrop in addition to being transmissive avenues of flow downdip.

Carrizo Formation

The Carrizo Formation unconformably overlies the Wilcox Group and is typically a massive to crossbedded well-sorted fine- to coarse-grained quartz sand about 100 ft (30 m) thick. In the southern half of the basin, the Carrizo is a relatively homogeneous sand and only locally contains a significant portion of mud interbeds. North of Smith County (figs. 6 and 7), however, the clean homogeneous sands of the Carrizo gradually disappear, and in many areas the presence of interbedded sands and muds makes the Carrizo indistinguishable on electric logs from the Wilcox Group.

Reklaw Formation

The Reklaw Formation consists of variable amounts of mud and sand thinning from about 250 ft (76 m) thick in the south to less than 75 ft (23 m) thick in the north part of the study area. Stenzel (1938) divided the Reklaw into the Marquez Shale (upper) and the Newby Sand (lower) in outcrops in Leon County along the southern margin of the basin. Similar units exist in the subsurface of Leon (Collins, 1980), Anderson, and Cherokee Counties (Guyton and Associates, 1972). In these areas, the upper half of the Reklaw is principally clay, and the lower half is a silty glauconitic fine-grained quartz sand. North of Cherokee and Anderson Counties, the Reklaw is generally not divisible; here, the formation consists of interbedded sand and mud.

The Reklaw is generally considered to be an aquitard, limiting flow between the overlying Queen City and underlying Wilcox and Carrizo aquifers. This is a reasonable assumption because the Reklaw contains laterally extensive clays and lacks clean sands containing good-quality water; also, wells that tap the underlying Carrizo are artesian. To understand better the aquitard characteristics of the Reklaw, a net-clay map of the unit was constructed using resistivity logs (fig. 8). The map could not be extended north of southern Smith County because north of this area the Reklaw is difficult or impossible to distinguish from the Queen City or the Carrizo Formations on resistivity logs. Consequently, in the northern half of the basin, the Reklaw may be a very leaky aquitard. The Reklaw also may be significantly leaky in Leon, Anderson, and Smith

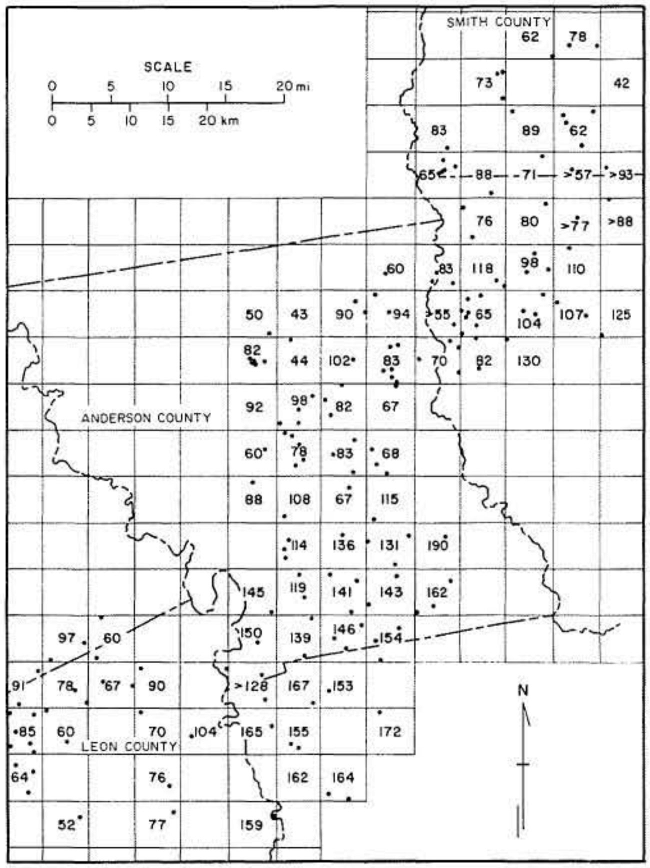

Figure 8. Mean net-clay-thickness map, Reklaw aquitard. The mapped area was constrained by availability of electric log data and distinguishability of the Reklaw from the Carrizo and Queen City on electric logs. North of the map area, Reklaw clays become more discontinuous, making it difficult to distinguish the Reklaw from interbedded strata of the Carrizo and Queen City Formations.

Counties (fig. 8), where clay strata appear to be somewhat discontinuous. Strata can typically be correlated over only a few miles before they pinch out or grade into strata of different lithologies. In general, the Reklaw appears least pervious south of central Anderson County (fig. 8), where the clay beds are thickest and most laterally continuous.

Queen City Formation

The Queen City Formation (fig. 4) is composed of interbedded quartz sands and muds, with a maximum thickness of about 700 ft (213 m) occurring in central Smith County. The unit thins in all directions from Smith County; it is approximately 200 ft (61 m) thick in Morris County to the northeast and in Houston County to the south. In southern Houston and Leon Counties, the Queen City Formation dips into the subsurface;

thickness here is approximately 400 ft (120 m). Fine- to medium-grained sand constitutes 50 to 80 percent of the Queen City Formation.

Hobday and others (1979) interpreted Queen City sediments to be of fluvial, deltaic, tidal-flat, barrier, and tidal-delta origins through observations of surface exposures lying between the Trinity River and the Texas-Louisiana border. They characterized the western half of the basin as predominantly fluvial deltaic, and the eastern half of the basin as tidal flat, barrier, and tidal deltaic. The sandy fluvial-deltaic sediments should be the most transmissive (D. K. Hobday, personal communication, 1980), provided that their saturated thickness has not been excessively diminished by erosion. Saturated thickness may be the most critical factor governing the productivity of the Queen City aquifer, since the unit has been complexly eroded by surface drainage systems (figs. 3 and 4).

Weches and Sparta Formations

In small areas in the middle and along the southern margin of the basin, the Queen City is overlain by the Weches and Sparta Formations (fig. 4). The Weches consists primarily of glauconitic muds and fine-grained quartz sands and is generally less than 90 ft (27 m) thick. High limonite content commonly makes the Weches resistant to erosion; consequently, it caps high hills and scarps. In central Anderson County, the Weches caps the highest hills in the study area at elevations greater than 700 ft (213 m) above mean sea level. Because sands in the Weches are generally very thin and dirty, it is considered an aquitard.

The Sparta Formation consists primarily of very fine grained to medium-grained quartz sand and mud. Maximum formation thickness is about 200 ft (61 m); sand is approximately 50 to 70 percent. This limited lateral extent, plus its distribution on topographically high areas, makes the Sparta a minor aquifer in the East Texas Basin compared with the Queen City, Carrizo, and Wilcox. Nevertheless, the Sparta supports some domestic ground-water production in Wood, Smith, Anderson, Cherokee, Nacogdoches, and Angelina Counties, and it is a chief source of ground water in Houston County.

Alluvium

Terrace and floodplain alluvium occur along all the major rivers and streams in the basin (fig. 4). Alluvium consists of mixtures of sand, mud, and gravel and probably attains a maximum thickness of about 60 ft (18 m) (E. W. Collins, personal communication, 1980). The most extensive alluvial deposits occur along the Trinity River. Few wells tap the alluvium, presumably because of its small saturated thickness. It would not be surprising, however, to find local zones of coarse-grained sediments of high permeability in the alluvium.

Structural setting

The structural framework of the East Texas Basin is shown by cross sections (figs. 5a, b, and c) and a structure map of the top of the Wilcox Group (fig. 9). Wilcox, Carrizo, and Reklaw strata crop out both along the western margin of the basin and, as a result of the Sabine Uplift (fig. 1), along the eastern margin. These strata dip generally toward the central axis of the basin. A northwest-trending structural high extends through Gregg and Upshur Counties (fig. 9), causing Eocene strata to dip both northeastward and southward. South of the Elkhart Graben-Mount Enterprise fault system, all formations dip relatively steeply toward the Gulf of Mexico.

The Elkhart Graben-Mount Enterprise fault system, which is the most extensive fault system displacing Eocene strata, consists of normal faults that offset Eocene rocks, usually by 50 to 300 ft (15 to 91 m) (Guyton and Associates, 1972). Underlying Cretaceous rocks are generally offset by 600 to 700 ft (183 to 213 m). Other faults exist in the basin, but none appear to have affected regional Eocene geology or hydrology.

Like many faults cutting nonindurated sediments, those of the Elkhart Graben-Mount Enterprise system are probably partial or total barriers to ground-water flow because of either the offset of sands or the formation of low-permeability gouge zones along the fault planes, or both. Such faults may create vertical avenues of flow by decreasing horizontal permeability in sands and increasing vertical permeability in fractured clays and shales.

Several salt domes have pierced and uplifted Eocene units in the East Texas Basin (figs. 4 and 5). Dome-specific structural geology generally varies between two types: (1) The dome may have caused surprisingly little uplift and faulting; thus, formations surrounding the dome remain relatively undeformed. Oakwood and Hainesville Domes are of this type. (2) The dome may have sharply uplifted other formations and typically exposed them within a complexly faulted outcrop. Butler, Palestine, Keechi (fig. 5a), and Boggy Creek Domes are of this type. Domes that have either aquifers exposed at the surface or disrupted aquitards, or both, are potential

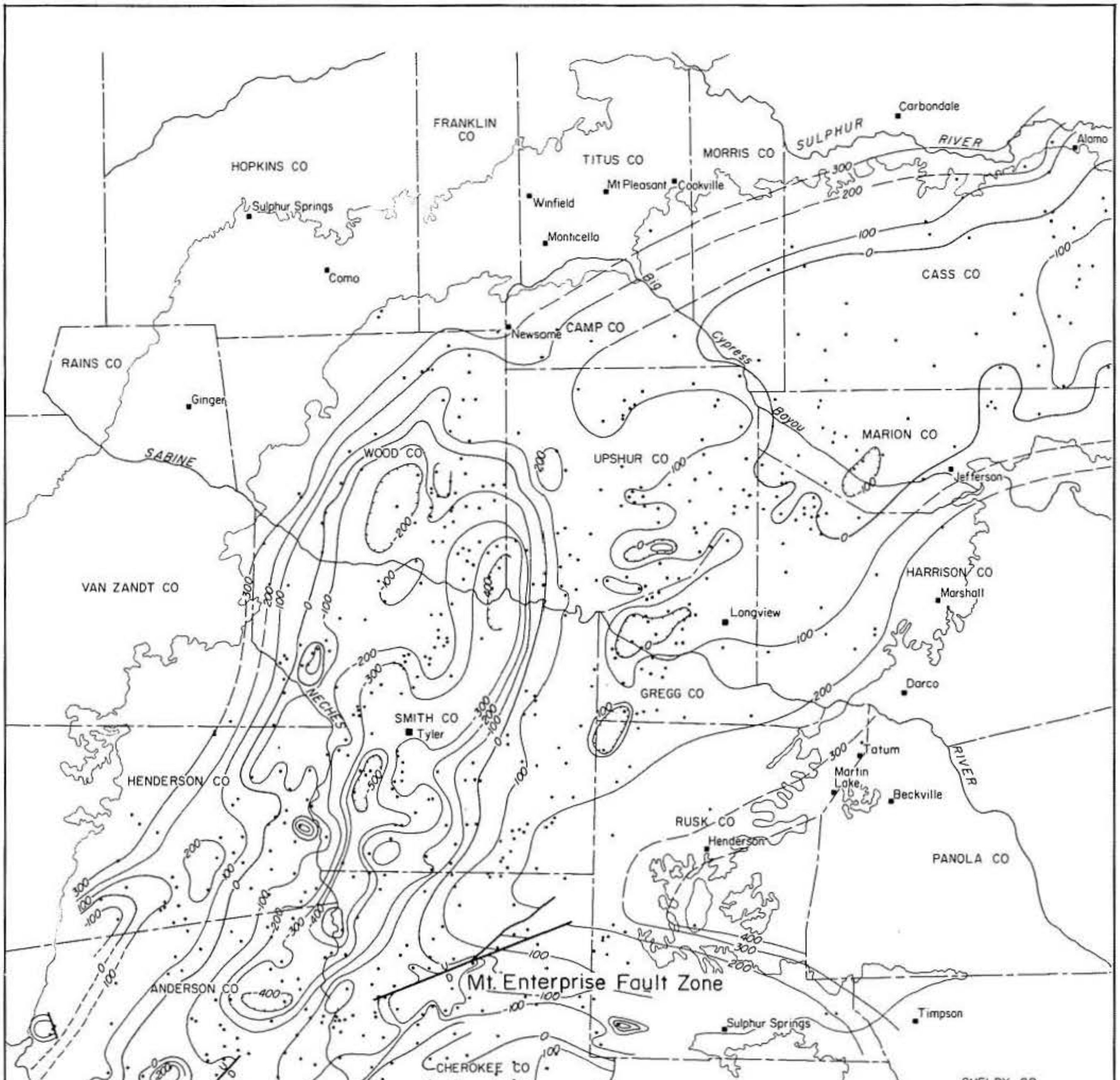

Figure 9. Structure map, top of Wilcox Group (from W. R. Kaiser, personal communication, 1980). The structural divide trends northwestward through Gregg and Upshur Counties and separates southward-dipping and east-northeast-dipping strata.

sites of recharge or discharge. At Oakwood Dome, the Carrizo and Reklaw crop out in a small area.

The youngest stratigraphic unit in contact with East Texas domes probably is the Reklaw Formation, which appears to be in contact with Bullard and Whitehouse Domes in Smith County (A. B. Giles, personal communication, 1980). The youngest units reached by all the other domes are Wilcox and older. The following domes appear to be in contact with the Wilcox Group: Bullard, Whitehouse, Keechi, Brooks, Bethel, Oakwood, Hainesville, Grand Saline, Steen, and Mount Sylvan (A. B. Giles, personal communication, 1980).

GROUND-WATER PUMPAGE AND USE

Ground water constitutes about 40 percent of the total water used in East Texas, and most of this water is pumped from the Wilcox and Carrizo aquifers. The 1974 ground-water and surface-water use figures have been compiled, by county, by the Texas Department of Water Resources (TDWR) (table 2) and include measured and estimated municipal, manufacturing, steam electric, irrigation, mining, and livestock uses. Most water was used for municipal and manufacturing purposes, and the remaining use composed a very small fraction of the total pumpage. In 1974, the greatest user of ground water was Angelina County, primarily owing to high rates of industrial pumpage. The second greatest user was Smith County because of relatively heavy municipal pumpage by Tyler, the largest city in the basin (70,058 people, according to the 1980 census [U.S. Government Printing Office, 1980]).

Annual rates of ground-water withdrawals for municipal and industrial use during the period 1955 to 1976, compiled for each county by the TDWR, are plotted in appendix A. These data were supplied to the TDWR through a voluntary system in which water users reported their measured or estimated volumes of pumpage, so data accuracy is questionable. However, the general trends shown in appendix A are probably reliable (Bill Moltz, Texas Department of Water Resources, personal communication, 1981). In general, pumpage is declining or slowly increasing. Declining pumpage results either from shifts from ground-water to surface-water resources or from reduced industrial activity, or both. The most significant industrial effect has been the recent decline in hydrocarbon production from the East Texas oil field. This is apparently responsible for declining ground-water withdrawals in Gregg, Harrison, Panola, Rusk, and Upshur Counties.

Table 2. Water use in the East Texas Basin, 1974.*

County	Ground water (acre-ft [ha-m])		Surface water (acre-ft [ha-m])		Total (acre-ft [ha-m])	
Anderson	6,450	(796)	4,168	(514)	10,618	(1,310)
Angelina	34,285	(4,229)	4,579	(565)	38,864	(4,794)
Camp	1,424	(176)	323	(40)	1,747	(215)
Cherokee	5,695	(702)	5,591	(690)	11,286	(1,392)
Franklin	678	(84)	1,032	(127)	1,710	(211)
Freestone	1,363	(168)	15,087	(1,861)	16,450	(2,029)
Gregg	4,194	(517)	17,010	(2,098)	21,204	(2,616)
Henderson	2,162	(267)	7,988	(985)	10,150	(1,252)
Hopkins	2,015	(249)	5,395	(665)	7,410	(914)
Houston	2,360	(291)	4,720	(582)	7,080	(873)
Leon	1,435	(177)	1,804	(223)	3,239	(400)
Limestone	1,570	(194)	2,990	(369)	4,560	(562)
Nacogdoches	7,524	(928)	1,126	(139)	8,650	(1,067)
Rains	256	(32)	339	(42)	595	(73)
Rusk	5,979	(738)	1,882	(232)	7,861	(970)
San Augustine	1,371	(169)	959	(118)	2,330	(287)
Smith	8,685	(1,071)	14,916	(1,840)	23,601	(2,911)
Titus	1,794	(221)	10,505	(1,296)	12,299	(1,517)
Upshur	3,357	(414)	1,524	(188)	4,881	(602)
Van Zandt	2,378	(293)	3,748	(462)	6,126	(756)
Wood	3,396	(419)	1,363	(168)	4,759	(587)
TOTAL	**98,371**	**(12,134)**	**107,049**	**(13,205)**	**205,420**	**(25,339)**

*Texas Department of Water Resources, B. Moltz, personal communication, 1980.

AQUIFER PARAMETERS

Aquifer parameters of transmissivity, hydraulic conductivity, and storativity coefficient have been calculated from pumping tests. These tests have been published by TDWR in county ground-water reports (see "Previous Work," p.3) and compiled by Myers (1969). Values of minima, maxima, and means are summarized for each county in table 3. Figure 10 is a map of mean values of transmissivity by county. Most of the tests are short term (2 to 12 h in duration) with either drawdown or recovery measurements, or both, recorded only in the production well. In each case, data were analyzed by the standard Theis or Jacob technique. As with most pumping test results, these data are subject to various errors, including non-ideal aquifer response and judgment error.

Aquifer parameters for the Wilcox and Queen City generally do not represent entire thicknesses of the geologic units, since the wells are generally screened only in individual sand bodies within these units. For example, figure 6 illustrates net-sand thicknesses exceeding 1,200 ft (400 m) in the Wilcox Group, but for practical reasons, wells rarely tap more than 100 to 200 ft (30 to 60 m) of the Wilcox. Individual sands are commonly 100 ft (30 m) thick.

To calculate transmissivity values for the entire thickness of the Wilcox Group, one would have to add together transmissivity values for all sands and

Table 3. Aquifer properties.

County	Aquifers	Transmissivity (gal/d/ft [m²/d]) Range	Transmissivity Mean	No. of wells	Hydraulic conductivity (gal/d/ft² [m/d]) Range	Hydraulic conductivity Mean	No. of wells	Storativity range	Approximate max. pumping rate (gal/min [L/min])
Anderson	Queen City	3,000 (37)	3,000 (37)	2	32-71 (1.3-2.9)	52 (2.1)	2	---	400 (1,500)*
	Carrizo	12,800-20,800 (159-258)	15,400 (191)	5	158-214 (6.4-8.7)	182 (7.4)	5	---	1,500 (5,700)*
	Wilcox	5,400-47,000 (67-580)	21,200 (263)	10	49-338 (2.0-13.8)	134 (5.5)	10	0.00037	1,500 (5,700)*
Angelina	Carrizo	14,300-45,300 (177-573)	30,800 (383)	36	204-336 (8.3-13.7)	259 (10.5)	23	0.00012-0.00016	1,500 (5,700)*
	Wilcox	---	---	--	---	---	--	---	<300 (1,100)*
	Sparta	---	---	--	---	---	--	---	500 (1,900)*
Camp	Cypress	340 (4.2)	340 (4.2)	1	4.4 (0.18)	4.4 (0.18)	1	---	310 (1,200)+
Cass	Cypress	900-14,000 (11-174)	4,400 (54)	7	5-118 (0.20-4.80)	58 (2.4)	7	---	475 (1,800)+
Cherokee	Queen City	3,000 (37)	3,000 (37)	1	67 (2.7)	67 (2.7)	1	---	400 (1,500)*
	Carrizo	4,200-34,000 (52-420)	26,100 (324)	9	117-476 (4.77-19.4)	203 (8.27)	9	0.00011	1,000 (3,800)*
	Wilcox	12,800-24,500 (159-304)	16,800 (209)	3	136-272 (5.54-11.1)	18.4 (7.50)	3	---	800 (3,000)*
Freestone	Wilcox	1,400-12,500 (17.4-155)	4,000 (50)	10	17-71 (0.69-2.9)	38 (1.5)	9	---	1,500 (5,700)*
Gregg	Wilcox-Carrizo	3,000-5,500 (37-68)	4,000 (50)	7	2.8 (0.11)	2.8 (0.11)	1	0.00006	300 (1,100)+
	Queen City	---	---	--	---	---	--	---	---
Franklin	Cypress	7,300-81,000 (91-1,000)	31,500 (391)	3	115-1,270 (4.6-51.7)	434 (17.7)	3	---	150 (550)+
Harrison	Cypress	1,300-4,300 (16-53)	3,150 (39)	5	17-83 (0.69-3.4)	52 (2.1)	5	---	250 (950)+
Henderson	Carrizo	2,000 (25)	2,000 (25)	1	22 (0.90)	22 (0.90)	1	---	500 (1,900)*
	Wilcox	1,400-12,500 (17-155)	4,900 (61)	10	18-156 (0.73-6.3)	56 (2.3)	10	---	800 (3,000)*
Houston	Carrizo	---	25,000 (310)	2**	---	---	--	---	750 (2,800)+
	Queen City	---	3,800 (47)	--	---	---	--	---	---
	Sparta	---	20,000 (250)	--	---	---	--	---	1,200 (4,500)*
Leon	Carrizo	30,000-31,000 (370-385)	30,500 (378)	2	338-480 (13.8-19.6)	409 (16.7)	2	---	---
	Wilcox	no data	--	--	---	---	--	---	---

Table 3 (continued).

County	Aquifers	Transmissivity (gal/d/ft [m²/d]) Range	Transmissivity Mean	No. of wells	Hydraulic conductivity (gal/d/ft² [m/d]) Range	Hydraulic conductivity Mean	No. of wells	Storativity range	Approximate max. pumping rate (gal/min [L/min])
Leon (cont.)	Queen City	2,790-8,000 (34.7-99)	5,400 (67)	2	50 (2.0)	30 (2.0)	1	---	130 (490)+
Marion	Cypress	200-13,000 (2.5-160)	7,000 (87)	2	5-178 (0.2-7.25)	92 (3.7)	2	0.00014	348 (1,300)+
Morris	Cypress	960-2,000 (12-25)	1,300 (16)	3	3.9-19 (0.16-0.77)	11 (0.45)	3	---	100 (380)+
Nacog-doches	Carrizo	500-38,000 (6.2-470)	21,700 (270)	17	99-282 (4.0-11.5)	202 (8.2)	16	0.00007-0.00016	1,500 (5,100)•
	Wilcox	1,100-5,800 (14-72)	2,300 (28)	6	20-100 (0.81-4.1)	46 (1.9)	6	0.00068	500 (1,900)•
	Sparta	1,000-58,100 (12-722)	15,800 (196)	9	22-632 (0.90-25.8)	224 (9.13)	9	0.00017-0.00048	200 (760)•
Navarro	---	---	---	--	---	---	--	---	---
Panola	Wilcox	3,610 (44.8)	3,610 (44.8)	1	116 (4.73)	116 (4.73)	1	---	---
Rains	Wilcox-Carrizo	600 (7.4)	600 (7.4)	1	14 (0.57)	14 (0.57)	1	---	275 (1,040)+
Smith	Carrizo	19,500 (240)	19,500 (240)	1	---	---	--	---	---
	Wilcox-Carrizo	10,400-38,000 (129-470)	18,900 (234)	14	85-416 (3.5-16.9)	---	--	0.0001-0.0002	1,100 (4,200)•
	Wilcox	4,930-19,300 (61-239)	11,400 (147)	10	---	---	--	---	---
	Queen City	2,720-3,260 (33.7-40.7)	3,000 (37)	3	10-30 (0.41-1.2)	---	--	---	400 (1,500)+
	Sparta	12,400 (154)	12,400 (154)	1	---	---	--	0.00017	250 (950)+
Titus	Cypress	250-2,500 (3.1-31)	1,700 (21)	4	2.6-29 (0.11-1.2)	14 (0.57)	4	0.00015	125 (475)+
Upshur	Carrizo	6,840 (84.9)	6,840 (84.9)	1	---	---	--	---	---
	Wilcox-Carrizo	4,200-11,000 (52-137)	7,800 (98)	4	3.6-15.5 (0.15-0.63)	8.4 (0.34)	4	---	810 (3,100)+
	Queen City	3,200-4,900 (40-61)	3,800 (47)	3	---	---	--	0.0003	---
Van Zandt	Wilcox-Carrizo	2,100-8,900 (26-110)	4,800 (60)	7	32-90 (1.3-3.6)	55 (2.3)	7	0.00038	250 (950)•
Wood	Wilcox-Carrizo	600-19,000 (7.4-235)	5,700 (71)	9	5-700 (0.2-28)	133 (5.42)	9	0.00034-0.00046	490 (1,900)+
	Queen City	---	---	--	---	---	--	---	---
	Sparta	---	---	--	---	---	--	---	---

+Highest reported yield for individual well.
•Estimated maximum yield for individual well.
••Data from Peckham and others (1963).

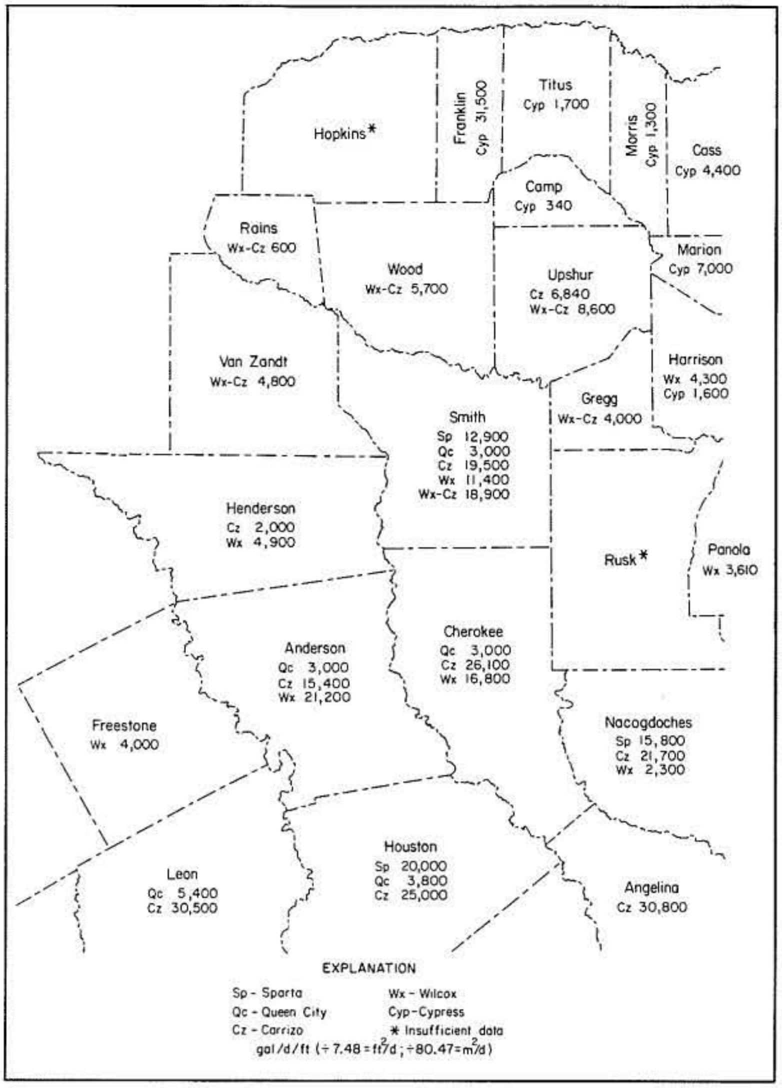

Figure 10. Mean transmissivity (T) map, Sparta, Queen City, Carrizo, Wilcox, and Cypress aquifers. The Cypress aquifer exists in the northern part of the basin and consists of Eocene strata, which appear to form one integrated unit in this area. The northward decrease in transmissivity of the Wilcox is due to a corresponding decrease in sand thickness (compare with figs. 6 and 7).

make assumptions about lateral interconnection of these sands. The Carrizo Formation is generally thin and sufficiently homogeneous so that wells are screened through its entire thickness.

Values of hydraulic conductivity (table 3) are generally absent or approximated because the corresponding values of aquifer thickness are commonly unknown or approximated from the lengths of well screens. The values of hydraulic conductivity should be considered good order-of-magnitude estimates.

The Carrizo aquifer generally yields the highest values of transmissivity and hydraulic conductivity (table 3) because of its laterally continuous well-sorted clean sands. Commonly, sands of the Wilcox are as thick as those of the Carrizo, but the silty Wilcox sands are frequently less permeable and less transmissive. Queen City wells generally yield lower values of transmissivity and hydraulic conductivity than do wells producing from the Wilcox and Carrizo, apparently because of thinner sands and higher silt content.

As mentioned earlier, for the Wilcox aquifer there should be a correlation between transmissivity and sand distributions (figs. 6 and 7). Such a correlation is illustrated to some degree in figure 10 and in plots of transmissivity and hydraulic conductivity versus net sand and sand percent in figure 11. Transmissivity values decrease northward from about 16,000 and 21,000 gal/d/ft (650 and 900 m^2/d) in Anderson and Cherokee Counties, respectively, to less than 5,000 gal/d/ft (200 m^2/d) at the northern end of the basin, where the Wilcox is included in the so-called Cypress aquifer (fig. 10). This relationship undoubtedly results from south- to north-decreasing sand thicknesses and increasing mud contents. Plots of transmissivity versus net-sand values and sand percent (figs. 11a and b) indicate general positive correlations. Transmissivity versus sand percent shows the poorer correlation of the two, possibly because there are only four categories of sand percent (fig. 7). Transmissivity versus net sand indicates as much as a twentyfold increase in transmissivity from sand thicknesses of about 250 ft (75 m) to sand thicknesses of about 950 ft (290 m). One might expect to find similar correlations for hydraulic conductivity because the coarsest sands tend to be located in the zones of either highest sand percent or net sand, or both. However, hydraulic conductivity correlates weakly, if at all, with net sand and sand percent in figures 11c and d.

Much of the scatter in figures 11a, b, c, and d presumably stems from (1) errors in the estimates of transmissivity and hydraulic conductivity and (2) the fact that the net-sand and sand-percent values (figs. 6 and 7) are regional averages measured through the entire thickness of the Wilcox Group, whereas transmissivity and hydraulic conductivity represent relatively smaller areas and individual sand bodies within the Wilcox Group.

Few estimates of the storativity coefficient have been made because of limited measurements of water-level response in observation wells during

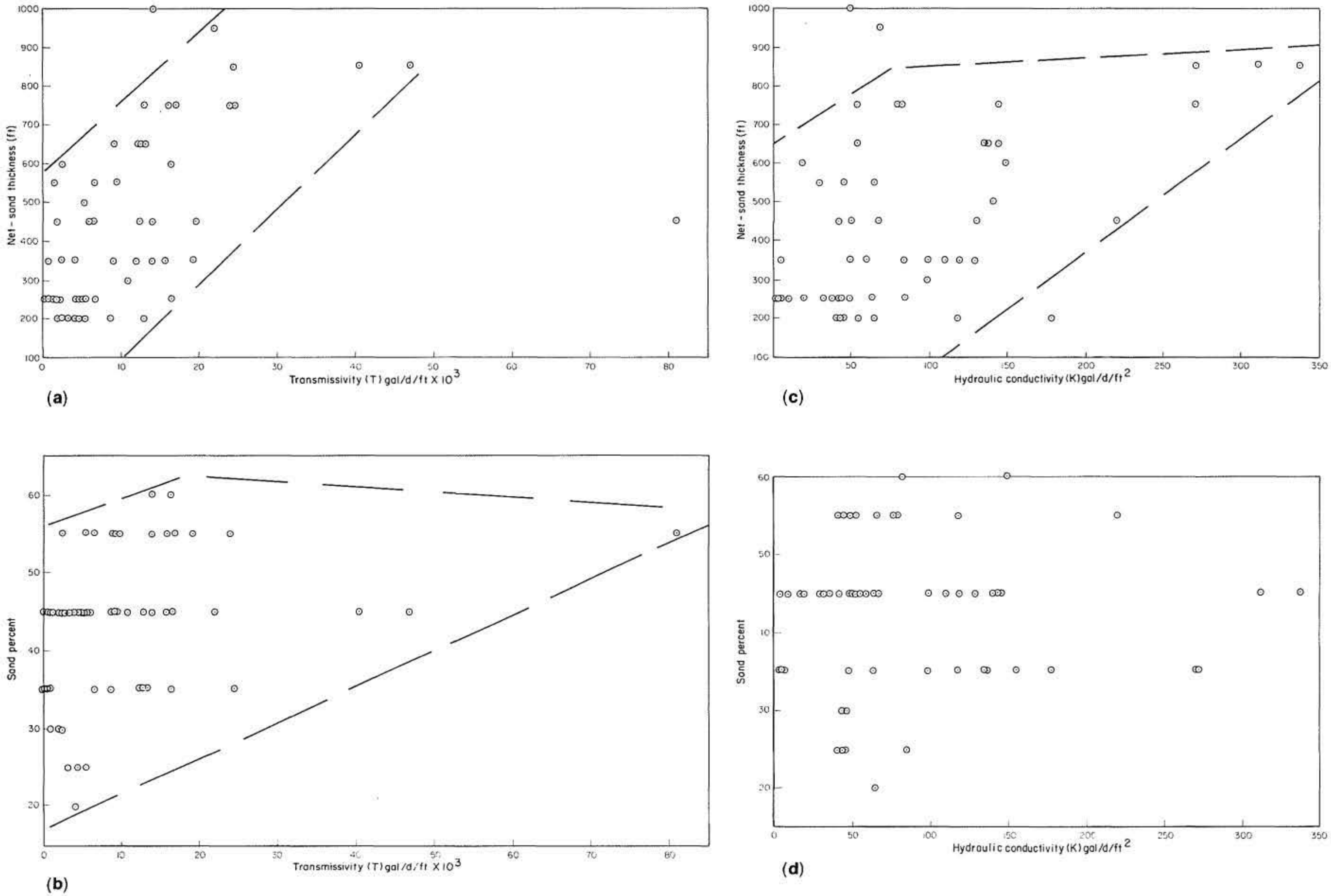

Figure 11. Plots of transmissivity (T) and hydraulic conductivity (K) versus sand-percent and net-sand values (figs. 6 and 7), Wilcox aquifer: (a) transmissivity versus net sand, (b) transmissivity versus sand percent, (c) hydraulic conductivity versus net sand, and (d) hydraulic conductivity versus sand percent. The plots show, at best, weak correlations. The best correlation occurs for transmissivity versus net sand, presumably because transmissivity is a direct function of sand thickness.

pumping tests. (The storativity coefficient can be measured accurately from pumping tests only when measurements are taken in at least one observation well.) Nearly all the measurements of storativity coefficient are for Wilcox-Carrizo sands, which have yielded values in the range of 0.00006 to 0.00068 (table 3). These low storativity-coefficient values indicate confining conditions; however, four of the wells tested for storativity coefficient are located in the Wilcox-Carrizo outcrop in Nacogdoches, Wood, Van Zandt, and Titus Counties, where one might expect higher values because of unconfined conditions. A probable reason for this discrepancy is the presence of local confining conditions in the outcrop; this is easy to visualize because the system is so heterogeneous. Another possible reason for the low storativity-coefficient values is the delayed gravity response of unconfined aquifers. Delayed gravity response, also called delayed yield or delayed gravity drainage, is a phenomenon in which an unconfined aquifer acts like a confined aquifer during the early phase of pumping and has a low storativity-coefficient value; after a transition period, it then behaves like an unconfined aquifer and has a higher storativity-coefficient value (Boulton, 1963; Neuman, 1972). When delayed gravity response occurs, the pumping test must proceed for a long time to establish an accurate value for storativity coefficient. Short-term tests like those currently used in the East Texas Basin are undoubtedly too short even to detect the phenomenon.

AQUIFER HYDRAULICS

Aquifer hydraulics is the study of ground-water circulation as a distribution of potential energy in the system. Ground-water circulation is controlled essentially by four factors: climate, topography, geology, and human activity such as pumpage, injection, and excavation. Climate controls the amount of water available for recharge to aquifers. Topography dictates the amount of potential energy (hydraulic head) available at the upper boundary of a subsurface flow system where fluids enter or leave the geosphere. Geology imposes physical restraints, such as permeability and aquifer geometry, on flow. Pumpage and injection artificially raise and lower potential energies (heads) in the system. In the East Texas Basin, topography and geology are the dominant controls on flow in the Eocene aquifers. Thousands of production wells supply fresh water in the basin, but only in a few localities are withdrawal rates sufficient to affect appreciably the regional flow systems (no injection takes place in the fresh-water aquifers).

In this study, ground-water circulation in the Queen City and Wilcox-Carrizo aquifer systems is defined by using hydraulic head data. The Sparta aquifer and its relation to flow in the Queen City will be mentioned briefly. Interpretation of regional flow conditions in the Queen City is straightforward because the aquifer is under water-table conditions over most of the basin. The Wilcox-Carrizo system is more complex and includes much more hydraulic head data. Evaluation of circulation in the Wilcox-Carrizo aquifer system includes two basic steps. First, horizontal components of flow are analyzed, using conventional potentiometric surface mapping. This step provides information on (1) regional ground-water flow patterns, (2) impacts of topography, geology, and pumpage on flow, (3) locations of major recharge and discharge areas, and (4) mechanisms of recharge and discharge. Second, vertical-flow components are analyzed, using the distribution of flowing wells, head differentials measured between aquifers, and pressure-versus-depth relationships. This second step provides more information on locations and mechanisms of recharge and discharge. Vertical flow is particularly important because it is the mechanism that moves contaminants toward or away from the biosphere. Ground-water flow is a three-dimensional phenomenon. The traditional approach that employs only analysis of potentiometric surface maps is inadequate because it neglects vertical-flow components.

QUEEN CITY

The Queen City system is under water-table conditions over most of the basin, and consequently, head values closely correspond to the irregular topography. Since significant variations in elevation of the water table occur between data points, the Queen City water table is a complex surface that is not adequately represented by the available head data. These data nonetheless were plotted as block-averaged quantities (fig. 12) to show the general configuration of the water table. More detailed water-table maps could be constructed by inference from topographic maps. Depth to the Queen City water table is generally about 50 ft (15 m).

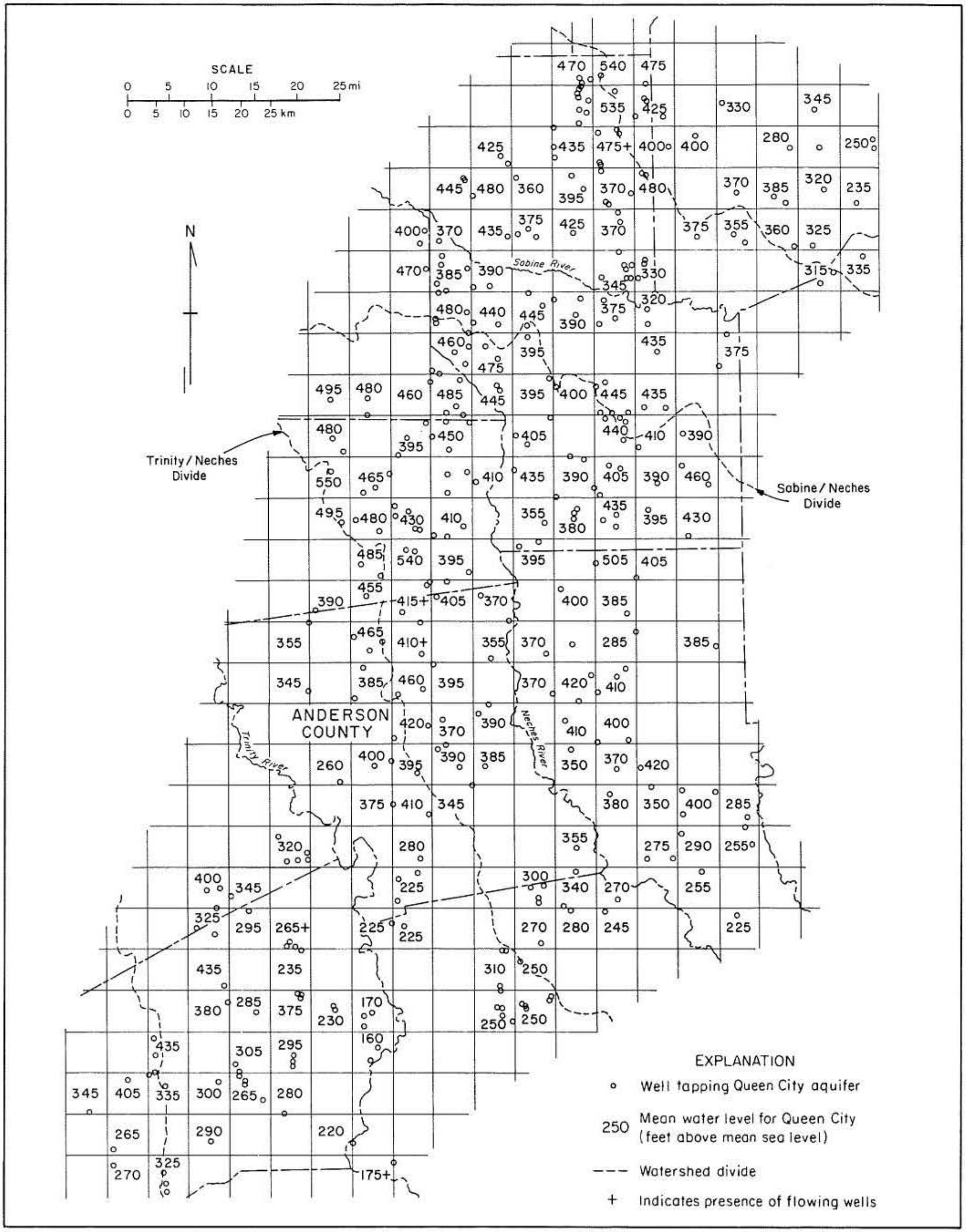

Figure 12. Potentiometric levels, Queen City aquifer. Irregular heads in the aquifer are caused by irregular topography. Closely spaced recharge and discharge areas are scattered throughout the aquifer.

The complex variations in head (water table) indicate an equally complex distribution of recharge and discharge in the Queen City aquifer. The aquifer does not constitute a regionally coherent flow system. Ground-water residence times in the Queen City are less than residence times in the Wilcox and Carrizo aquifers.

The head map of the Queen City aquifer reflects the regional topography. Head values are consistently high beneath the regional topographic highs or the watershed divides (fig. 12) and slope generally toward stream valleys. This is true even in Smith County, where the Queen City is confined by the Weches aquitard, suggesting a significant amount of hydrologic communication, or leakage, across the aquitard.

Effects of regional geology are not evident in the head map because of the predominance of topographic effects. Locally, geology is probably a strong influence on ground-water flow because the Queen City is a heterogeneous distribution of sands and muds.

Although the Queen City aquifer does not constitute a regional flow system, it has regional importance for the deeper aquifers. It affects the vertical hydraulic gradients available for moving fluids vertically into or out of the deeper aquifers.

WILCOX-CARRIZO

Potentiometric surface map

A potentiometric surface map (fig. 13) was constructed from a total of 1,678 water-level measurements in wells tapping the Wilcox and Carrizo aquifers. Approximately 350 (20 percent) of these wells tap the Carrizo. The two units are combined on the map because *at a regional scale* they appear sufficiently interconnected hydrologically to form one integrated flow system. This interconnection is indicated by two factors. (1) When plotted together on the map, the Wilcox and Carrizo heads generally appear to differ little. (2) No regionally continuous aquitard restricts flow between them. For the rest of this chapter, the Wilcox and Carrizo will be considered as one system.

Caution should be exercised when studying the Wilcox and Carrizo on a local scale because upper Wilcox muds are commonly in contact with the Carrizo, effectively isolating the two units from each other. Investigations on the local scale should map conditions in the Wilcox and Carrizo as if they were two separate systems and should perhaps subdivide the Wilcox further. Although Wilcox sands typically appear to be distributed randomly in the vertical dimension, detailed stratigraphic analysis shows that they are commonly clustered within local intervals of the Wilcox Group (Seni and Fogg, in preparation). Subdividing the Wilcox is especially recommended in the extreme southwest part of the study area, where the Simsboro Sand Member of the Wilcox comprises a distinct highly transmissive unit.

Unlike the water table of the Queen City, that of the Wilcox-Carrizo exhibits a relatively smooth surface that can be contoured, apparently because of the gentler topography in the Wilcox-Carrizo outcrop (fig. 3) and better well control. The smoother surface of the water table may also be related to better interconnectedness of Wilcox-Carrizo sands.

Water-level measurements used to construct figure 13 were selected from data collected between 1936 and 1976. Nearly all of the values, however, were measured between 1962 and 1971. The reliability of data collected during different years depends upon how rapidly water levels are declining because of pumpage. In most areas of the East Texas Basin, annual water-level declines in the Wilcox-Carrizo system generally have been negligible (less than a few feet), and most of the data are therefore sufficiently valid for constructing 50-ft (15-m) intervals. Nevertheless, information on water-level fluctuation was compiled for each data point plotted, and the reliability of each measurement was assessed subjectively. During contouring, those points at which water levels were changing most rapidly were given the least weight. Pumpage has greatly lowered water levels in only a few areas of the basin, usually near cities.

Another potential source of error stems from water-level measurements that have been made in wells shortly after those wells were pumped; thus, the water level recorded may have been significantly below the static water level. In a few cases such errors were obvious, and these points were eliminated. Some faulty data undoubtedly went undetected and were used in the final analysis. The net effect of erroneous data on the head contours in figure 13 and on the final interpretation, however, is thought minimal; when analyzed collectively, the data create a physically reasonable model of the system.

The Wilcox-Carrizo potentiometric surface map is a reliable representation of regional ground-water flow. However, it undoubtedly misrepresents local hydraulic gradients in several areas and should therefore be applied judiciously to site-specific problems. The most reliable areas of the map are the outcrops (where head data are most abundant) and the interior counties of Leon, Anderson, Cherokee, Nacogdoches, Henderson, Smith, Gregg, and Wood. Although these counties encompass all the salt domes in the basin, the hydraulic head map

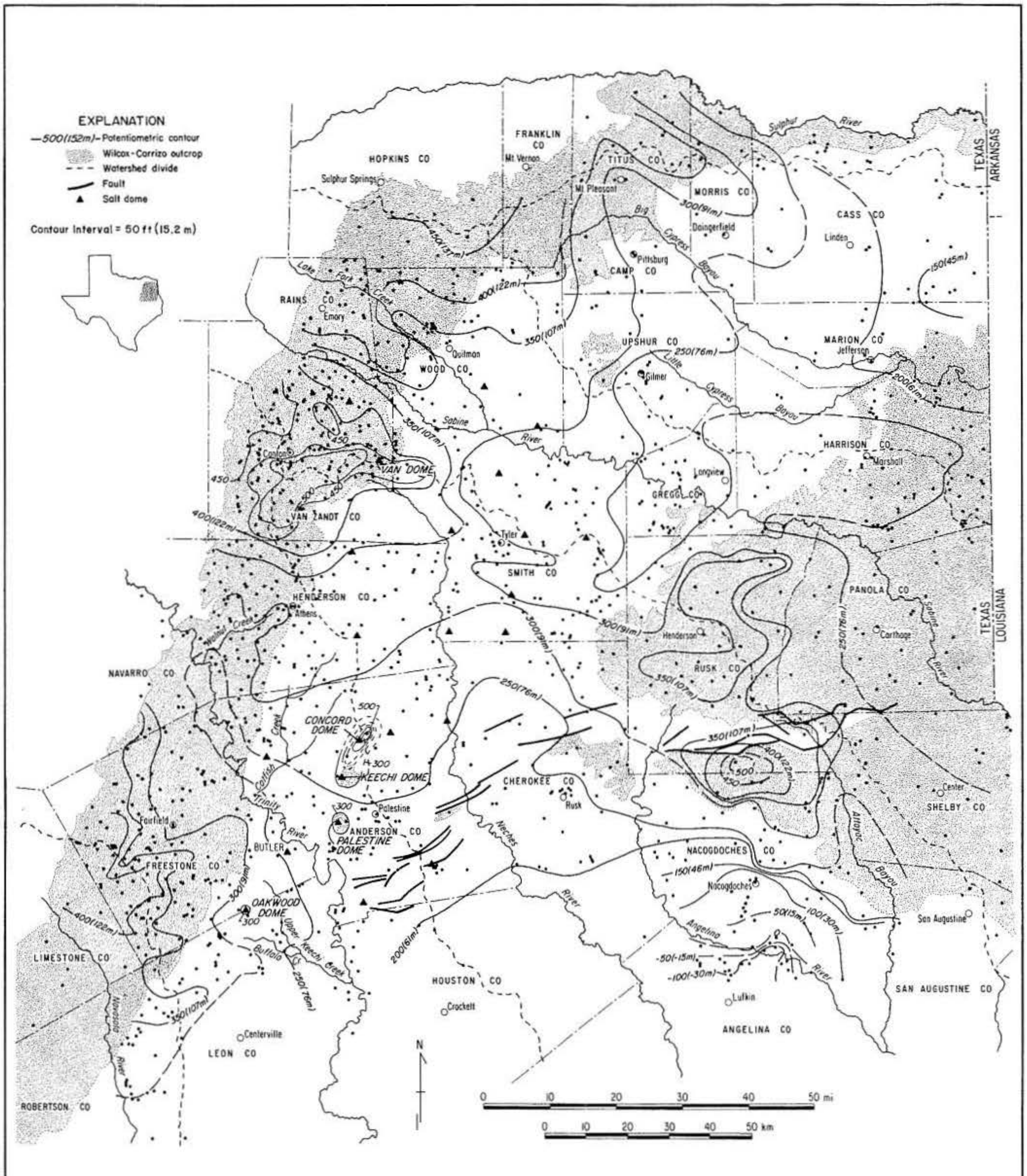

Figure 13. Potentiometric surface, Wilcox-Carrizo aquifer system. Water-level data are from 1936 through 1976; however, most of the data were selected from measurements made during 1962 through 1971. Local hydraulic gradients and fluxes may differ significantly from those indicated here. Configuration of the potentiometric surface can be attributed to impacts of either topography, geology, or pumpage. Topographic effects can even be seen in the central artesian section; the best example is the recharge mound in central Anderson County. A regional ground-water divide traverses southern Smith County.

(fig. 13) was extended several miles farther east and north to delineate better the whole basin. From the northern margin of the basin in Camp, Franklin, Morris, and Titus Counties, only a fraction of the available data was used to construct figure 13 because a general picture of flow was desired in this area. In these four counties, as well as in Harrison and Marion Counties, the Texas Department of Water Resources has grouped all Eocene formations into one aquifer unit called the Cypress aquifer, because none of these formations can be distinguished on electric logs (Broom and others, 1965; Broom and Myers, 1966; and Broom, 1969). Thus, in this six-county area, Wilcox and Carrizo wells were determined approximately by comparing depths of screens and elevation of the Wilcox Group (fig. 9).

To aid interpretation of the potentiometric surface map, ground-water flow lines have been drawn on the basis of potentiometric contours (fig. 14). The stream lines are only general indicators of flow direction and do not constitute a quantitative flow net.

Impacts of topography

Figures 13 and 14 indicate that in general, ground water in the Wilcox-Carrizo flows away from large potentiometric mounds in the eastern and western outcrops toward streams in the outcrops and toward structurally downdip areas, where flow continues to veer toward streams. These potentiometric mounds always underlie regional topographic highs, which are delineated in figures 13 and 14 by the watershed divides of the Trinity, Neches, and Sabine River basins. The most extensive recharge mound lies in the western outcrop belt in Van Zandt County, where an extensive topographic high is formed by the coalescence of three watershed divides. Effects of topography are also evident on a much larger scale, as flow lines originating from the western outcrop belt extend over nearly the entire basin, whereas those originating from the topographically lower eastern outcrop extend over a much smaller area.

The flow lines clearly indicate major discharge areas in the Wilcox-Carrizo outcrop to be the Trinity River and its tributary, Walnut Creek; the Sabine River and its tributary, Lake Fork Creek; Big Cypress Bayou; and the Sulphur River.

The flow patterns also show evidence of topographic influence in the artesian section, albeit more subtle than that for the outcrop areas. The evidence is most obvious in the Trinity Basin, where there is a recharge mound in central Anderson County underlying the Trinity/Neches watershed divide and flow lines converge almost at right angles on the Trinity River. Flow in the artesian section also appears to converge more or less toward the Neches and Sabine Rivers and Big Cypress Bayou. The correlation between topography and flow strongly suggests that the Reklaw aquitard is significantly leaky. Such leakage may occur as flow through the clays of the Reklaw or as flow around them as a result of its interbedded lithology (see the earlier discussion of the Reklaw aquitard on p. 12).

The shape and size of the recharge mound in central Anderson County are hypothesized from only three data points. The reliability of these three points has been verified through field measurement of the water levels. The high vertical relief of the mound can be partly attributed to the high relief of the overlying hills that reach more than 725 ft (220 m) above mean sea level (fig. 3), marking some of the highest elevations in the basin. Additionally, Keechi and Concord salt domes apparently affect the mound (fig. 13). Keechi uplifts the Wilcox-Carrizo to the surface, creating a recharge area of approximately 15 mi^2 (28 km^2) at the southwestern extension of the mound. This uplift alone, however, cannot account for the mound: The uplift affects a relatively small area away from the center of the mound, and the maximum land-surface elevation in the outcrop over the dome is about 100 ft (30 m) lower than maximum heads on the mound. Concord Dome, on the other hand, directly underlies the center of the potentiometric mound, and although it has perturbed the Wilcox-Carrizo less than Keechi Dome has, the dome has locally uplifted the base of the Wilcox by approximately 100 ft (30 m) (A. B. Giles, personal communication, 1980) and faulted overlying sediments. These faults may disrupt the Reklaw and Weches aquitards enough to increase their vertical permeabilities and allow increased leakage rates. Thus, high rates of recharge at the mound could be attributed primarily to high topography supplying the downward-driving force and to disruption of aquitards by faults associated with Concord Dome.

Impacts of geology and pumpage

Geology appears to affect regional ground-water circulation in the Wilcox-Carrizo in five areas: (1) the Sabine Uplift (fig. 1), (2) the structural ridge shown in the Wilcox structure map (fig. 9), (3) the Elkhart Graben-Mount Enterprise fault system (fig. 1), (4) salt dome growth, and (5) sand distribution in the Wilcox (figs. 6 and 7).

The Sabine Uplift has had the most significant effect on regional Wilcox-Carrizo hydrogeology. Most Tertiary aquifers of the Texas Gulf Coast dip steeply into the subsurface a short distance away

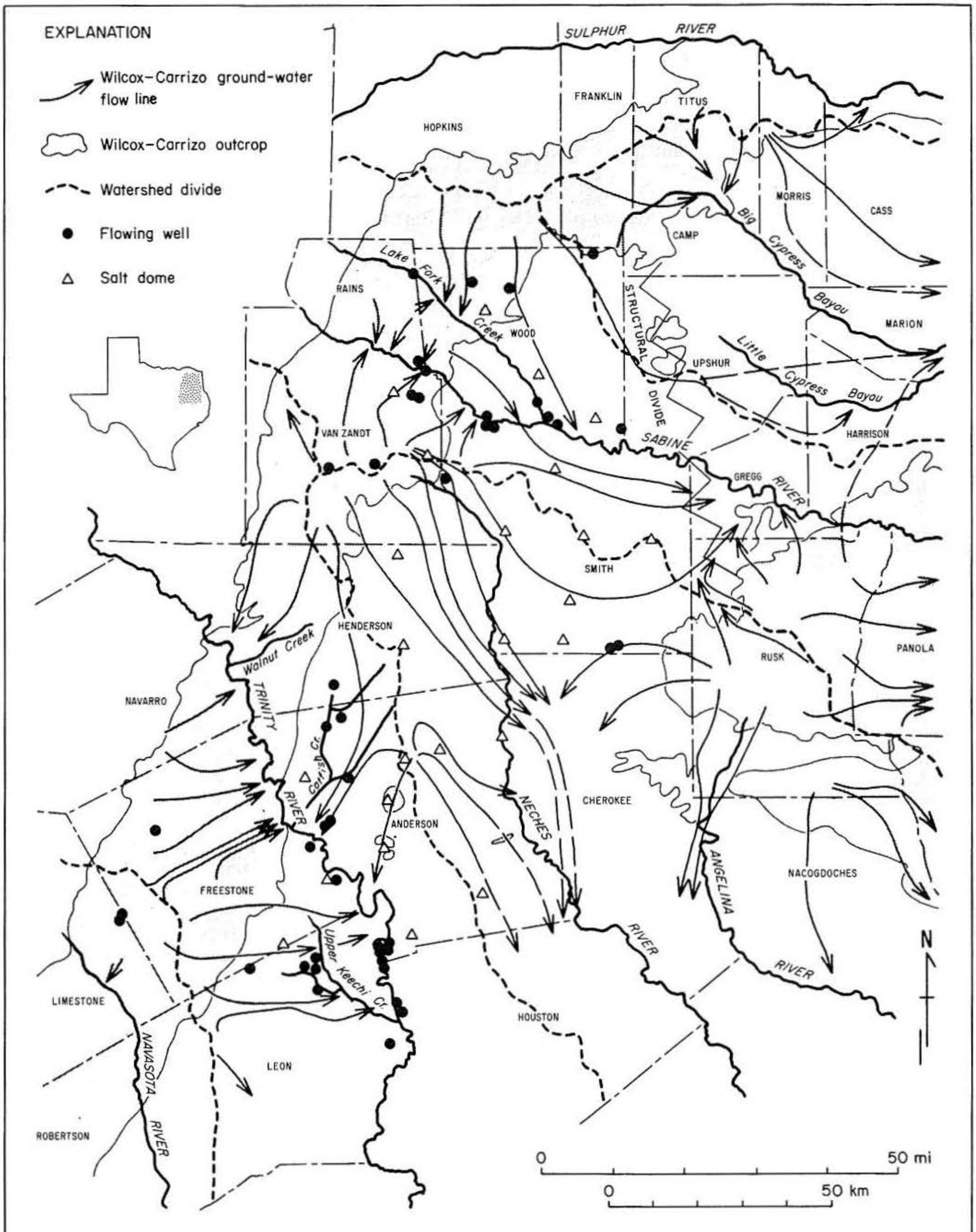

Figure 14. Ground-water flow lines drawn from the Wilcox-Carrizo potentiometric surface. Local flow directions may differ significantly from those shown here.

from the outcrops and become relatively isolated from shallower systems. The Sabine Uplift has prevented this isolation in the East Texas Basin by creating a major outcrop (recharge area) of Wilcox-Carrizo strata on the eastern side of the basin. Consequently, the system contains great thicknesses of fresh water having total dissolved solids (TDS) of less than 1,000 mg/L.

A structural high mapped on top of the Wilcox Group trends approximately southeast to northwest through Gregg and Upshur Counties (figs. 9 and 14). The Wilcox dips gradually away from the high toward the northeast and south. This is probably the principal reason that the Wilcox-Carrizo drains northeastward (toward the North Louisiana Basin) in the northern part of the basin and southward in the southern part of the basin (figs. 13 and 14). The ground-water divide, however, is located in southern Smith County, about 30 mi (55 km) southwest of the structural divide. The structural and ground-water divides may have coincided at one time, and the ground-water divide may have later shifted southward owing to extensive drawdowns caused by the high rates of pumpage in Gregg and Smith Counties. On the other hand, the ground-water divide may have always been located where it is today because of the topographic influence imposed by the overlying Neches/Sabine watershed divide (fig. 14). The regional topography tilts toward the northeast from the Sabine watershed (fig. 3); this may be related to the structural tilting and may be another cause of the northeastward component of ground-water flow.

Faults of the Elkhart Graben-Mount Enterprise system apparently are partial (low permeability) barriers to horizontal ground-water flow. In general, flow perpendicular to a fault that is a partial barrier will result in greatly steepened hydraulic gradients across the fault. This appears to be the case along the eastern half of the fault zone, where contours in Cherokee and Rusk Counties are relatively uneven and more closely spaced. However, these features may be more the result of the complex arrangement of outcrop-recharge areas created in this region by faults than the result of faults acting as barriers (fig. 13). In Anderson County, the head contours seem to indicate no effects from faulting; however, here the map (fig. 13) is misleading because the contours fall north and south of the fault zone, thereby missing details of flow within the fault zone. Water-level data lying between the 200- and 250-ft (61- and 76-m) contours in southern Anderson County indicate an approximate fourfold increase in the hydraulic gradient from about 1 ft/mi (0.2 m/km) north of the fault zone to about 4.2 ft/mi (0.7 m/km) south of the fault zone, implying that the faults are partial barriers.

Uplift of strata by growth of Keechi and Concord salt domes has already been mentioned as affecting the recharge mound in central Anderson County. The only other domes that have noticeably perturbed the potentiometric surface map are Palestine (Anderson County), Oakwood (Leon and Freestone Counties), and Van (Van Zandt County). Structural uplifts of the Wilcox-Carrizo aquifer system over Palestine Dome and the Carrizo aquifer over Oakwood Dome are recharge areas, as evidenced by the 300-ft (90-m) closed potentiometric contours at these domes (fig. 13). Van Dome is a very large and deep-seated structure that has uplifted the base of the Wilcox as much as 600 ft (180 m) over an area approximately 15 mi (24 km) in diameter (fig. 9 of White, 1973). The uplift, plus subsequent erosion, has shifted the eastern boundary of the Wilcox-Carrizo outcrop about 5 mi (8 km) farther to the southeast, resulting in a prominent bulge in the outcrop belt over Van Dome (figs. 4, 13, and 14). In addition, the Van uplift appears to have elevated land surface to the extent that the Neches/Sabine watershed divide directly overlies the dome. Structure and topography have enlarged the outcrop area, have elevated heads, and have extended the large potentiometric (recharge) mound centered in Van Zandt County to the east (fig. 13).

Sand distribution in the Wilcox Group was discussed earlier as an important control on transmissivity. Since ground water tends to flow into the zones of highest transmissivity, the head map theoretically should reflect flow into the Wilcox sand bodies (figs. 6 and 7). However, few correlations can be made between the flow patterns and locations of the sand bodies. In fact, in the northern subbasin (that is, north of the structural divide), flow is completely contrary to sand distribution; flow is oriented normal to the sand belts and in the direction of decreasing sand thickness.

Apparently, two areas in the artesian section of the aquifer are affected by sand distribution. One is in northwestern Cherokee County, where flow lines (fig. 13) converge in the area where the 250-ft (75-m) contour is deflected northward. In this same area lies a sand body oriented north to south, just east of the Neches River (fig. 7). It is unclear whether the sand body causes the observed flow patterns, because the sand body does not line up exactly with the converging flow lines (perhaps because of sparse hydraulic head data in the area) and because the same flow pattern may also be induced by drawdowns resulting from pumpage in nearby Jacksonville (Guyton and Associates, 1972).

The second area in the artesian section is centered in Gregg County; here, flow lines converge from several directions, and two high-sand-percent systems have been identified (fig. 7). Unlike the closely spaced high-sand-percent systems in the southern half of the basin, those in Gregg County are relatively isolated east to west by broad muddy parts of the aquifer. Thus, the elongate sand systems in Gregg County should provide a relatively large-scale permeability contrast, which might be the cause of the large-scale convergence of flow there. Again, however, effects of permeability may be overshadowed by effects of pumpage; drawdowns of several tens of feet in Gregg County (Broom, 1969) were enough to cause the observed depression in heads. Note that this head depression (marked by the 250-ft [76-m] contour in fig. 13) is elongate parallel to the sand systems, suggesting that the regional cone of depression is spreading anisotropically along the axes of the sand systems.

Effects of aquifer heterogeneities on heads appear greatest in the western Wilcox outcrop belt in Freestone County. Just southwest of Fairfield is a northeast-trending elongate depression (or trough) in the hydraulic head surface; contours are elongate to the southwest (fig. 13). This is not a topographic effect but appears to be the result of flow into the Simsboro Sand, which crops out parallel to and just north of the trough (Barnes, 1970). The Simsboro Formation is an interval of massive sands in the Wilcox Group. On the basis of well depths in the trough and Wilcox dip of approximately 0.5° to 1° (about 46 to 92 ft/mi [9 to 17 m/km]), we conclude most of these wells tap the Simsboro. Although Teague and Fairfield are both located in the trough and pump Wilcox water for municipal use, the observed drawdowns have been generally less than 50 ft (15 m), which is insufficient to cause the roughly 100-ft (30-m) drop in head across the trough. Thus, the Simsboro seems to exert important control on flow. Again, pumpage may exaggerate this effect by lowering heads along the sand trend.

Effects of pumpage on Wilcox-Carrizo heads are particularly obvious near the Angelina River in Nacogdoches and Angelina Counties. Here, hydraulic heads have been lowered below sea level, as indicated by the negative contour elevations in the southeastern corner of the head map (fig. 13).

In summary, the most important geologic control on regional flow appears to be geologic structure, such as Sabine Uplift, structural divides, dome uplifts, and faults. That sand systems appear to exert less influence may be an artifact of the regional scale of our investigation. Smaller scale investigations with more detailed data bases would undoubtedly reveal more and clearer examples of sand bodies controlling flow. However, because the sand bodies are commonly pumped by water wells, one must take care not to confuse potentiometric lows resulting from pumpage with those resulting from natural flow into the sand bodies.

Vertical leakage across the Reklaw aquitard

The correlation between topography and the potentiometric surface in the artesian sections of the Wilcox-Carrizo aquifer system suggests that vertical leakage occurs through the Reklaw aquitard. To investigate this apparent leakage in greater detail, three methods of mapping were applied: (1) vertical head differentials between the Queen City and Wilcox-Carrizo, (2) vertical differential between elevations of stream beds of major streams and head in the Wilcox-Carrizo, and (3) distributions of flowing wells that tap the Wilcox-Carrizo. These methods provide a means of verifying whether vertical leakage can account for the observed correlation between topography and potentials and, in turn, a means of defining recharge and discharge in the artesian section. The inferred components of leakage are summarized in the regional cross sections (figs. 5a, b, and c), where vertical-flow components are sketched.

To interpret the vertical head differentials, a conceptual model is helpful. Figure 15 shows how recharge and discharge might occur in an artesian aquifer because of topographically controlled leakage across the confining bed. The direction of leakage is controlled by the relative elevations of the water table in the unconfined aquifer and potentiometric surface of the artesian aquifer. Downward leakage occurs where the water table lies above the artesian heads and upward where the reverse occurs. As illustrated in figure 15, downward leakage occurs beneath the higher land-surface elevations caused by the higher water-table elevation. As the topographically controlled water table slopes toward the stream, the rate of downward leakage decreases because of a decrease in the head differential. Where the water table drops below the artesian head surface, the leakage turns upward. Vertical leakage can also be described mathematically with Darcy's equation for vertical flow:

$$\underline{q} = K_v \frac{h_{wt} - h_a}{b} = K_v \nabla h$$

where $\underline{q}$ = the flux vector,
K_v = vertical hydraulic conductivity of the aquitard,
h_{wt} = head in the water-table aquifer,
h_a = head in the artesian aquifer,
b = aquitard thickness, and
∇h = vertical hydraulic gradient across the aquitard.

If the artesian section of the Wilcox-Carrizo system is recharging and discharging by means of

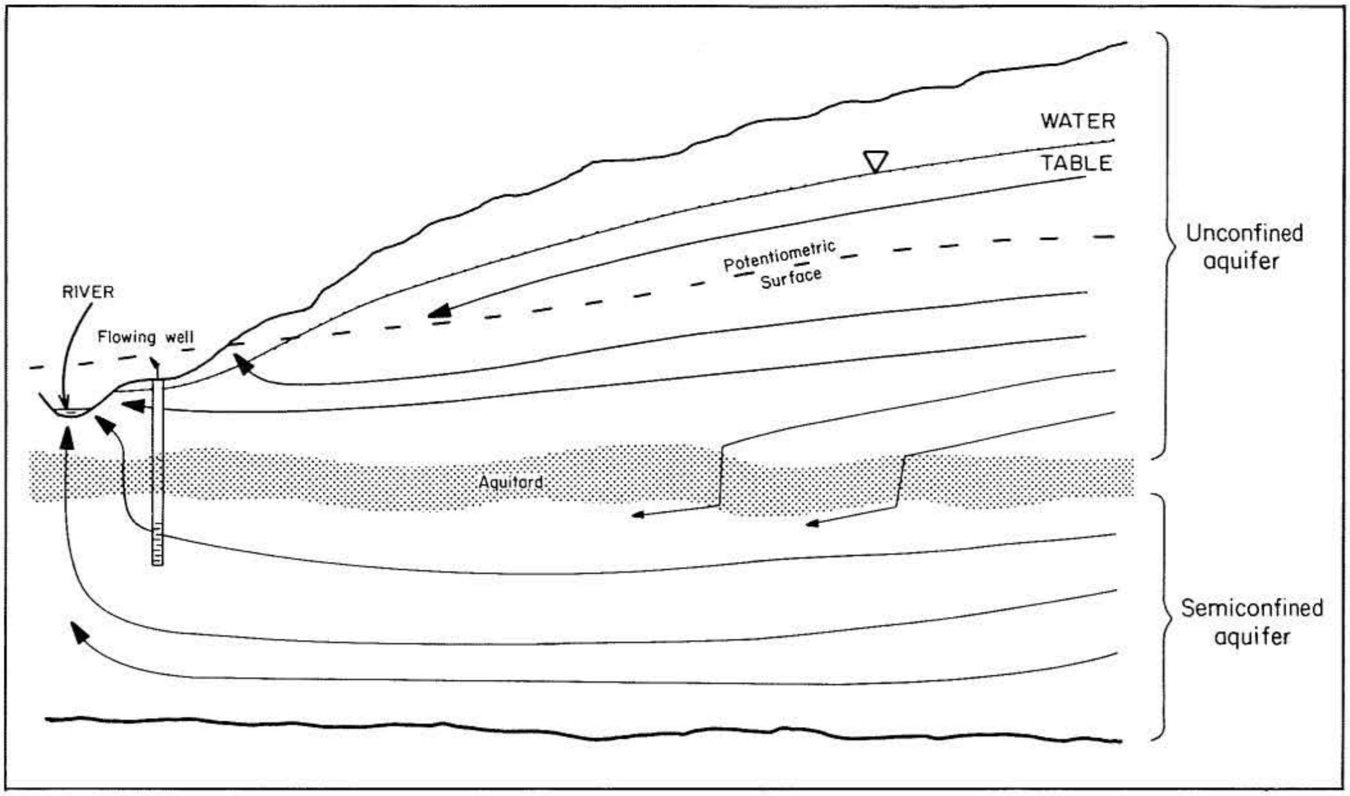

Figure 15. Sketch showing topographically controlled leakage across an aquitard. Topography influences the relative positions of the water table and the potentiometric surface of the semiconfined aquifer, thereby influencing both direction and rate of leakage.

topographically controlled leakage, head differentials between the Queen City and Wilcox-Carrizo aquifers will follow a pattern similar to that in the conceptual model. Figure 16 is a map of head differentials measured between the two aquifers. The map was constructed by (1) subtracting the underlying Wilcox-Carrizo head values (obtained from fig. 13 by linear interpolation) from Queen City head values (measured at each Queen City well location) and by (2) block-averaging these values. On the basis of inspection of head differentials at each data point, the block averages do not detract significantly from the accuracy of the data. Interestingly, the map illustrates positive head differentials, indicating downward leakage, over most of the basin. Negative values occur in only three blocks on the map: -15 ft (-4.5 m) along Upper Keechi Creek, -1 ft (-0.3 m) near the Trinity River, and -35 ft (-10.7 m) at the southwest corner. The general absence of negative head differentials is in part an artifact of the data. Along the major streams, where the probability of upward leakage (and hence negative head differentials) is greatest, Queen City head data are sparse because the aquifer is commonly very thin or missing owing to downcutting of the streams.

To obtain greater detail about vertical flow beneath the streams, plots showing elevation of Wilcox-Carrizo heads relative to stream beds of the Trinity, Neches, and Sabine Rivers were made (fig. 17). The head data were selected from an area extending 2 mi (3.2 km) on either side of the streams in both the confined and the unconfined sections of the Wilcox-Carrizo. The plots show that beneath the Trinity and Sabine Rivers in the artesian section of the aquifer, head differentials are indeed negative because Wilcox-Carrizo heads are generally above the elevation of the stream beds.

Additionally, head differentials (listed in fig. 16) tend to increase from the rivers to the watershed divide. The best example is in the Trinity watershed in Anderson County, where differentials range from -1 to 135 ft (-0.3 to 41 m) near the river and from 105 to 175 ft (32 to 53 m) along the Trinity/Neches divide. A similar trend can be found in the Sabine watershed, where the range increases from 20 to 90 ft (6 to 27 m) near the river to 35 to 145 ft (11 to 44 m) near the divides. Only sketchy trends appear in the Neches watershed, except perhaps in Henderson and Smith Counties, where values along the river range from 55 to 85 ft (17 to 26 m) and values along the divides range from 35 to 230 ft (11 to 70 m). Only for the Neches River are artesian head values in the Wilcox-Carrizo system below the stream bed, indicating no potential for upward leakage (fig. 17).

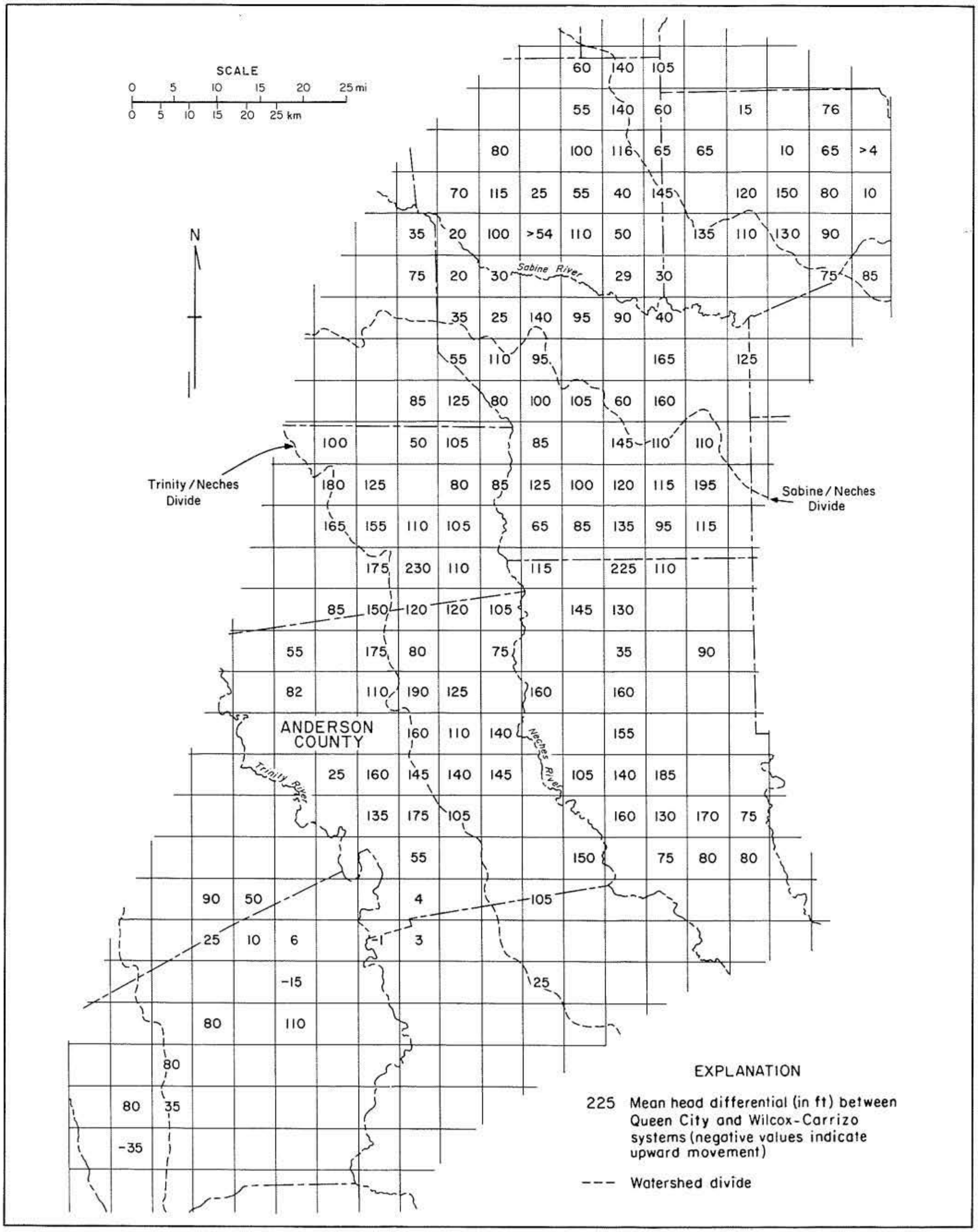

Figure 16. Vertical head differentials measured between Queen City and Wilcox-Carrizo aquifers. Widespread positive values indicate downward leakage from the Queen City to the Wilcox-Carrizo everywhere except along major stream valleys, where data are insufficient. In many areas, hydraulic head differentials increase toward watershed divides because of topographic effects.

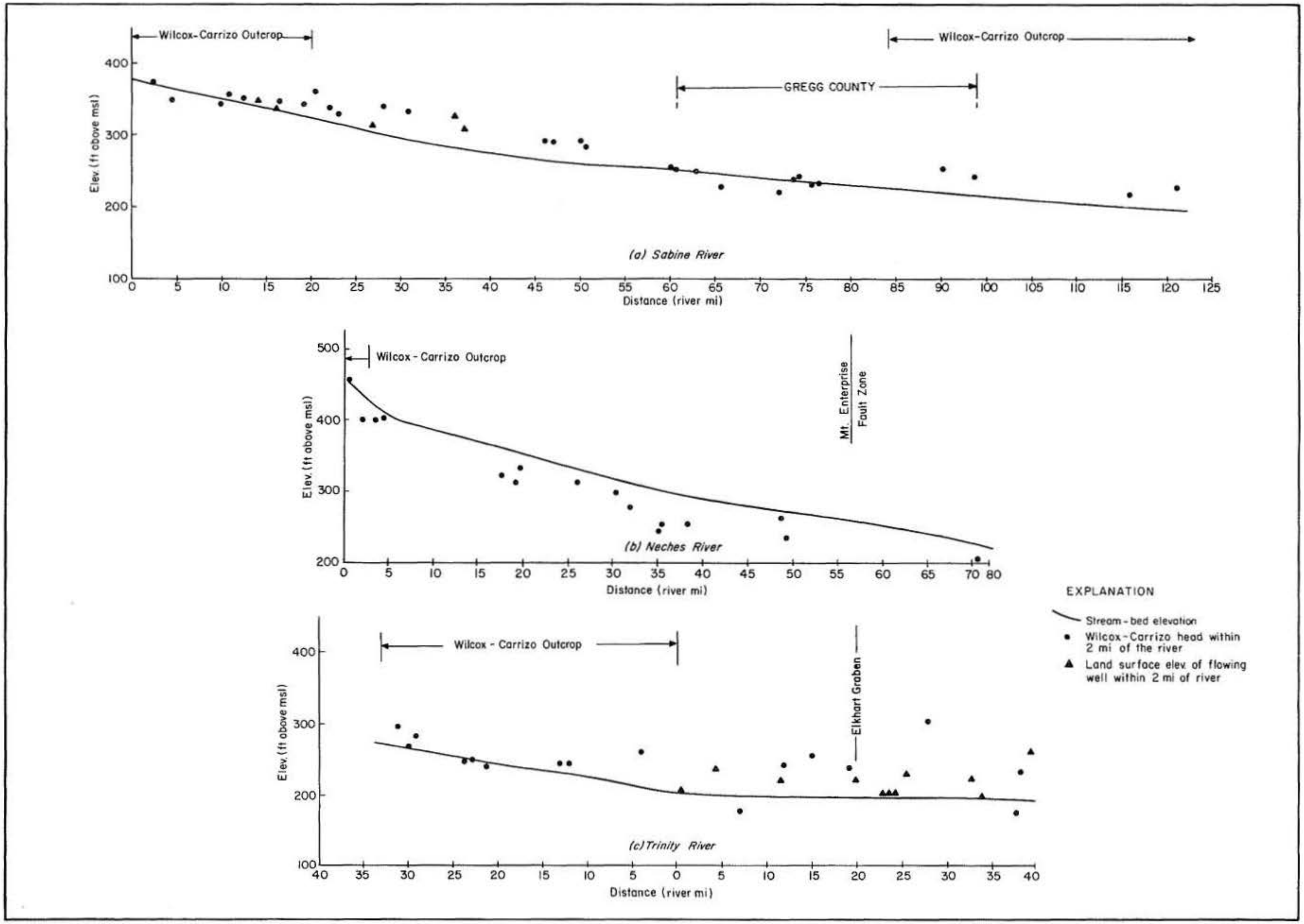

Figure 17. Profiles showing elevations of Wilcox-Carrizo water levels above major stream beds: (a) Sabine River, (b) Neches River, and (c) Trinity River. Water levels are from wells located within 2 mi (3.2 km) of the rivers. Any reaches where water levels are above the stream beds are potential discharge sites.

In other words, base flow of the Neches River does not include any contributions from the Wilcox-Carrizo.

Thus, the head differential data fit the conceptual model of topographically controlled leakage in the Trinity and Sabine basins but not in the Neches basin. This is not surprising because the correlation between topography and the potentiometric surface appeared strongest in the Trinity and Sabine basins (figs. 13 and 14), where flow lines converge toward the streams in the artesian section. The Neches River appears to have little or no effect on flow lines of the Wilcox-Carrizo.

Since the Neches is a river of considerable size, one might expect it to induce upward leakage from the Wilcox-Carrizo system just as the Trinity and Sabine do. The controls here are probably related to the comparatively lower flow rates in the Neches (table 1) and its location relative to the major recharge areas. Lower flow rates may have prevented the Neches River from incising deeply enough to intersect the potentiometric surface of the Wilcox-Carrizo. The location of the Neches about midway between the outcrop belts may place it far enough from the major recharge areas so that by the time ground water reaches the river, hydraulic heads have declined to depths well below the stream-bed elevation.

Elevations of head along the Sabine River (fig. 17a) strongly suggest that the leakage in Gregg County has been reversed from upward to downward as a result of pumpage. Heads in the county are just below the stream bed, and given drawdowns of several tens of feet in the area, it appears that heads were probably once above the stream bed. The relatively rapid rates of drawdown in Gregg County can be in part attributed to lower values of transmissivity in that area (fig. 10; table 3).

Where heads lie above land surface, one should also find flowing wells. Accordingly, the distribution of flowing Wilcox-Carrizo wells plotted in figure 14 shows that most of the wells are located in the artesian section near the Trinity and Sabine Rivers and some of their respective tributaries: Upper Keechi, Catfish, and Lake Fork Creeks. No flowing wells are found near the Neches and Angelina Rivers. A substantial number of flowing wells are located in the western Wilcox-Carrizo outcrop belt (fig. 14). These do not necessarily indicate confined conditions, because flowing wells can occur in discharge areas, where deepest heads are commonly above land surface. A comparison of locations of flowing wells in the outcrop belt with U.S. Geological Survey topographic maps shows that each flowing well lies near the bottom of a local stream valley.

Vertical flow in the Wilcox-Carrizo system

Head differential maps help define vertical flow between the Queen City and the Wilcox-Carrizo aquifers, but they demonstrate nothing about vertical flow within the Wilcox-Carrizo itself. In areas where leakage occurs, there may be corresponding downward- or upward-flow components in the Wilcox-Carrizo. Knowledge of such components and the depths to which they extend in the system is particularly important to the understanding of the potential for upward migration of contaminants from the lower part of the system to the water wells, which generally tap the upper part, or to surface-water systems. One way of detecting vertical-flow components is by analyzing pressure-versus-depth (P-D) relationships, which can be used to determine if fluid movement is directed upward, downward, or horizontally. Basic axioms of P-D analysis are outlined in appendix B.

Most P-D analyses have been conducted in deep petroliferous aquifers where pressures, rather than hydraulic heads or water levels, are measured directly from drill-stem-test data (for example, Tóth, 1978). No such pressure measurements have been made in the Wilcox-Carrizo aquifer, and therefore pressures had to be computed indirectly from the head data, as shown schematically in figure 18. Since water-density variations caused by differences in TDS and temperature are negligible in the Wilcox-Carrizo system, there was no need to correct the data for fluid-density variations. Thus, pressures are presented in units of feet of fresh water. For analysis, depth values (D) were defined as the midpoint of the screened interval or, if such information was unavailable, total depth of the well. The midpoint of the screened interval was used because head may vary vertically within the screened interval, and the level to which water rises in the well bore is generally a function of the average head in the aquifer within this interval. This method has one disadvantage: Water levels in wells that screen more than one sand unit may primarily reflect heads in only the most transmissive sands, and the midpoint of the total screened interval or depth of the well may therefore not be an accurate estimate of D. To help minimize this source of error, wells having several screens over thick intervals (for example, intervals thicker than about 300 ft [90 m]) were eliminated. Several more points had to be eliminated because of lack of data about D.

Another potential source of error in P-D data stems from ground-water pumpage, which may lower water levels and result in abnormally low pressure estimates. Since only a small percentage of the hydraulic head data is significantly affected by

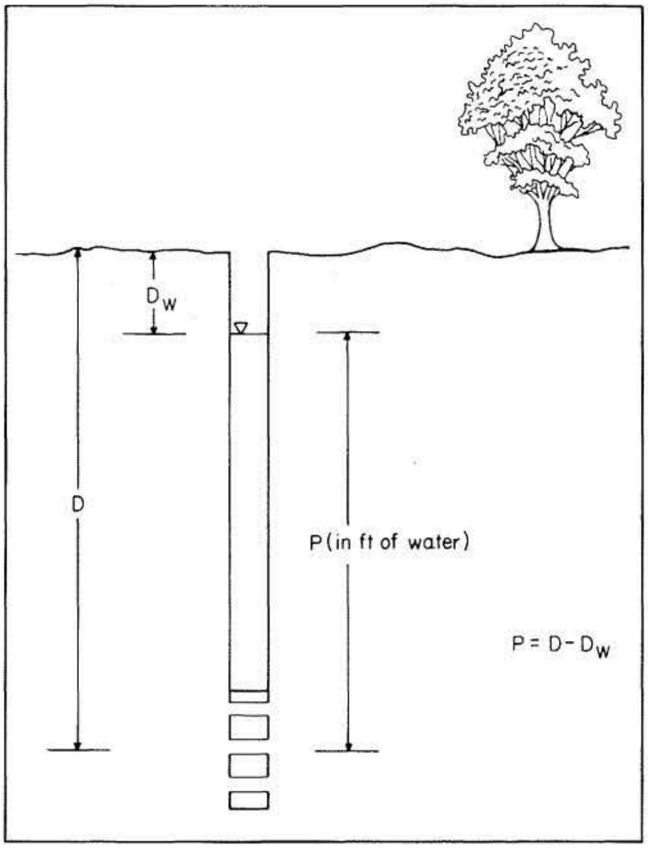

Figure 18. Method of computing pressure head from conventional water-well data.

pumpage, pressures computed from these data generally represent natural conditions. Errors stemming from pumpage are considered in the discussion that follows.

Pressure-versus-depth data were compiled for most of the counties in the basin: Anderson, Cherokee, Freestone, Gregg, Henderson, Houston, Leon, Nacogdoches, Rusk, Smith, Van Zandt, and Wood. (Data were excluded from counties that were data poor or were located far away from the region containing the salt domes.) Pressure-versus-depth plots were then constructed and linear regression statistics calculated for (1) all the data (fig. 19), (2) data from 50-ft (15.2-m) intervals of land-surface elevation within each county for confined and unconfined sections of the system (table 4), and (3) data within 2 mi (3.7 km) of the Trinity, Neches, and Sabine Rivers (figs. 17 and 20; table 5).

The plot of all the data (fig. 19) was constructed to detect any errors or large-scale trends that exist. The data were segregated geographically into smaller groups to approximate true P-D gradients at various localities. Ideally, the P-D measurements for each plot should be made in small areas because lateral variations occur in the depth of the potentiometric surface or water table and in the depth of the aquifer and also because permeability variations can create noise in the data. Data segregation by confined or unconfined aquifers, by county, and by land-surface elevation was chosen primarily for convenience and to facilitate comparison of data from areas where the vertical-flow component might be expected to be different. From this method, trends became evident. For example, since the unconfined sections (outcrop areas) are the principal recharge areas, they should contain the greatest downward-flow components. Similarly, if topography exerts appreciable influence on flow in the system, the downward-flow components should increase toward higher elevations. As will be shown, these trends are indeed evident in the data.

The linear regression statistics shown in figures 19 and 20 and tables 4 and 5 were computed by the least-squares method with the statistical computer package SPSS (Nie and others, 1975). The statistics include slope (m) of the regression line and the 95-percent confidence interval for m (for example, $0.96 \pm .02$), coefficient (r) of correlation, number (n) of data points, and, in the tables, the range of depths (D-range) represented in each data group. The 95-percent confidence intervals of m were calculated using the standard error of m computed by SPSS and assuming a Student's t distribution (Nie and others, 1975). In several instances, the regression analysis yielded a slope that was statistically not significant at a 95-percent confidence level (Nie and others, 1975). These cases are indicated by "n.s." for "not significant" in table 4. In each case, lack of significance can be traced to excessive drawdowns resulting from pumpage.

One will find that many of the values of m have 95-percent confidence intervals, which range from ≤ 1.00 to ≥ 1.00. These values are indicated by asterisks in tables 4 and 5. This highlights a major limitation of the P-D analysis: The method often is insufficiently sensitive to reliably indicate the direction of the vertical-flow component. Reasons for this lack of sensitivity are (1) that significant vertical-flow components can register values of m that differ only slightly from a value of 1 and (2) that small errors in the data may obliterate this difference. Nevertheless, the analysis of data shows several important trends that appear consistent with the physical system and would be worth considering in more detailed investigations.

The plot of all the P-D data (fig. 19) yields an excellent correlation of 0.97 and a slope (m) of $0.84 \pm .01$. The increased scatter of the data between approximate depths of 300 and 900 ft (91 and 274 m) is caused by excessive drawdowns resulting from pumpage. Because of the large

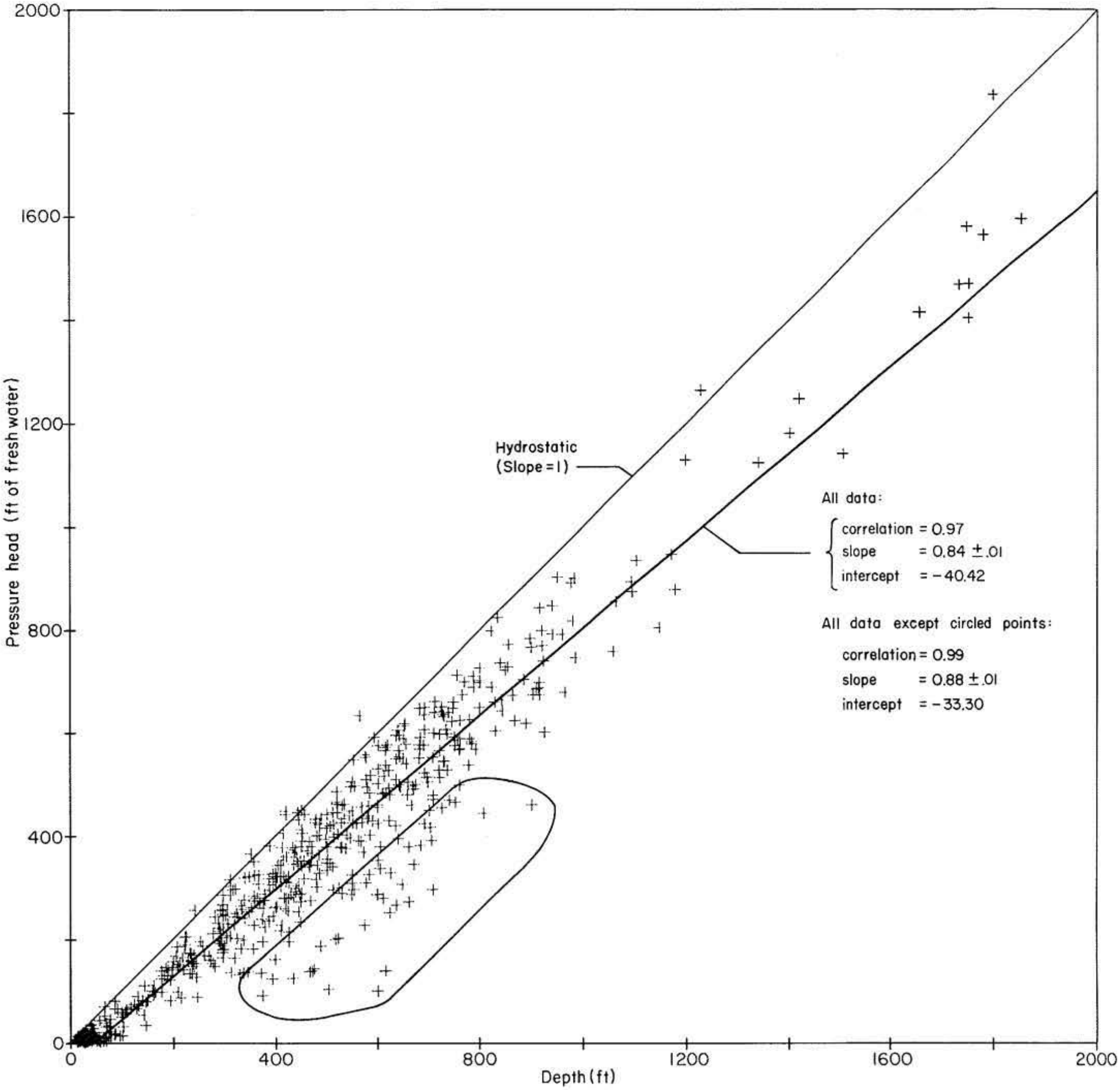

Figure 19. Pressure-versus-depth (P-D) plot of all data from the Wilcox-Carrizo system. The vertical component of flow is upward when *m* (slope) > 1 and downward when *m* < 1. One can infer from the plot that the component of vertical flow is generally downward. Data representing excessive drawdowns owing to pumpage are circled; they do not significantly affect the results.

number of data points in the plot, however, this scatter does not affect the significance of *m*; when the data that cause the scatter are removed from the regression analysis, *m* does not change significantly (fig. 19).

The *m* value of 0.84 suggests that the vertical component of flow is generally downward in the Wilcox-Carrizo system. Such a downward component could be attributed (1) to the widespread occurrence of recharge and downward leakage from the Queen City or (2) to the fact that flow is generally directed down the structural dip. The other P-D plots (fig. 20; table 4) support the first explanation because nearly all these plots yield *m* values that are <1.00 and that correlate quite well with topography and presence or absence of confining conditions. This correlation is illustrated graphically in figure 21, where the mean values of *m* for the confined and

Table 4. Linear regression statistics for the Wilcox-Carrizo pressure-versus-depth (P-D) data from confined

						Confined section						
Land surface, ft (m)	200-250 (61-76)			250-300 (76-91)			300-350 (91-107)			350-400 (107-122)		
	m (D-range)	r	n	**m** (D-range)	r	n	**m** (D-range)	r	n	**m** (D-range)	r	n
Anderson	n.d.	—	—	**1.07±.17*** **(215-835)**	0.97	9	**1.07±.14*** **(260-614)**	0.99	7	0.88±.04 (136-1,345)	0.99	16
Cherokee	n.d.	—	—	n.d.	—	—	0.86±.15* (112-915)	0.96	10	0.77±.11 (153-465)	0.99	5
Freestone	n.d.	—	—	n.d.	—	—	0.95±.33* (295-856)	0.97	4	0.94±.10* (480-800)	0.99	4
Gregg	n.d.	—	—	0.99±.03* (135-950)	0.99	4	1.00±.15* (300-800)	0.99	6	**1.03±.09*** **(342-915)**	0.99	11
Henderson	n.d.	—	—	n.d.	—	—	n.d.	—	—	1.00±.08* (521-1,200)	0.99	11
Houston	n.d.	—	—	**1.05±.02** **(360-1,800)**	0.99	3	n.d.	—	—	n.d.	—	—
Leon	n.d.	—	—	n.s.	—	—	n.s.	—	—	0.91±.34* (614-724)	0.85	11
Nacogdoches	0.73±.48* (400-901)	0.79	7	0.87±.45* (426-831)	0.85	7	n.s.	—	—	n.s.	—	—
Smith	n.d.	—	—	n.d.	—	—	0.86±0 (443-755)	1.00	3	**1.07±.06** **(328-983)**	0.99	12
Van Zandt	n.d.	—	—	n.d.	—	—	n.d.	—	—	n.d.	—	—
Wood	n.d.	—	—	n.d.	—	—	n.d.	—	—	n.d.	—	—
***MEAN* m**	*0.73?*	—	—	*1.03*	—	—	*0.95*	—	—	*0.94*	—	—
						Unconfined section (outcrop)						
Anderson	n.d.	—	—	0.96±.02 (228-520)	0.99	3	0.98±.05* (58-531)	0.99	7	n.d.	—	—
Cherokee	n.d.	—	—	n.d.	—	—	0.77±.12 (23-211)	0.99	4	0.75±.05 (37-295)	0.99	4
Freestone	n.d.	—	—	n.d.	—	—	0.95±.13* (17-306)	0.98	8	0.79±.09 (28-330)	0.97	16
Henderson	n.d.	—	—	0.96±.04* (25-325)	0.99	6	0.82±.14 (21-400)	0.98	4	0.79±.08 (16-455)	0.96	23
Rusk	n.d.	—	—	n.d.	—	—	n.d.	—	—	0.81±.16 (31-315)	0.97	8
Van Zandt	n.d.	—	—	n.d.	—	—	n.d.	—	—	n.d.	—	—
Wood	n.d.	—	—	n.d.	—	—	n.d.	—	—	n.d.	—	—
***MEAN* m**	—	—	—	*0.96*	—	—	*0.90*	—	—	*0.79*	—	—

m - slope
D-range - depth (ft) range of data
r - correlation coefficient
n - number of data points

n.d. - no data
n.s. - not significant
*Indicates the 95-percent confidence interval ranges from ≤ 1.00 to ≥ 1.00.
Boldface indicates **m** > 1.00.

and unconfined sections and 50-ft (15.2-m) intervals of land-surface elevation within each county.

400-450 (122-137)			450-500 (137-152)			500-550 (152-168)			550-600 (168-183)			600-650 (183-198)		
m (D-range)	r	n	**m** (D-range)	r	n	**m** (D-range)	r	n	**m** (D-range)	r	n	**m** (D-range)	r	n
Confined section														
0.96±.05* (420–1,745)	0.99	17	0.98±.05* (462–2,120)	0.99	10	0.94±.03 (600–1,855)	0.99	7	n.d.	—	—	n.d.	—	—
0.93±.08* (235–1,095)	0.99	14	0.78±.14 (150–720)	0.97	8	**1.07±.22* (376–1,097)**	0.99	5	n.s.	—	—	n.s.	—	—
n.d.	—	—	n.d.	—	—	n.d.	—	—	n.d.	—	—	n.d.	—	—
n.d.	—	—	n.d.	—	—	n.d.	—	—	n.d.	—	—	n.d.	—	—
0.76±.09 (368–1,180)	0.95	21	0.82±.05 (21–885)	0.99	17	0.76±.07 (239–1,150)	0.98	13	n.d.	—	—	n.d.	—	—
n.d.	—	—	0.89±.47* (735–903)	0.91	5	n.d.	—	—	n.d.	—	—	n.d.	—	—
0.96±.12* (337–840)	0.99	6	n.s.	—	—	n.d.	—	—	n.d.	—	—	n.d.	—	—
n.s.	—	—	n.d.	—	—	n.d.	—	—	n.d.	—	—	n.d.	—	—
0.86±.07 (75–745)	0.98	18	0.87±.08 (70–980)	0.99	10	**1.02±.19* (728–915)**	0.96	9	0.71±.30* (415–985)	0.94	5	**1.47±.31 (809–965)**	0.99	3
n.d.	—	—	n.s.	—	—	0.32±.07 (315–690)	0.99	3	n.d.	—	—	n.d.	—	—
0.84±.23* (238–690)	0.92	10	0.94±.06* (242–920)	0.99	7	n.d.	—	—	n.d.	—	—	n.d.	—	—
0.89	—	—	*0.88*	—	—	*0.82*	—	—	*0.71?*	—	—	*1.47?*	—	—
Unconfined section (outcrop)														
n.d.	—	—	n.d.	—	—	n.d.	—	—	n.d.	—	—	n.d.	—	—
0.75±.07 (14–501)	0.99	9	n.d.	—	—	n.d.	—	—	n.d.	—	—	n.d.	—	—
0.85±.04 (23–525)	0.99	26	0.80±.04 (16–668)	0.99	42	0.86±.06 (20–822)	0.99	20	n.d.	—	—	n.d.	—	—
0.87±.05 (21–500)	0.99	19	0.80±.07 (31–185)	0.99	5	0.85±.40 (12–70)	0.93	5	n.d.	—	—	n.d.	—	—
0.77±.09 (36–750)	0.98	13	0.48±.08 (48–599)	0.98	6	0.75±.13 (82–480)	0.99	3	n.s.	—	—	n.d.	—	—
0.93±.06 (13–471)	0.99	17	0.88±.04 (12–522)	0.98	37	0.79±.03 (15–680)	0.99	24	0.79±.03 (18–416)	0.99	10	n.d.	—	—
0.84±.13 (11–599)	0.98	8	0.88±.09 (97–540)	0.98	11	n.d.	—	—	n.d.	—	—	n.d.	—	—
0.84	—	—	*0.77*	—	—	*0.81*	—	—	*0.79*	—	—	—	—	—

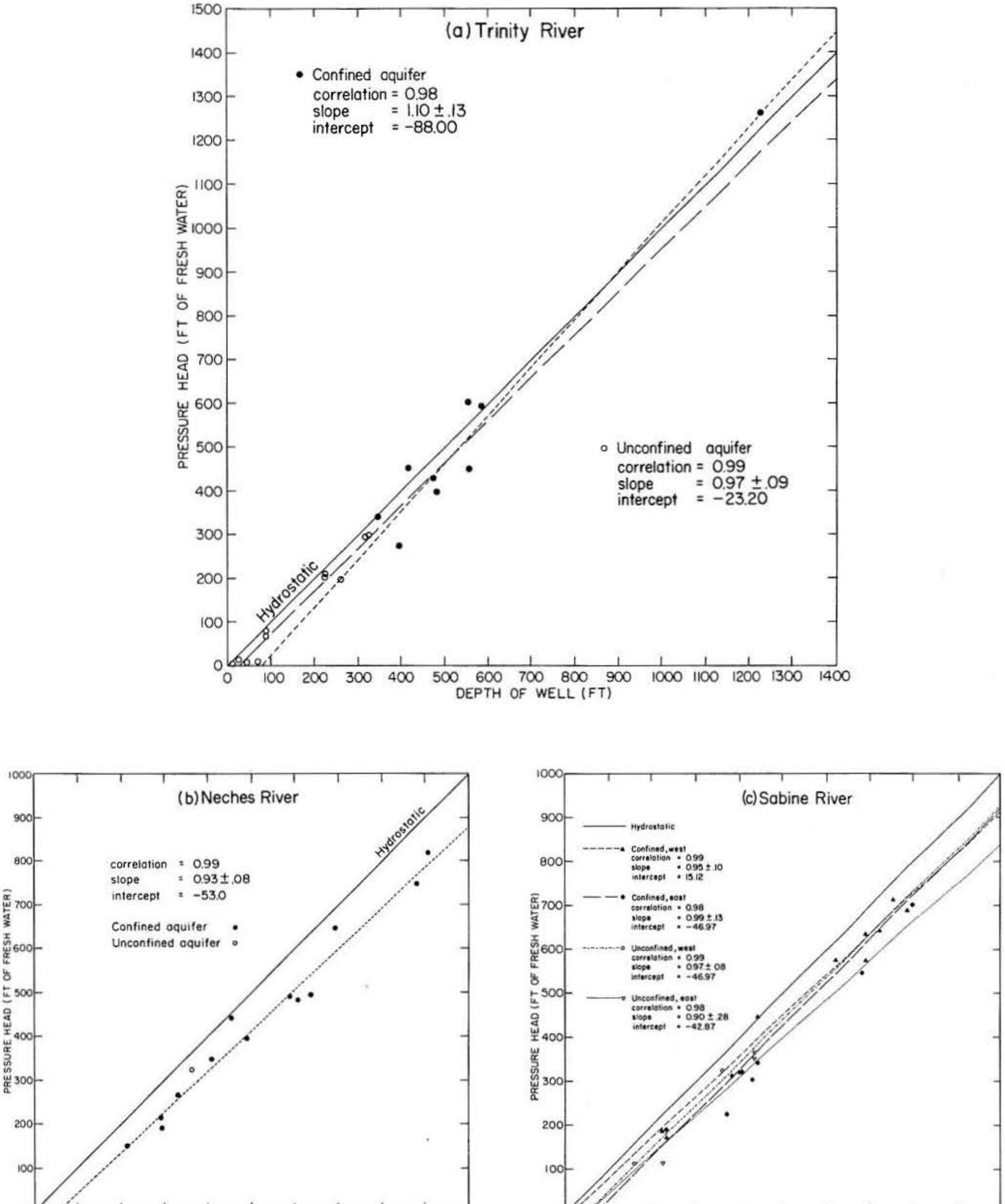

Figure 20. Graphs of pressure versus depth (P-D) for areas within 2 mi (3.2 km) of (a) Trinity River, (b) Neches River, and (c) Sabine River. Slope (*m*) of the P-D line indicates whether vertical component of flow is upward ($m > 1$) or downward ($m < 1$). Only data along the Trinity River indicate an upward component of flow.

unconfined (outcrop) sections (table 4) are plotted against land-surface elevation. The mean values of m show a remarkably consistent decrease from low to high elevation, as would be expected if there were increasing rates of recharge and downward leakage in the same direction. The graph of confined data (fig. 21) correlates well with topography only if the two questionable points situated at either end of the graph are disregarded. These points are questionable because each is based on only one m value, which has an unusually wide 95-percent confidence interval. Again, pumpage is the cause of the wide confidence intervals.

Values of m for the unconfined section are generally below those in the confined section (fig. 21; table 4). This is attributed to the presence of a water table and to the relatively high recharge rates in the unconfined section of the Wilcox-Carrizo aquifer system.

Only 8 of the 36 plots for the confined section yield $m > 1.00$ (table 4). These plots are scattered over nearly the entire range of elevations. Half of them occur in topographically low areas where upward leakage across the Reklaw aquitard is documented or suspected (table 4). These plots occur in Anderson County (250 to 300 ft [76 to 91 m] and 300 to 350 ft [91 to 107 m]), Houston County (250 to 300 ft [76 to 91 m]), and Gregg County (350 to 400 ft [107 to 122 m]). These parts of Anderson and Houston Counties lie along the Trinity River, where we earlier proved that there is a certain amount of upward leakage or discharge from the Wilcox-Carrizo system. Gregg County was discussed earlier as perhaps being an area of natural discharge in the past and an area of relatively large drawdowns owing to pumpage during the recent past. These drawdowns may invalidate the Gregg County data, but it is worth noting that all the values of m in table 4 from Gregg County are between 0.99 and 1.03 and are higher than average.

The remaining plots where $m > 1.00$ (table 4) occur in Smith County (350 to 400 ft [107 to 122 m], 500 to 550 ft [152 to 168 m], and 600 to 650 ft [183 to 198 m]) and Cherokee County (500 to 550 ft [157 to 168 m]). The three Smith County cases are of questionable validity because the other m values in the county are consistently low and have narrower confidence intervals. On the other hand, the variability of m in Smith County may reflect a complex system of both upward and downward fluid movement.

One might speculate that the high m values in Smith and Cherokee Counties are caused by the presence of an additional confining bed, the Weches aquitard. The Weches is present in most of Smith County and in the higher elevations of Cherokee County (figs. 2 and 4). The combined influence of

Table 5. Linear regression statistics for the Wilcox-Carrizo pressure-versus-depth (P-D) data from areas within 2 mi (3.7 km) of the major rivers.

Data group	Slope (m)	Depth range (ft)	Correlation (r)	No. of points
Trinity River				
confined	1.10±.13*	359.0-1,230.0	0.98	10
	1.30±.46*	359.0-593.0	0.90	9
unconfined	0.97±.09*	17.0-325.0	0.99	11
Neches River	0.93±.08*	212.0-940.0	0.99	15
Sabine River				
confined-west	0.95±.10*	225.0-788.0	0.99	9
confined-east	0.99±.13*	237.0-800.0	0.98	9
unconfined-west	0.97±.08*	52.0-400.0	0.99	7
unconfined-east	0.90±.28*	39.0-448.0	0.98	4

*Indicates the 95-percent confidence interval ranges from ≤1.00 to ≥1.00.

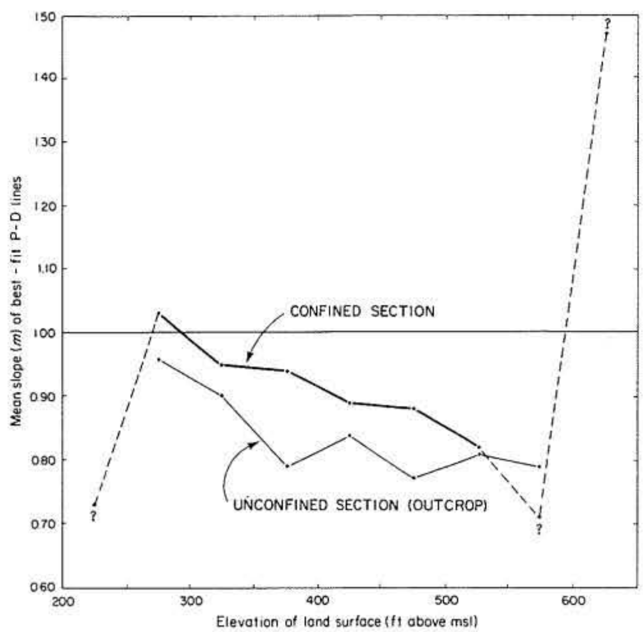

Figure 21. Graph of mean slope (m) of pressure-versus-depth (P-D) regression lines (table 4) versus land-surface elevation. Both the unconfined and confined data show a general trend of decreasing m with increasing elevation, reflecting greater recharge (and, hence, greater downward movement) at higher elevations. The points with question marks are tenuous because they are each based on sparse data having wide error bars (± .30 to ± .48).

the Weches and Reklaw aquitards may totally isolate the Wilcox-Carrizo from any topographic effect. This would, in turn, tend to lessen or reverse any downward-flow components that are present.

Finally, the P-D plots for the Trinity, Neches, and Sabine Rivers (figs. 20a, b, and c; table 5) corroborate the implications of the other P-D data and provide greater detail regarding these important areas. The highest value of m for these data ($m = 1.10 \pm .13$) is that of the Trinity where it traverses the confined section (fig. 20a). This indicates upward movement, but again the error bar of $\pm .13$ suggests an appreciable amount of uncertainty. Nonetheless, the interpretation of an upward-flow component appears reasonable because ground-water flow lines in figure 14 converge most strongly on the Trinity, and the potential for upward leakage is consistently present along this reach of the Trinity (fig. 17).

Since data from the Trinity River (fig. 20a) do not exist for depths below 1,200 ft (365 m), the upward-flow component apparently persists at least to this depth. However, these data include only one point below about 600 ft (180 m). Regression statistics computed without this point still indicate upward movement ($m = 1.30 \pm .46$) (table 5). Total thickness of the Wilcox-Carrizo in the area is approximately 1,300 to 3,000 ft (395 to 915 m).

Pressure-versus-depth data from along the Sabine River (fig. 20c) where it crosses the confined section were divided into a confined-west group (data from Smith and Wood Counties) and a confined-east group (data from Gregg and Upshur Counties) because of the effects of pumpage in the latter group. The slope for the confined-west group ($m = 0.95 \pm .10$) (fig. 20c; table 5) suggests that the upward leakage there does not induce upward flow within the Wilcox-Carrizo. The slope for the confined-east group ($m = 0.99 \pm .13$), like the m values for Gregg County (table 4), may imply a tendency for upward flow there, or the slope may be merely an artifact of pumpage.

Along the Trinity River, the greater upward-flow components could be attributed to locations of recharge areas. The major recharge area in the Sabine River basin is the western outcrop belt, which is oriented normal to the river (fig. 13). In contrast, the Trinity River basin contains two recharge areas that are located on either flank of the river: the western outcrop belt and central Anderson County (fig. 13). Recharge to either side of the Trinity River creates a convergence of opposing hydraulic gradients at the river, which may cause relatively high pressures at depth beneath the river and high rates of upward leakage. For the Sabine River, much lower rates of recharge to either side of the river allow ground water to flow essentially parallel to the river without causing excessive pressure buildup and high rates of upward leakage beneath the river.

The Neches River is known to be an area of downward leakage. Accordingly, the P-D plot yields $m = 0.93 \pm .08$.

Values of m where the Trinity and Sabine Rivers cross the Wilcox-Carrizo outcrops are less than 1.0 (table 5). Theoretically, these m values should be greater than 1.0, because these streams are known discharge areas in the outcrops (on the basis of the head data and axioms of unconfined ground-water flow). This discrepancy is not necessarily due to errors or to lack of data and could be attributed to a problem of data distribution. Ground-water modeling studies have shown that the zone of upward flow beneath streams is much narrower for unconfined systems than for confined systems (compare figures 6.2a and 6.4b of Freeze and Cherry, 1979). In fact, the zone of upward flow beneath the rivers in the unconfined section may be too narrow to be intersected by wells that are not located immediately adjacent to the stream bed. Conversely, the greater width of the discharge zone in a confined system would be easily intersected by wells spaced within 2 mi (3.2 km) of the river. The wells in the unconfined section near the Trinity and Sabine Rivers, therefore, may still be in a recharge zone or a transitional zone between recharge and discharge. Pressure heads measured directly beneath the stream beds should yield $m > 1.00$.

In summary, the P-D relationships have helped to confirm that the Trinity River is a potentially important ground-water discharge area. Furthermore, they suggest that topographic effects and vertical leakage may significantly affect vertical flow within the Wilcox-Carrizo system itself. One should bear in mind that the P-D data indicate only the direction of the vertical component of the hydraulic gradient. This component may be rendered insignificant by vertical hydraulic conductivities that are much lower than the horizontal hydraulic conductivities. Such anisotropy is highly probable in the Wilcox-Carrizo owing to its horizontally stratified lithology.

Rate of ground-water flow

Rates of ground-water flow ($K \times \nabla h$) can be inferred from the hydraulic gradients (∇h) measured on the potentiometric surface map (fig. 13) and values of hydraulic conductivity (K) estimated from pumping tests (table 3). Flow rates computed for Wilcox-Carrizo sand bodies generally range from 10^{-3} to 10^{0} ft/d (3.0×10^{-4} to 3.0×10^{-1} m/d) and can be quite variable owing to variations in both K and ∇h. Divide these numbers by a representative porosity (for example, 0.30) to obtain pore-water velocities. The value of 10^{0} ft/d is probably rare, except at shallow depths in outcrop areas having steep slopes. Flow rates can be estimated best by construction of detailed numerical ground-water flow models, which include effects of heterogeneous K distributions and appropriate boundary conditions.

SUMMARY—AQUIFER HYDRAULICS

Ground-water circulation in Eocene aquifers of the East Texas Basin is controlled primarily by topography and structure. In outcrop areas, flow patterns closely follow land-surface gradients as water moves away from topographically high recharge areas to topographically low discharge areas. Since the Queen City is topographically controlled over most of the basin, it does not form a regionally coherent flow system but, instead, a series of smaller flow cells of closely spaced recharge and discharge areas. In the confined Wilcox-Carrizo system, flow approximately follows the structural dip as ground water moves toward the Texas-Louisiana border in the northern half of the basin and toward the Gulf of Mexico in the southern half of the basin. The ground-water divide lies in southern Smith County, but originally may have been located farther north before ground-water pumpage caused lowering of water levels in Gregg, Upshur, and Smith Counties.

Topography affects flow in the confined Wilcox-Carrizo indirectly through leakage between the Queen City and Wilcox-Carrizo. The leakage is indicated by a subtle correlation between the Wilcox-Carrizo potentiometric surface and topography. Analyses of vertical head differentials and the distribution of flowing wells confirm the occurrence of leakage and show its direction. The leakage is predominantly downward, except beneath the Trinity and Sabine Rivers, which appear to be discharge areas for the confined section. In comparison, the Neches River is not a discharge area because it does not incise deeply enough into the stratigraphic column to intersect the Wilcox-Carrizo potentiometric surface.

Vertical leakage influences vertical flow within the Wilcox-Carrizo to a certain extent, as evidenced in P-D data. These data agree with the analysis of leakage, indicating that the vertical-flow component is downward nearly everywhere in the basin. The vertical-flow component is upward only along the Trinity River. The P-D data also indicate a general trend of increasing downward movement with increasing land-surface elevation in both the unconfined and confined sections, reflecting greater recharge (and leakage) in the higher elevations.

Aquifer heterogeneity appears to exert little influence on regional ground-water circulation. The only correlation between flow and heterogeneity is in the Wilcox-Carrizo outcrop in Freestone County, where flow lines veer toward the relatively transmissive Simsboro Sand Formation of the Wilcox Group. In the confined section, the sand-percent and net-sand-thickness maps of Kaiser and others (1978) delineate zones that should be relatively transmissive. Flow lines converge on these zones only in areas, such as Gregg and northern Cherokee Counties, that have undergone excessive drawdowns because of pumpage. The role of transmissivity variations in these areas is therefore unclear. Possible reasons for lack of correlation between flow and the sand-facies maps are (1) that mapped variations in sand thickness may not represent variations in transmissivity that are large enough to significantly affect regional flow, and (2) that the head data may be too sparse to show local changes in flow near transmissivity changes. Investigations conducted on a local scale with more data might find better correlation between flow and sand thicknesses in the Wilcox.

WATER CHEMISTRY

Ground-water chemistry is an effective tool for delineating general geochemical environments, spatial geochemical variations, and regional direction of ground-water movement. Direction of ground-water flow can be inferred in many aquifer systems if the mechanisms that modify water chemistry are known and if sufficient data along the flow path are available.

In a simple monomineralic rock, the water will become saturated with that mineral phase (assuming pressure and temperature remain constant). In a limestone aquifer, the calcium and bicarbonate concentration will rise to saturation with respect to calcite. Similarly, in a bed of salt, the water will become saturated with sodium and chloride. The time needed for water to reach equilibrium is dependent on kinetics of the reaction: that is, how fast the solid reacts with the water. In a polymineralic aquifer such as a sandstone, the ground water reacts simultaneously with several different mineral species. As one reaction approaches saturation, a second reaction with another mineral species may use a product of the first reaction and thus may prevent the first reaction from reaching equilibrium. The dissolution of calcite and cation exchange of clays is an example of two chemical reactions working in opposition to each other. Calcite in a sandstone will dissolve until the water is saturated. However, with clay in the aquifer, the calcium from the dissolution of the calcite will be exchanged for sodium. Because of the exchange, the solution becomes undersaturated with respect to calcite, and more calcite dissolves. Sodium and bicarbonate concentrations continue to increase to relatively high concentrations because of these simultaneous reactions. In the polymineralic aquifer, the chemical composition of the water will continue to change as it flows through the rock. Mapping the trends identifies probable pathways of ground-water flow. Within the polymineralic aquifer, some chemical reactions may still be controlled by a single chemical reaction and its kinetics. Variation in sulfate concentrations is an example. As the ground water becomes more reducing, sulfate will be altered to the reduced species of H_2S or HS^-. Commonly, several geochemical variations are available to indicate directions of ground-water movement. The coincidence of two or more trends substantiates the general direction of ground-water flow.

In Texas, the generation of sodium bicarbonate waters is typical in Tertiary sandstone aquifers. The longer the water is in the aquifer (or the greater distance of transport), the higher the sodium and bicarbonate concentrations become. Conversely, low-sodium (high-calcium) and low-bicarbonate waters are commonly indicative of recharge waters. By plotting ionic constituents on maps or graphs, the chemical evolution of the water can be discerned, and therefore, the general direction of ground-water flow can be determined.

By understanding the regional trends, perturbations of the natural system can be identified more easily. In the East Texas Basin, salt domes provide appropriate examples. Intrusion of salt domes into the Eocene aquifers has uplifted the Wilcox-Carrizo aquifer to the land surface and provided recharge points in an area where the aquifer is predominantly confined. If recharge is occurring, it may be geochemically identifiable. Similarly, salt dome dissolution may be geochemically identifiable. This requires an understanding of the sodium and chloride variations. Increases in sodium are more closely related to generation of sodium bicarbonate waters. Therefore, an increase in chlorinity is a better indicator of sodium chloride waters, but in this case their spatial distribution is important in identifying evidence of dome dissolution. As will be discussed later, increased salinity correlates better with fault zones, high mud zones, and deep sections of the aquifer than with dissolution of salt domes. Understanding the regional geochemical distribution in an aquifer is critical to interpretation of the local perturbations.

The movement of contaminants in an aquifer will be controlled by the geochemistry of the aquifer as well as its hydraulics. The geochemical environment of the Wilcox-Carrizo aquifer shifts from an oxidizing acidic water in the recharge zone to a reducing basic water deep in the aquifer. Many contaminants are nonconservative compounds and will be attenuated in the aquifer. The degree of attenuation (such as ion-exchange and adsorption and precipitation) is dependent on the aquifer geochemistry. For example, trace metals such as uranium, molybdenum, or selenium that are mobile in the oxidizing environment of the recharge zone will become insoluble in reducing conditions farther downdip within the aquifer (Henry and others, 1982).

Chemical trends of ground waters in the Queen City-Sparta and Wilcox-Carrizo aquifers have been determined from results of water-chemistry analyses from the Texas Natural Resources Information System (TNRIS) and the Texas Department of Water Resources. One hundred and fifty chemical analyses for the Queen City and Sparta aquifers were processed with the computer program WATEQF (Plummer and others, 1976) to ensure validity of the data by cation/anion balances. These data were then plotted as equivalent parts per million on a Piper (trilinear) diagram. Chemical data for the Queen City and Sparta aquifers have been combined because they both are shallow and have similar water chemistries. Chemical data for the Wilcox-Carrizo aquifer were run through both WATEQF and SOLMNEQ (Kharaka and Barnes, 1973) at different stages of this study to ensure validity of the data. If cation/anion balance for any chemical analysis was in error by more than 5 percent, the data were excluded. Results of 530 water-chemistry analyses from the Wilcox-Carrizo aquifer were plotted in 3 different ways: (1) by Piper diagrams, (2) according to distribution in the aquifer, and (3) by species-correlation diagrams.

Shallow ground waters (less than 100 ft [30 m] to the water table) located near oil fields in the outcrop of the Wilcox-Carrizo commonly contain high chloride concentrations. These waters probably are contaminated by oil-field brine and do not represent natural compositions. Therefore, these data were eliminated. Data from Gregg County were also eliminated because waters there exhibit unusually high chloride concentrations with depth and may represent a mixing of deeper formation waters with the meteoric ground waters in the Wilcox-Carrizo. Therefore, Gregg County data do not represent the normal geochemical evolution of the ground water.

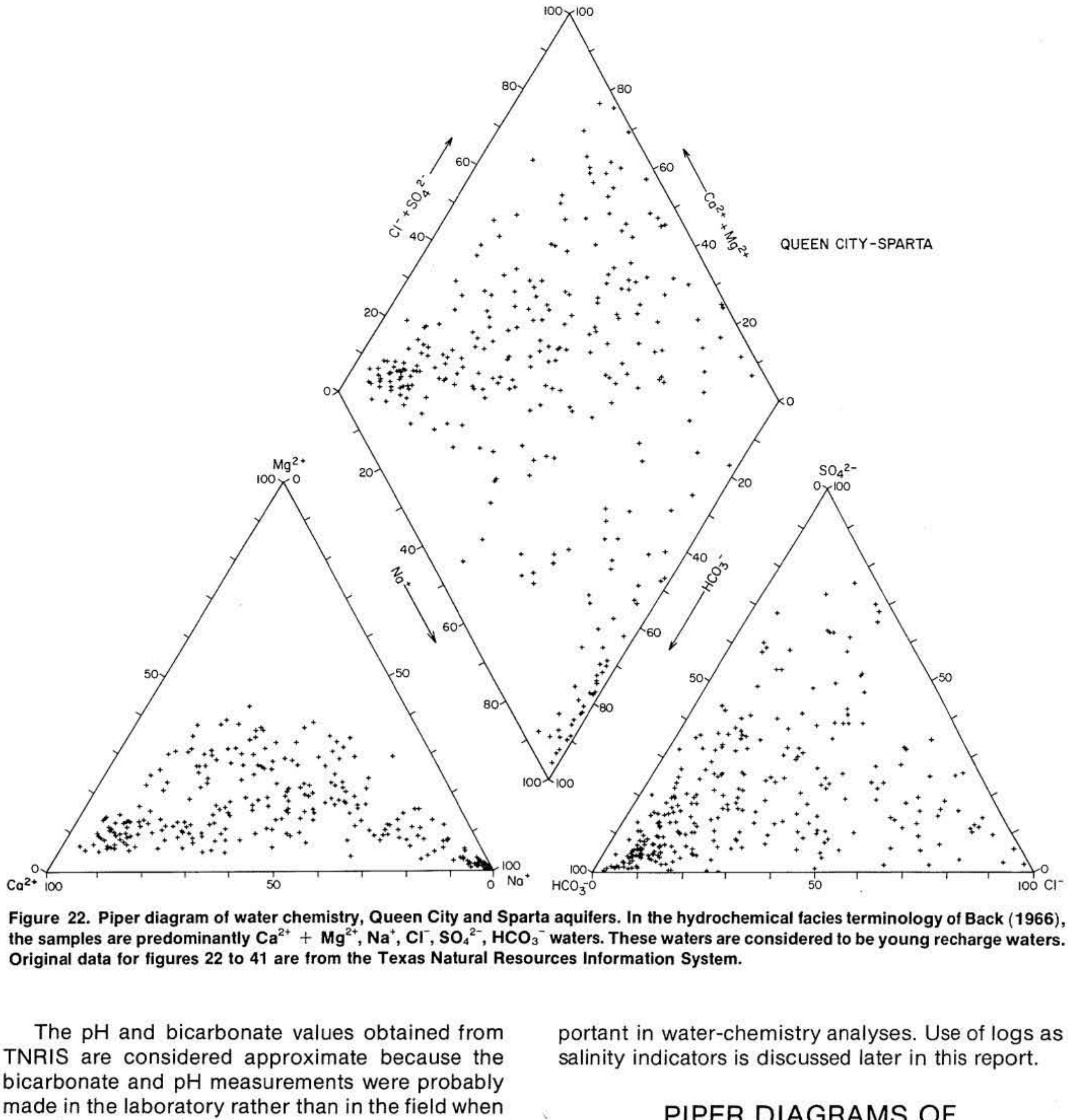

Figure 22. Piper diagram of water chemistry, Queen City and Sparta aquifers. In the hydrochemical facies terminology of Back (1966), the samples are predominantly $Ca^{2+} + Mg^{2+}$, Na^+, Cl^-, SO_4^{2-}, HCO_3^- waters. These waters are considered to be young recharge waters. Original data for figures 22 to 41 are from the Texas Natural Resources Information System.

The pH and bicarbonate values obtained from TNRIS are considered approximate because the bicarbonate and pH measurements were probably made in the laboratory rather than in the field when samples were collected.

Problems are inherent in water-chemistry data from water wells. Drillers typically drill to the shallowest high-producing good-water-quality sands. As a result, the collection of water-chemistry data is biased against the deep sections of an aquifer, the low-permeability sections, and the poor-water-quality sections. Using electric logs for analyses of water quality in an aquifer permits semiquantitative salinity measurements of large thicknesses of the aquifer, unlike using water-chemistry data. Electric log interpretation is important in water-chemistry analyses. Use of logs as salinity indicators is discussed later in this report.

PIPER DIAGRAMS OF QUEEN CITY-SPARTA AND WILCOX-CARRIZO WATER

Piper diagrams (Piper, 1944) of ground-water composition provide summaries of ground-water evolution for both the Queen City-Sparta and the Wilcox-Carrizo aquifers. The Queen City-Sparta waters range in composition from a calcium or calcium-magnesium water to a sodium water (fig. 22). In the anion triangle, there is a slight tendency toward a bicarbonate water. In the

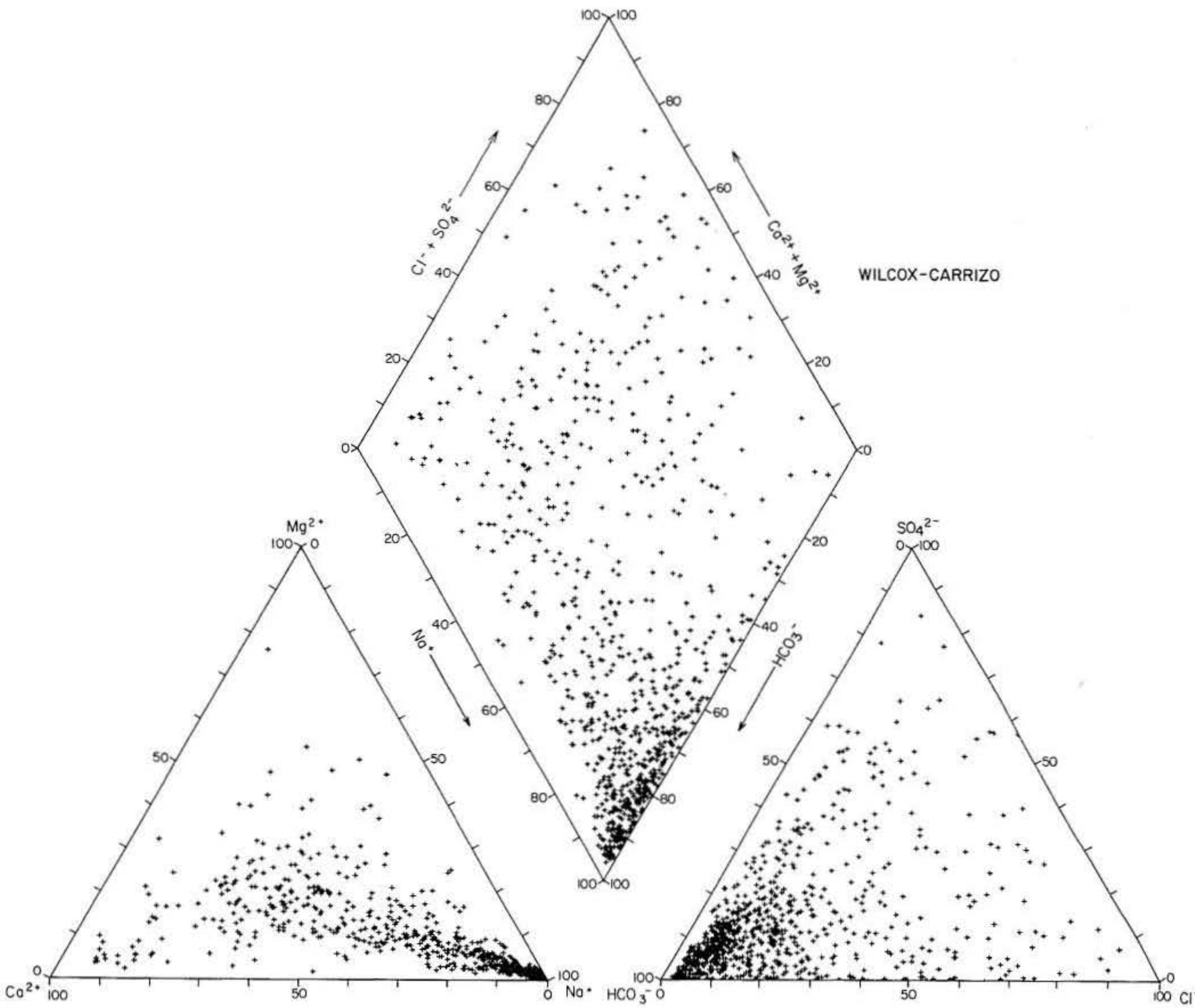

Figure 23. Piper diagram of water chemistry, Wilcox-Carrizo aquifer. Ground-water composition shifts from a $Ca^{2+} + Mg^{2+}$, Na^+, Cl^-, SO_4^{2-}, HCO_3^- water to an Na^+, HCO_3^-, Cl^- to SO_4^{2-} water. This evolution follows predictable trends as ground water flows from the recharge zone to the deep artesian section.

diamond figure, chemically the waters are calcium-magnesium to chloride-sulfate; only a few waters are in the sodium bicarbonate corner. The resulting chemical interpretation agrees with the hydraulic interpretation discussed previously. Waters in the Queen City-Sparta are recharge waters, and their transit time in the aquifer is short. These waters have not had the time or the transit distance to evolve into sodium bicarbonate waters.

The Piper diagram for the Wilcox-Carrizo aquifer shows similar distributions, but a more pronounced development of a sodium bicarbonate water is evident (fig. 23). The cation triangle shows a shift from a calcium or calcium-magnesium water to a sodium-dominated water. In the anion triangle, there is a much higher density of points in the bicarbonate field. Samples in the diamond figure were plotted in all fields of the diagram, with increased density in the sodium bicarbonate corner. When the Wilcox-Carrizo waters are grouped into shallow ground waters (less than 150 ft [46 m]) and deeper ground waters (greater than 150 ft [46 m]), the Piper diagrams show an interesting shift in the location of high densities of data points (figs. 24 and 25). For the shallow Wilcox-Carrizo waters, the Piper diagram is similar to the Piper diagram for Queen City-Sparta waters. Data points concentrate in the calcium-magnesium to chloride-sulfate field of the diamond figure. In

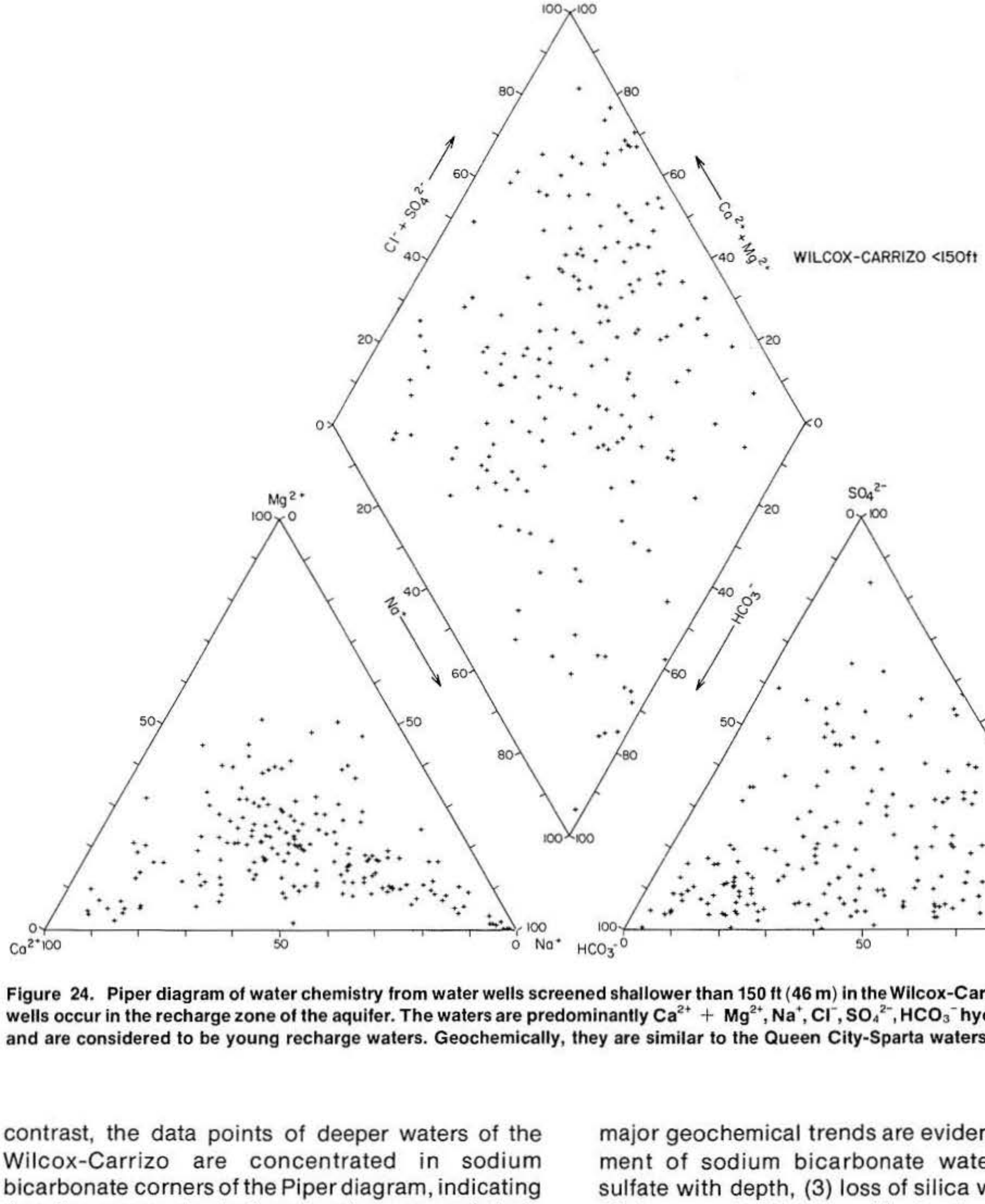

Figure 24. Piper diagram of water chemistry from water wells screened shallower than 150 ft (46 m) in the Wilcox-Carrizo aquifer. These wells occur in the recharge zone of the aquifer. The waters are predominantly Ca^{2+} + Mg^{2+}, Na^+, Cl^-, SO_4^{2-}, HCO_3^- hydrochemical facies and are considered to be young recharge waters. Geochemically, they are similar to the Queen City-Sparta waters.

contrast, the data points of deeper waters of the Wilcox-Carrizo are concentrated in sodium bicarbonate corners of the Piper diagram, indicating that the waters in shallow sections are relatively young (like the Queen City-Sparta waters), whereas the deeper waters are well-developed older sodium bicarbonate waters.

Piper diagrams show general qualitative trends in aquifer water chemistry. However, comparison of six ionic species within one diagram (as is done in the diamond figure of the Piper diagram) provides little quantification of the chemical processes occurring in the aquifer. Plotting of one ion versus another frequently provides additional information about the evolution of the water composition. Four major geochemical trends are evident: (1) development of sodium bicarbonate water, (2) loss of sulfate with depth, (3) loss of silica with depth, and (4) decreased chloride with depth. The following sections describe each of these trends.

DEVELOPMENT OF SODIUM BICARBONATE WATER

The development of a sodium bicarbonate water is controlled by two reactions (Foster, 1950):

$$CaCO_3 + H_2CO_3 \rightleftharpoons Ca^{2+} + 2HCO_3^- \qquad (1)$$

$$Ca^{2+} + \text{Na-clay} \rightleftharpoons 2Na^+ + \text{Ca-clay} \qquad (2)$$

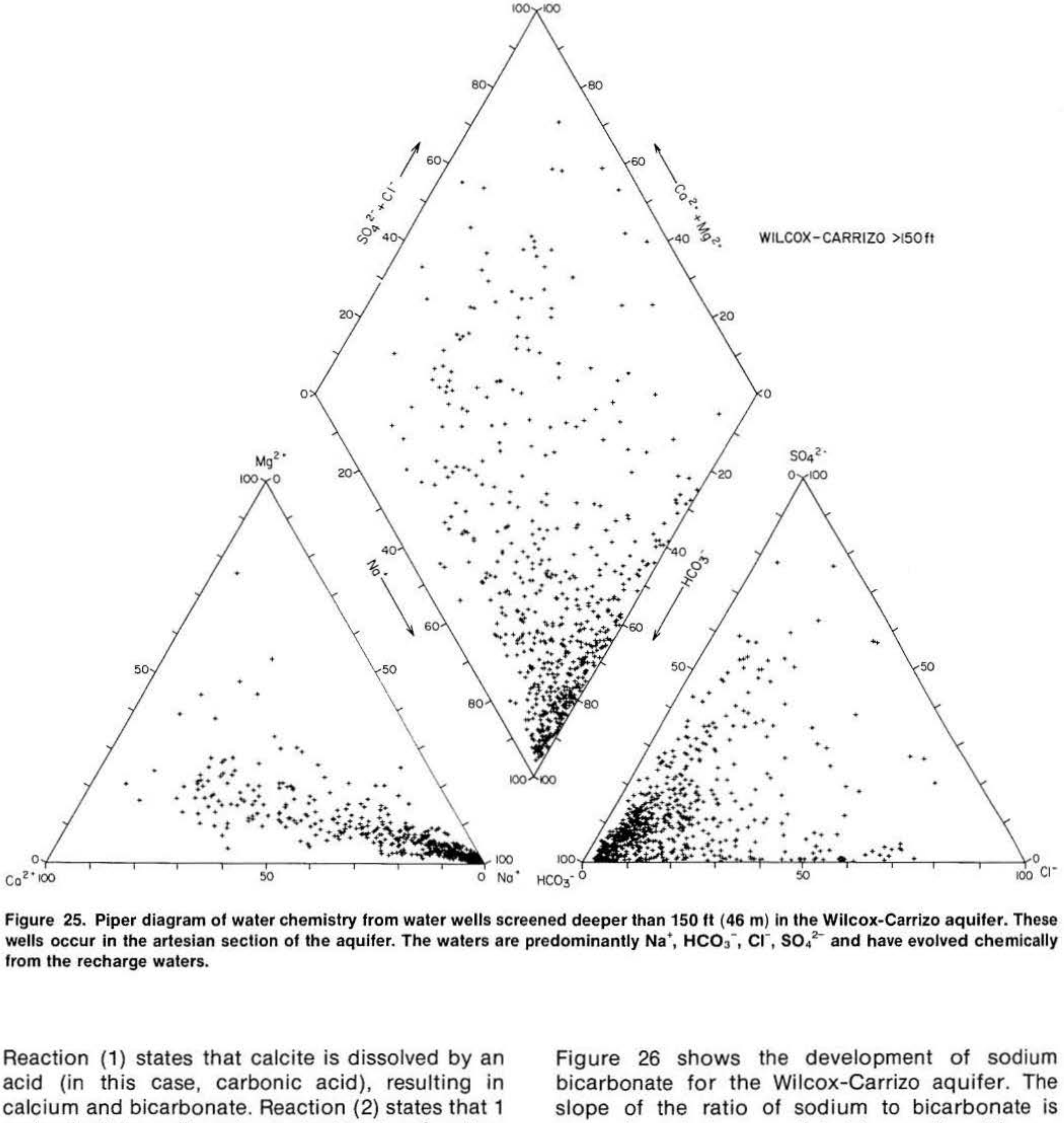

Figure 25. Piper diagram of water chemistry from water wells screened deeper than 150 ft (46 m) in the Wilcox-Carrizo aquifer. These wells occur in the artesian section of the aquifer. The waters are predominantly Na^+, HCO_3^-, Cl^-, SO_4^{2-} and have evolved chemically from the recharge waters.

Reaction (1) states that calcite is dissolved by an acid (in this case, carbonic acid), resulting in calcium and bicarbonate. Reaction (2) states that 1 mole of calcium will exchange for 2 moles of sodium on the clays. Magnesium and potassium will also be involved in this reaction. Together, reactions (1) and (2) yield reaction (3). This reaction is observed in many sandstone aquifers, such as the Magothy aquifer in Delaware (Back, 1966), the Fox Hills aquifer in South Dakota (Thorstenson and others, 1979), and the Gulf Coast aquifer in Texas (Kreitler and others, 1977).

$$CaCO_3 + H_2CO_3 + \text{Na-clay} \rightleftharpoons 2Na^+ + 2HCO_3^- + \text{Ca-clay} \quad (3)$$

Figure 26 shows the development of sodium bicarbonate for the Wilcox-Carrizo aquifer. The slope of the ratio of sodium to bicarbonate is approximately 1, as predicted by reaction (3).

Examination of reaction (3) indicates that other geochemical reactions should be occurring concurrently with the generation of sodium bicarbonate water:

1. Ground water should become progressively depleted with calcium the farther the water flows through the aquifer. A plot of calcium versus depth shows this to be occurring (fig. 27). A map view of calcium distribution also indicates that ground waters in the shallow outcrop are high in calcium, whereas deeper waters downdip are depleted in

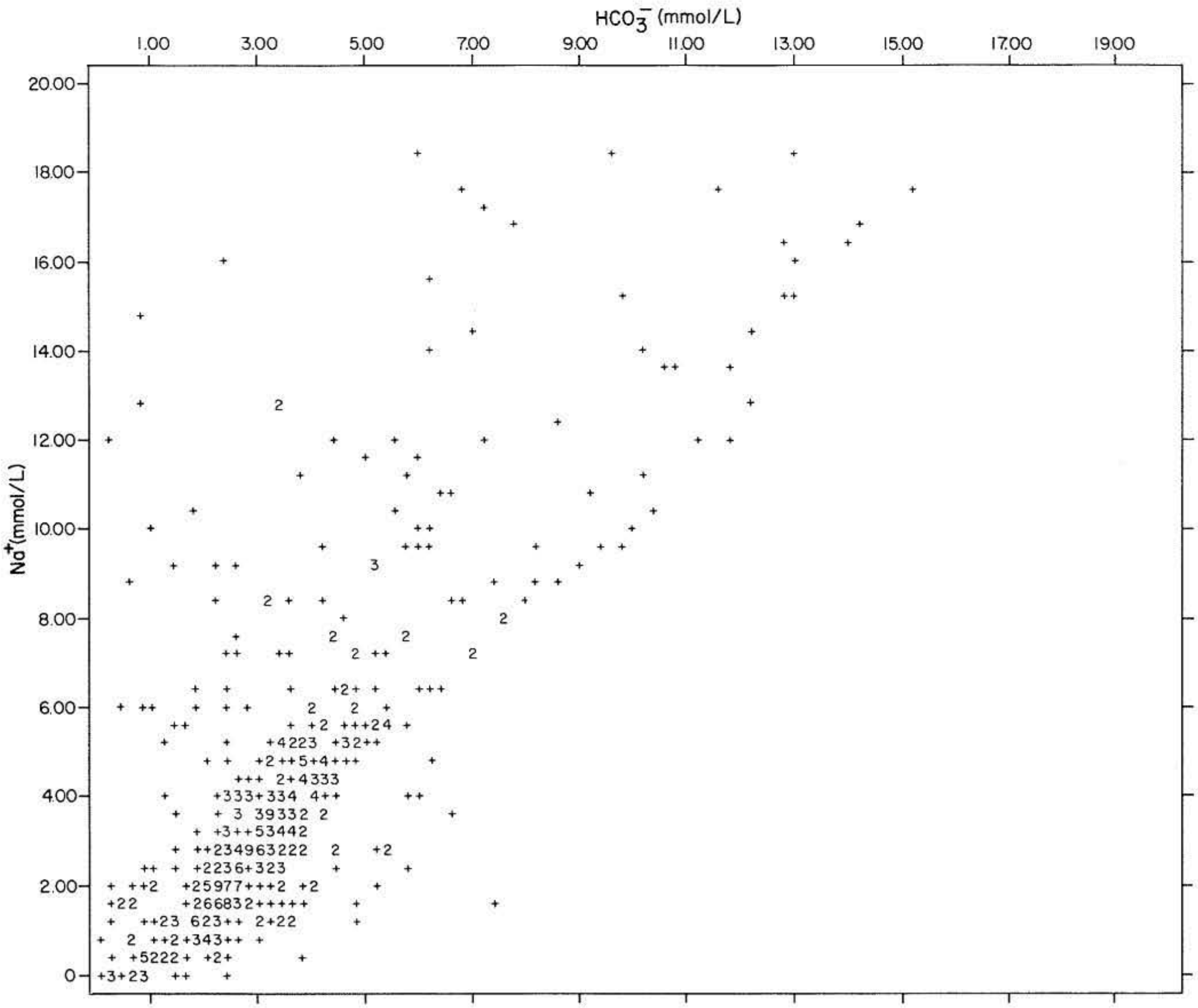

Figure 26. Generation of Na^{+}-HCO_3^{-} ground water in the Wilcox-Carrizo aquifer. Increased Na^{+} and HCO_3^{-} activities result from the reactions of $CaCO_3$ dissolution and cation exchange.

calcium (fig. 28). Magnesium is a similar divalent cation and reacts similarly to calcium. The Piper diagram for the Wilcox-Carrizo shows a downdip depletion of both calcium and magnesium and enrichment of sodium (fig. 23).

2. If the Wilcox-Carrizo aquifer is functioning as a closed system for carbonic acid, then the pH will rise as the sodium and bicarbonate concentrations increase. The dissolution of calcite uses up the carbonic acid, and the hydrogen joins with the carbonate ion, forming bicarbonate. The carbonic acid (dissolved carbon dioxide) is derived primarily from plant decay and respiration in the soil zone. If no additional carbon dioxide is added to the water, the ground water is considered to be functioning in a closed system. If additional carbon dioxide is being added either by decay of organic material in the aquifer or by an external source of carbon dioxide (deeper gas fields leaking into the aquifer or coalification), then the aquifer is considered an open system. A plot of pH versus total carbonate shows that most of the aquifer is functioning as a closed system. There is a continual increase of pH with increased total carbonate (fig. 29). In shallow ground waters, the pH range is approximately 5 to 7, whereas the deeper water range is from 8 to 9 (fig. 30). At very high bicarbonate concentrations, bicarbonate appears to increase independently of pH, suggesting that at great depths, the aquifer is an open system (fig. 29).

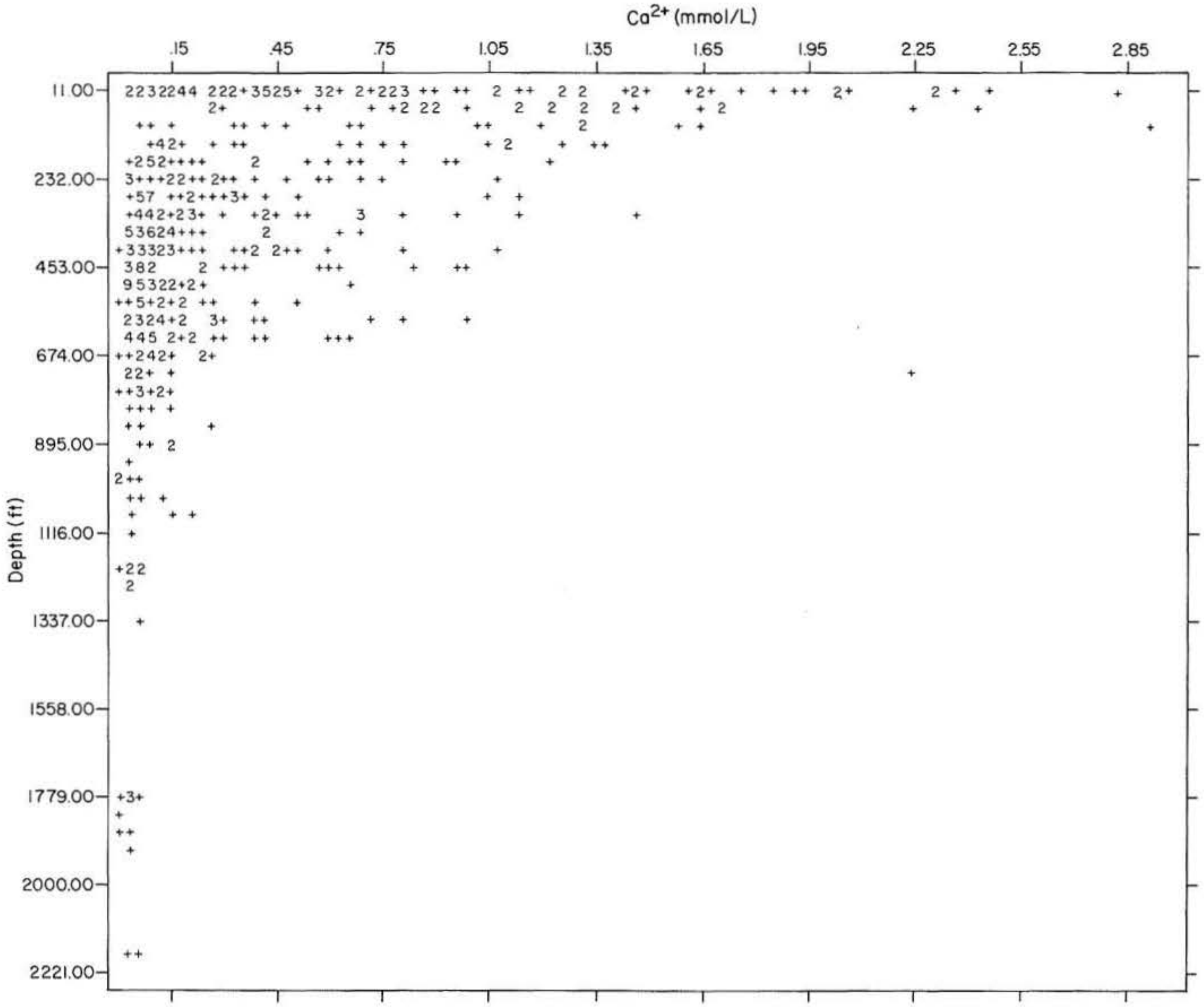

Figure 27. Graph of Ca^{2+} versus depth in Wilcox-Carrizo aquifer. Higher Ca^{2+} activities occur in the shallower ground waters. The loss of Ca^{2+} with depth results from cation exchange.

The pH of ground water is an effective indicator of recharge zones (fig. 31). Low pH waters are typical of recharge areas, and conversely, high pH waters occur in the artesian section. The pH is a sensitive tracer because a pH change of one unit (for example, from pH 5 to 6) is a change of one order of magnitude of the hydrogen activity. Ionic concentrations generally exhibit increases of no more than two or three times. Recharge areas for the Wilcox-Carrizo aquifer are characterized by pH values that are lower than those of downdip waters. In the outcrop, recharge waters typically have pH values less than 8.0, whereas downdip waters generally have pH values greater than 8.0 (fig. 30).

This pH change is a useful tool in identifying recharge or leakage in the confined section of the aquifer. At the recharge mound in central Anderson County (fig. 13), several low pH values are in the ground water. Similarly, north of the ground-water divide in Smith County, where the Reklaw is relatively sandy and permeable, numerous low-pH waters are in the confined section (fig. 31).

SULFATE REDUCTION AND REDUCING CONDITIONS

Sulfate ions appear to be reduced in the Wilcox-Carrizo ground waters; sulfate concentrations decrease with depth (fig. 32). Similarly, higher sulfate values exist in the outcrop rather than

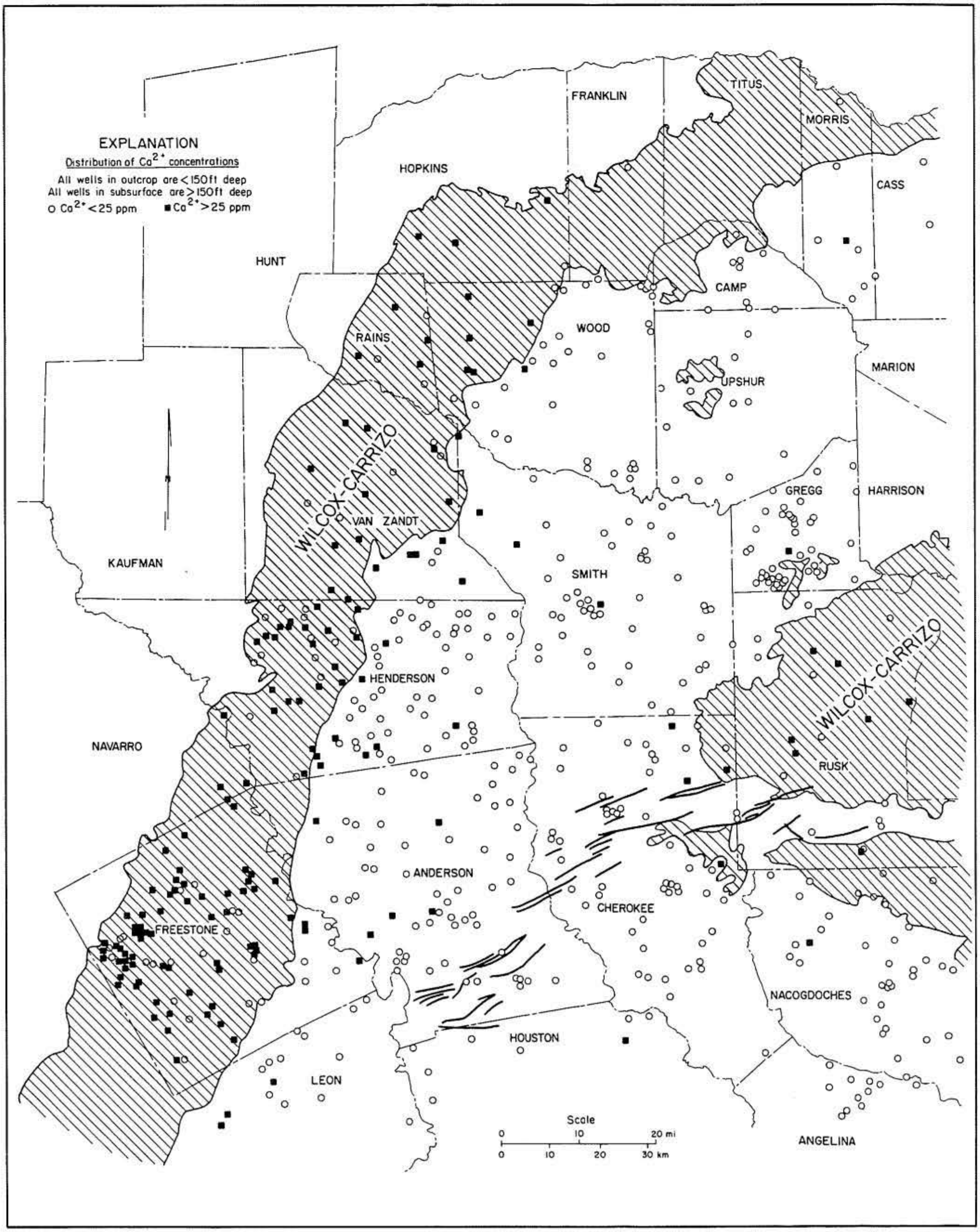

Figure 28. Map view of Ca^{2+} concentrations in Wilcox-Carrizo aquifer. Higher concentrations of Ca^{2+} occur in the outcrops of the Wilcox-Carrizo and are not present downdip. Outcrop indicated by diagonal-line pattern.

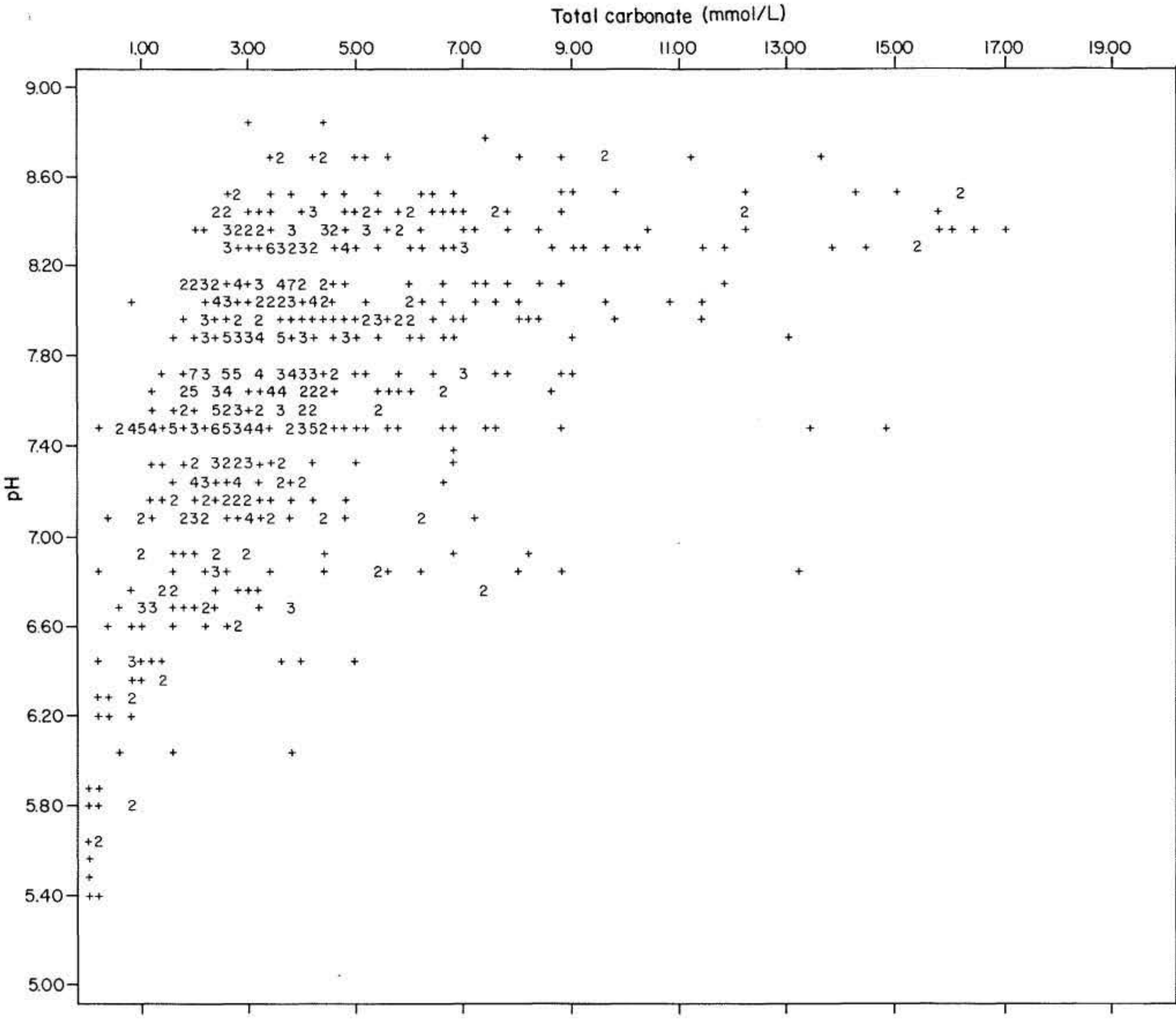

Figure 29. Graph of pH versus total carbonate activity (HCO_3^-, CO_3^{2-}, and complexed CO_3^{2-} and HCO_3^- species). The graph shows a trend of increasing pH with increasing total carbonate, implying a closed carbonate system. The graph also shows a trend of high concentrations of total carbonate that increases independently of pH, implying an open system where coalification deep in the aquifer is adding CO_2.

downdip in the confined section (fig. 33). The product of the sulfate reduction is unknown. Reduction of sulfate with subsequent oxidation of organics (for example, lignite) to produce bicarbonate does not appear to be as important a reaction in the Wilcox-Carrizo aquifer as in the Fox Hills-Hill Creek aquifer (Thorstenson and others, 1979) because the concentration of sulfate (generally less than 0.6 mmole/L) is limited in the Wilcox-Carrizo recharge zone (fig. 33). If sulfate reduction and oxidation of organics is an important reaction in the main part of the aquifer, then the Wilcox-Carrizo would be functioning as an open system and the pH would not rise.

Ground water may become more reducing after sulfate reduction. Deep Wilcox-Carrizo waters commonly contain high bicarbonate content. These products suggest coalification of organics in the aquifer, a process that should occur after sulfate reduction in a more reducing environment (Freeze and Cherry, 1979).

SILICA

Higher silica concentrations occur in ground water at the outcrop than in the confined part of the aquifer (fig. 34). Silica activity values decrease with

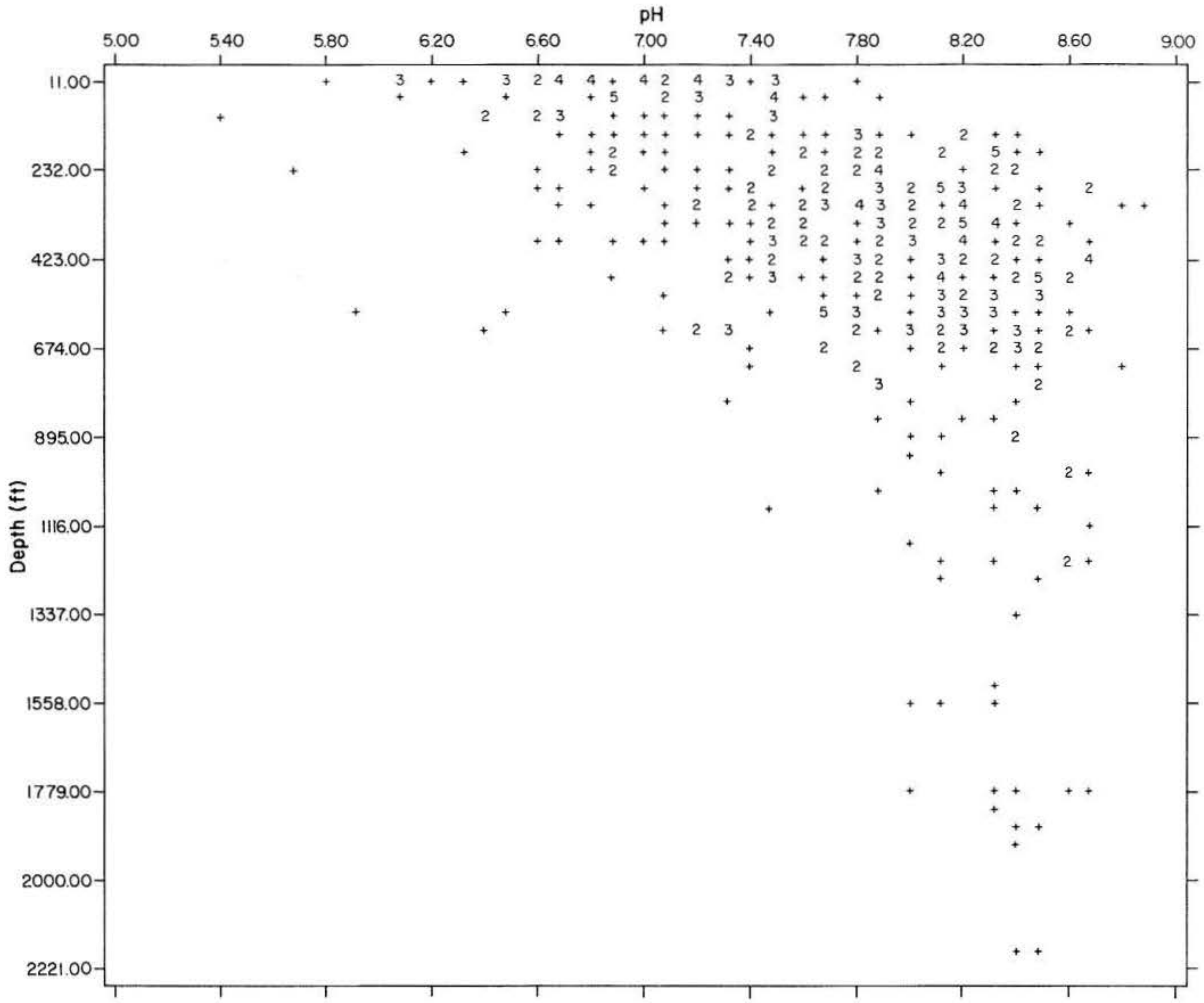

Figure 30. Graph of pH versus depth, Wilcox-Carrizo aquifer. Values of pH increase from 5 to 7 in the outcrop to 7 to 9 in the deeper artesian section of the aquifer. The increase in pH is attributed to $CaCO_3$ dissolution in a closed system.

depth from activities as great as 1 mmole/L to approximately 0.2 mmole/L of silica (fig. 35). High silica activity values in the recharge waters may result from dissolution of amorphous silica in the soil zone (Davis, 1964). Figure 36 shows that maximum silica activity values are at amorphous silica saturation. Some of the silica may be derived from leaching of feldspars. Petrographic analyses of Wilcox thin sections indicate leaching of feldspars (Dutton, 1980). The lower activity values of silica approach quartz equilibrium, suggesting that quartz cements could form. Dutton (1980) has identified epigenetic clays in the Wilcox, but not quartz cements. The excess silica may be used in the precipitation of authigenic clays.

Leaching of feldspars generates a cation (for example, sodium or calcium), bicarbonate, silica, and clay:

$$NaAlSi_3O_8(S) + H_2CO_3 + 9/2\ H_2O \rightleftharpoons Na^+ + HCO_3^- + 2H_4SiO_4 + 1/2\ Al_2Si_2O_5(OH)_4(S) \qquad (4)$$

Without calcium carbonate or clay minerals in the aquifer, this reaction can be important in generating sodium bicarbonate water (Garrels and MacKenzie, 1967). This process (if it is ongoing) in the Wilcox-Carrizo aquifer is contributing a relatively insignificant amount of bicarbonate to the ground water. According to reaction (4), 2 moles of silica should be generated for every mole of sodium and

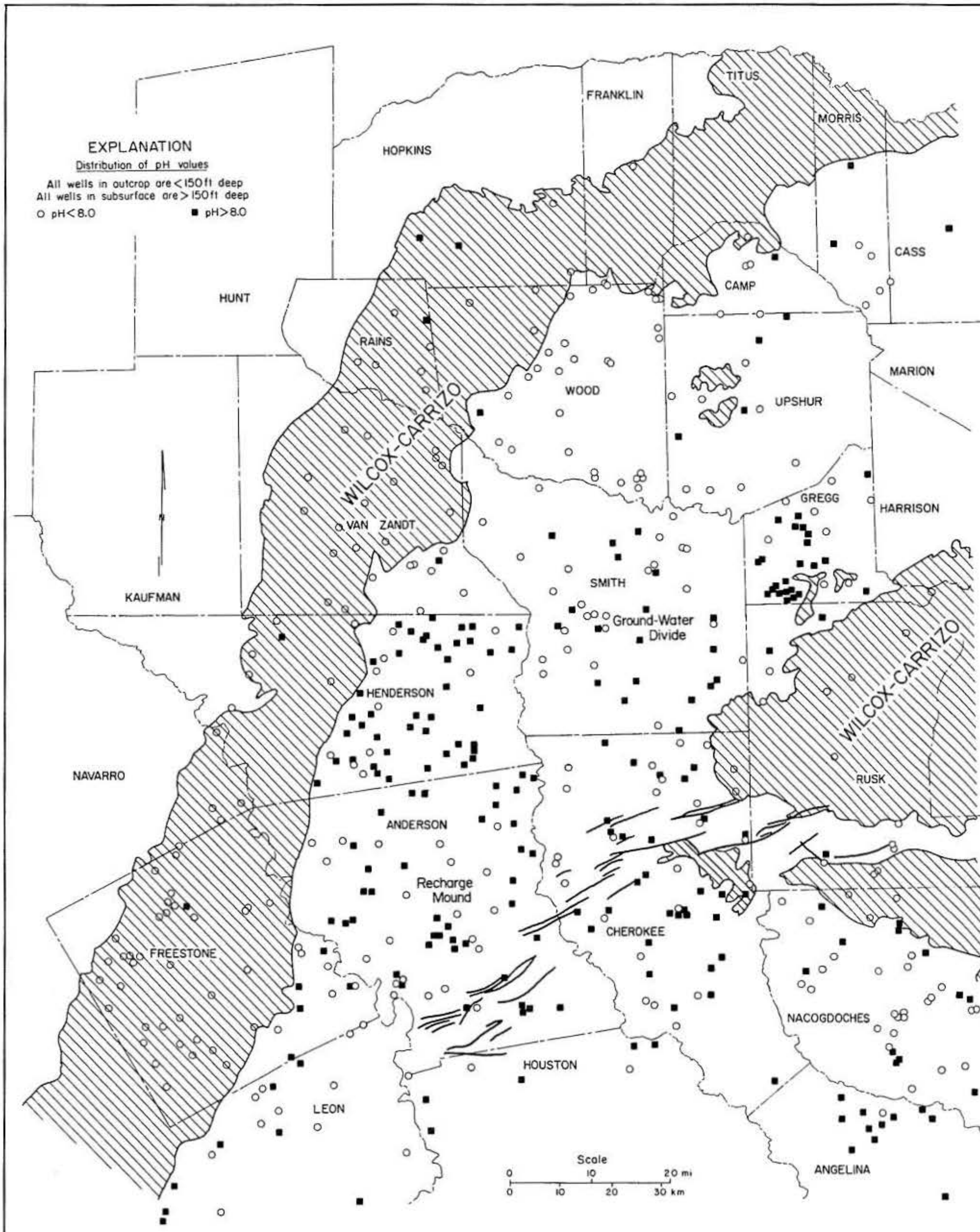

Figure 31. Map view of pH values, Wilcox-Carrizo aquifer. The highest pH values occur in the downdip artesian section. Low pH values in the artesian section are indicative of recharge (or leakage). This occurs in central Anderson County and in the northern part of the basin, where the overlying Reklaw may be relatively leaky. Outcrop indicated by diagonal-line pattern.

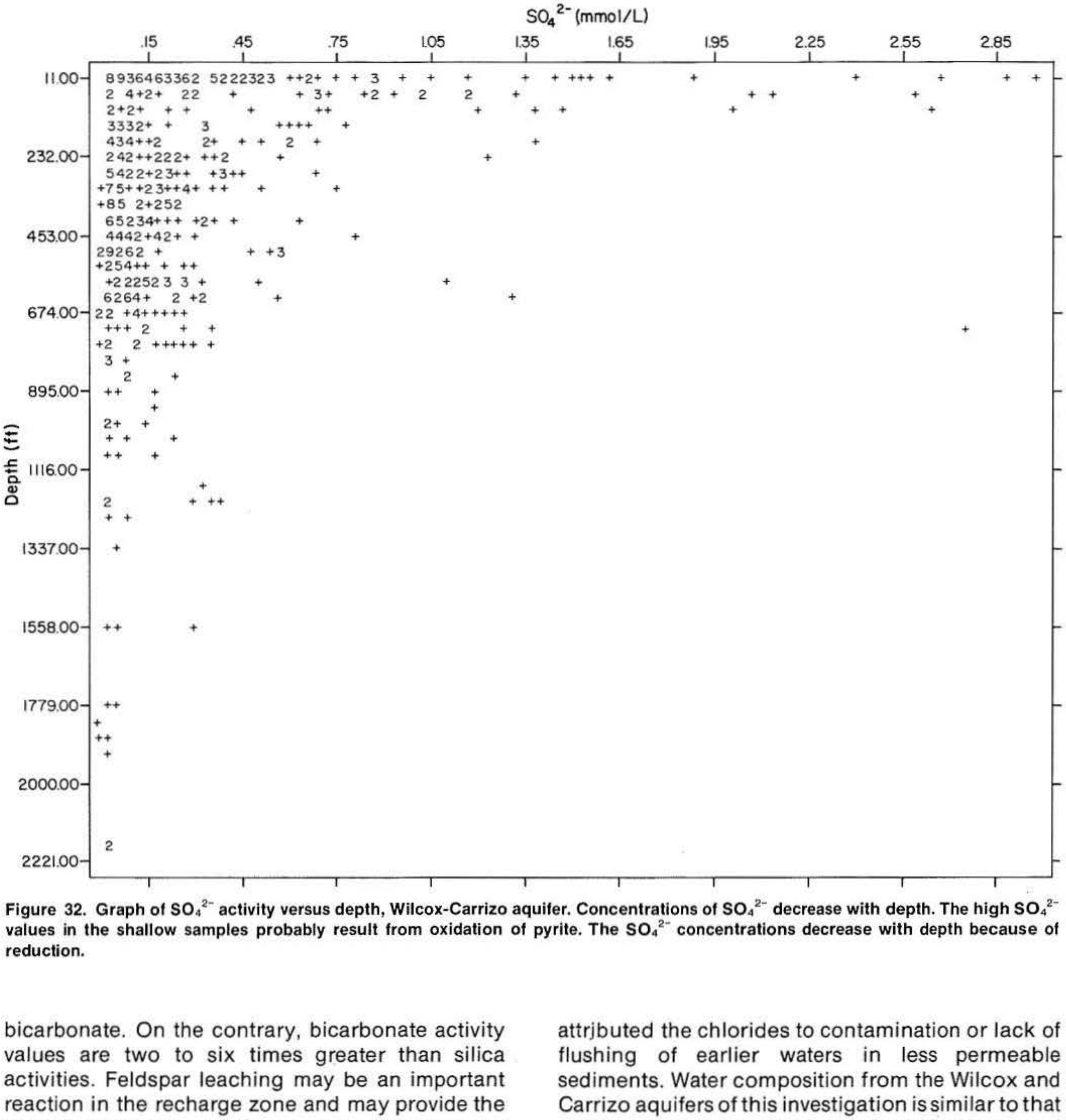

Figure 32. Graph of SO_4^{2-} activity versus depth, Wilcox-Carrizo aquifer. Concentrations of SO_4^{2-} decrease with depth. The high SO_4^{2-} values in the shallow samples probably result from oxidation of pyrite. The SO_4^{2-} concentrations decrease with depth because of reduction.

bicarbonate. On the contrary, bicarbonate activity values are two to six times greater than silica activities. Feldspar leaching may be an important reaction in the recharge zone and may provide the initial calcium, sodium, and bicarbonate concentrations.

CHLORIDE

High chloride concentrations occur in shallow ground waters, whereas the deeper waters in the confined section are generally low in chloride (figs. 37 and 38). Henry and others (1979) also identified similar high chloride concentrations in the Wilcox outcrop south of the study area. They attributed the chlorides to contamination or lack of flushing of earlier waters in less permeable sediments. Water composition from the Wilcox and Carrizo aquifers of this investigation is similar to that of the Wilcox water samples analyzed by Henry and others (1979). The Wilcox and Carrizo aquifers are considered as a single aquifer in this discussion of water chemistry because they appear to be hydraulically interconnected on the regional scale. Lithologically, however, the Wilcox and Carrizo aquifers are different. The Wilcox aquifer is muddier, has lower permeabilities, more variable lithologic composition (thick mud sections and lignites), and represents a greater variety of depositional facies (for example, fine-grained meanderbelts, crevasse splays, and deltaic distributary-channel fills). In

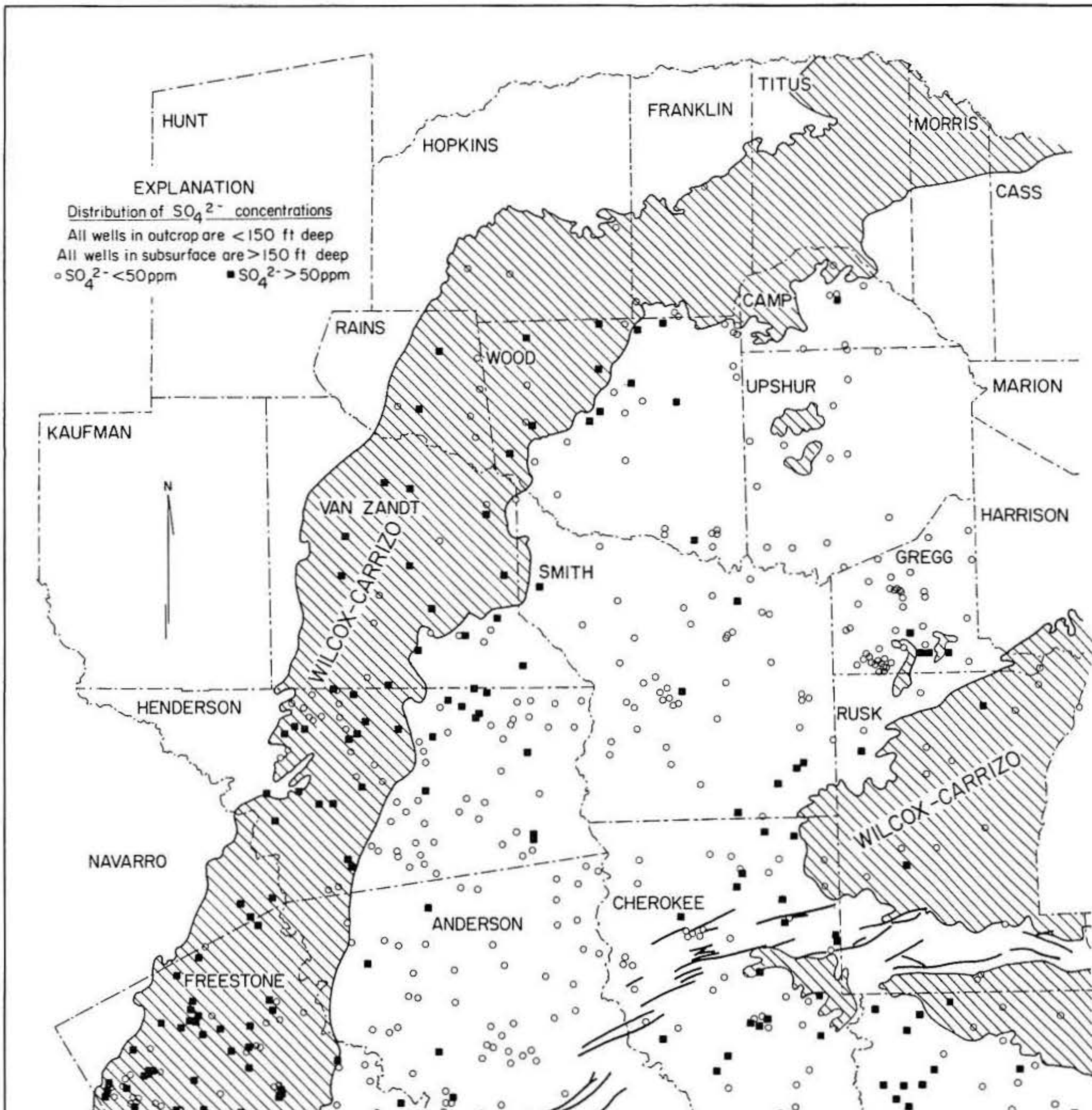

Figure 33. Map view of SO_4^{2-} concentrations, Wilcox-Carrizo aquifer. Note the high SO_4^{2-} concentrations in the outcrop. Outcrop indicated by diagonal-line pattern.

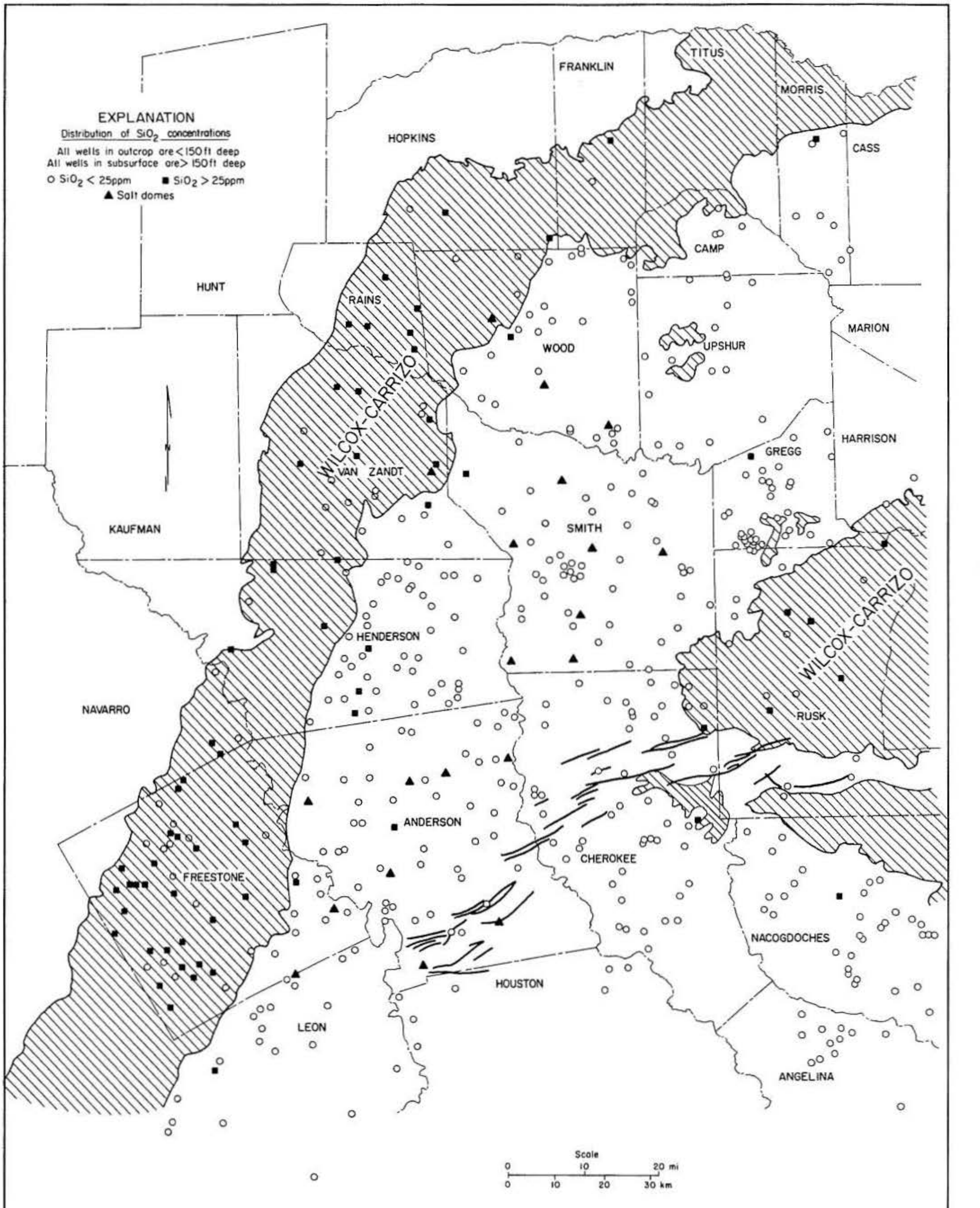

Figure 34. Map view of SiO_2 concentrations, Wilcox-Carrizo aquifer. Note the high SiO_2 concentrations in the outcrop. Outcrop indicated by diagonal-line pattern.

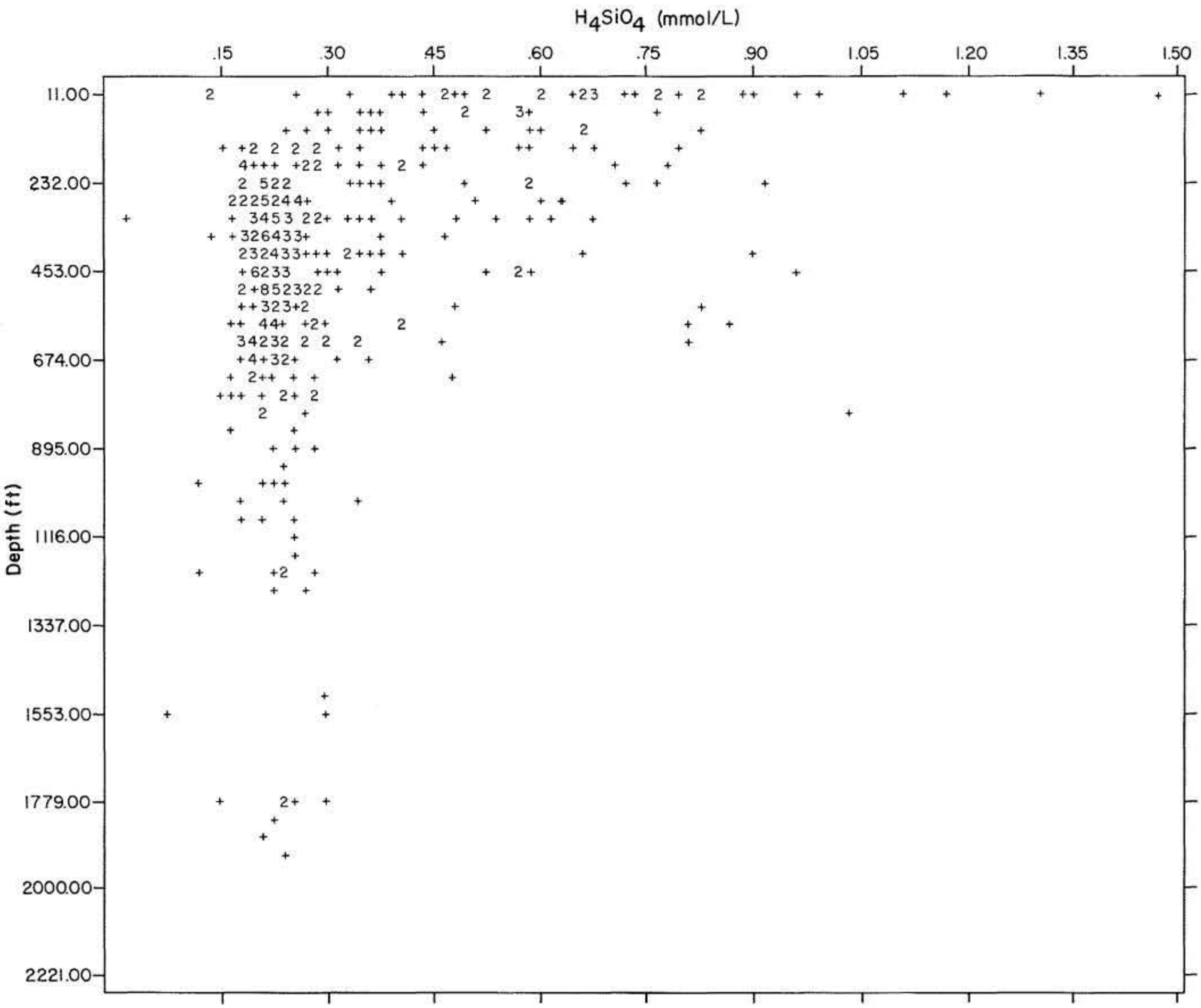

Figure 35. Graph of H_4SiO_4 versus depth. Activities of H_4SiO_4 decrease with depth. High H_4SiO_4 in the shallow samples may result from either solution of amorphous SiO_2 in soils or dissolution of feldspars. The loss of H_4SiO_4 with depth results from either precipitation of authigenic clays or quartz cement. No quartz cements, however, have been identified in core samples. Authigenic kaolinite has been identified.

contrast, the Carrizo is a relatively clean highly permeable ancient fluvial deposit. On the basis of these lithologic variations, it would be expected that the Wilcox aquifer would have a greater variation in water composition than the Carrizo. The following figures support this point. Graphs of sulfate versus depth and chloride versus depth for the Carrizo (figs. 39 and 40) do not exhibit the high concentrations at shallow depths that are exhibited in the Wilcox graphs (figs. 32 and 37). Even though there is a greater diversity of water composition in the Wilcox than in the Carrizo, the two aquifers can be treated as one because these geochemical trends are the same.

In contrast to most of the East Texas Basin, the Wilcox-Carrizo in Gregg County shows increasing chloride content with depth (fig. 41). This may be related to the East Texas field, which is one of the largest oil and gas fields in the Western Hemisphere and is located in Gregg and Rusk Counties. The hydrocarbons may have accumulated here as a result of regional flow of deep basinal fluids toward the field and then discharge of these fluids into shallower aquifers. Brines would probably be mixing with the overlying meteoric ground waters of the Wilcox-Carrizo, and consequently, higher chloride concentrations would occur in the Wilcox-Carrizo aquifer.

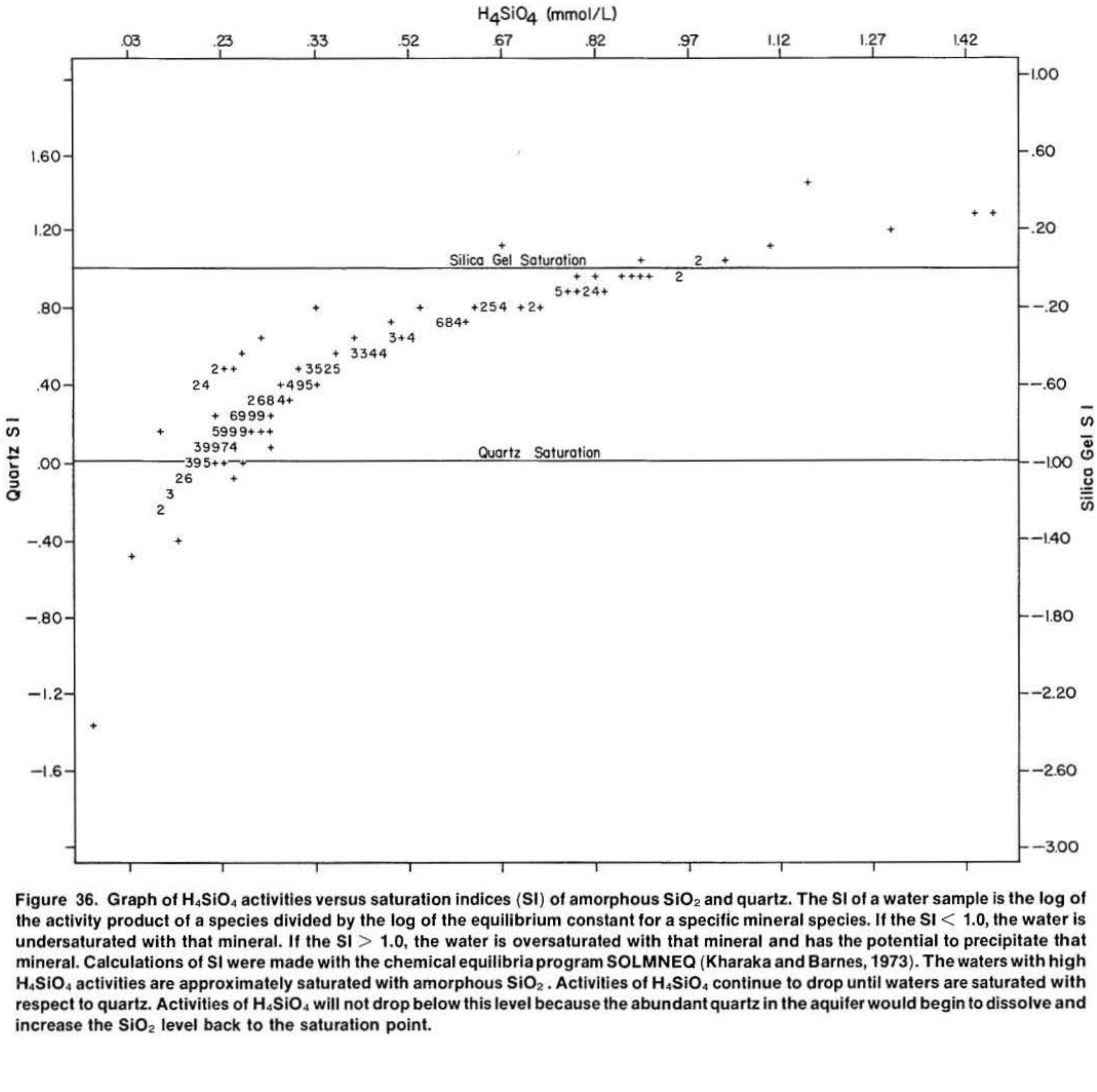

Figure 36. Graph of H_4SiO_4 activities versus saturation indices (SI) of amorphous SiO_2 and quartz. The SI of a water sample is the log of the activity product of a species divided by the log of the equilibrium constant for a specific mineral species. If the SI $<$ 1.0, the water is undersaturated with that mineral. If the SI $>$ 1.0, the water is oversaturated with that mineral and has the potential to precipitate that mineral. Calculations of SI were made with the chemical equilibria program SOLMNEQ (Kharaka and Barnes, 1973). The waters with high H_4SiO_4 activities are approximately saturated with amorphous SiO_2. Activities of H_4SiO_4 continue to drop until waters are saturated with respect to quartz. Activities of H_4SiO_4 will not drop below this level because the abundant quartz in the aquifer would begin to dissolve and increase the SiO_2 level back to the saturation point.

SUMMARY—EVOLUTION OF WATER CHEMISTRY

A sodium bicarbonate water in the Wilcox-Carrizo aquifer is derived from the interaction of calcite solution and cation exchange. Most of the aquifer appears to be functioning as a closed system. The continuous rise of pH with depth indicates the existence of a closed carbonate system. Excess bicarbonate may be generated at depth by coalification of organics. Sulfate reduction is occurring, but its effect on generation of additional bicarbonate is negligible because of its generally low initial concentration in the recharge zone. High silica concentrations in the shallow aquifer can be attributed either to leaching of feldspars or to dissolution of amorphous silica. Leaching of feldspars may be important during the initial generation of bicarbonate in the shallow recharge zone. It is not, however, an important reaction in the overall generation of the high bicarbonate concentrations. The loss of silica with depth can be accounted for by precipitation of either quartz cements or authigenic clays.

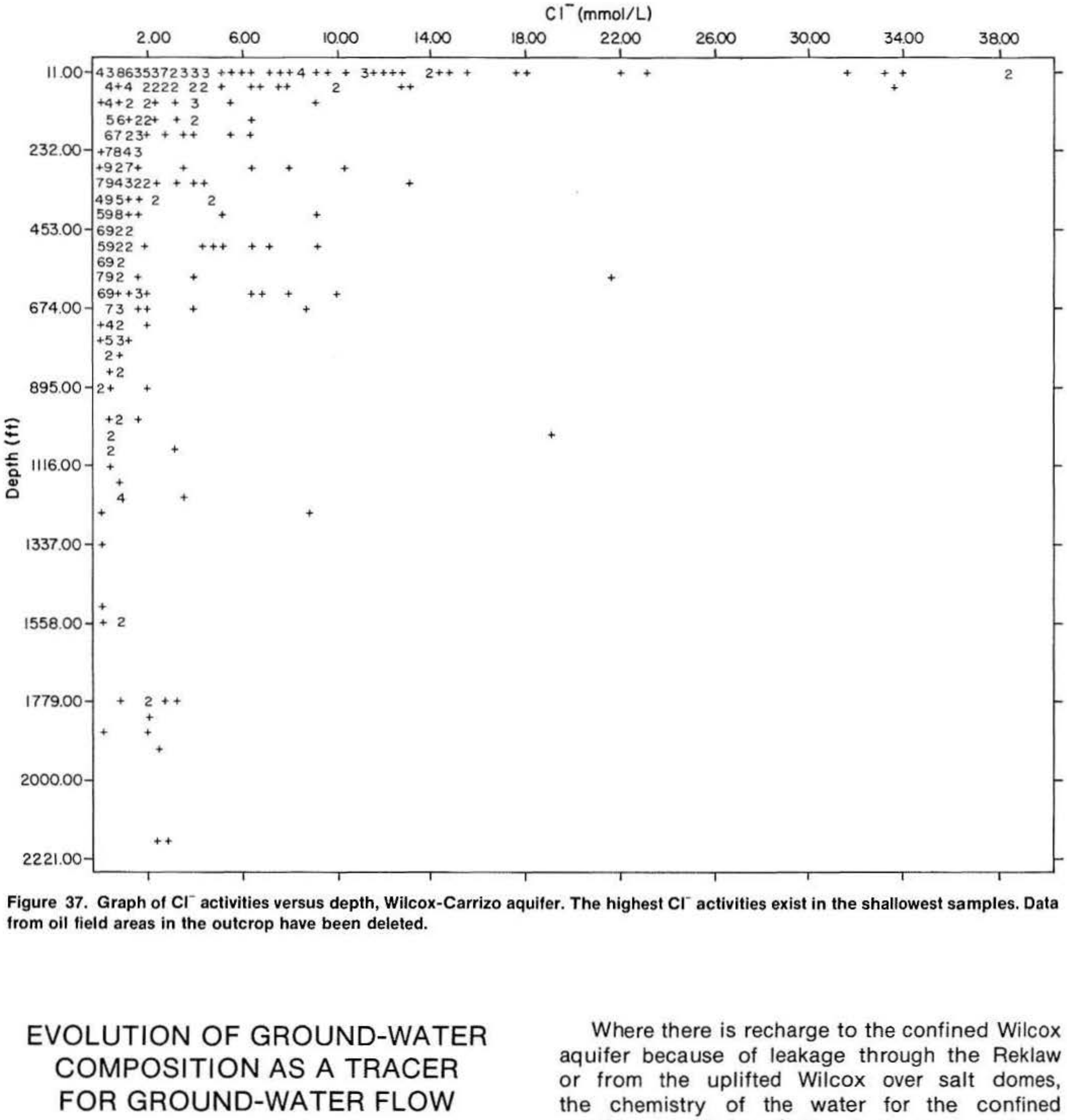

Figure 37. Graph of Cl^- activities versus depth, Wilcox-Carrizo aquifer. The highest Cl^- activities exist in the shallowest samples. Data from oil field areas in the outcrop have been deleted.

EVOLUTION OF GROUND-WATER COMPOSITION AS A TRACER FOR GROUND-WATER FLOW

The general chemical trends established by geochemical evolution of ground waters in the aquifer can be used to evaluate anomalous flow conditions. Waters in the shallow recharge zone of the Wilcox-Carrizo typically have neutral to acidic pH values, high calcium, low sodium, moderate sulfate, and high silica concentrations. The waters in the confined downdip section of the aquifer have higher pH values, low calcium, high sodium, low sulfate, and low silica concentrations.

Where there is recharge to the confined Wilcox aquifer because of leakage through the Reklaw or from the uplifted Wilcox over salt domes, the chemistry of the water for the confined aquifer should be similar to that of recharge waters. The following three examples document this occurrence.

In central Anderson County, the hydraulic head data indicate that a recharge mound results from leakage through the Reklaw aquitard from the overlying Queen City aquifer (fig. 13). Values of pH in this region also confirm the occurrence of this recharge because the waters are less basic than expected for this region (fig. 31).

Around two salt domes, Keechi and Oakwood, there is evidence of recharge. At both domes, uplift

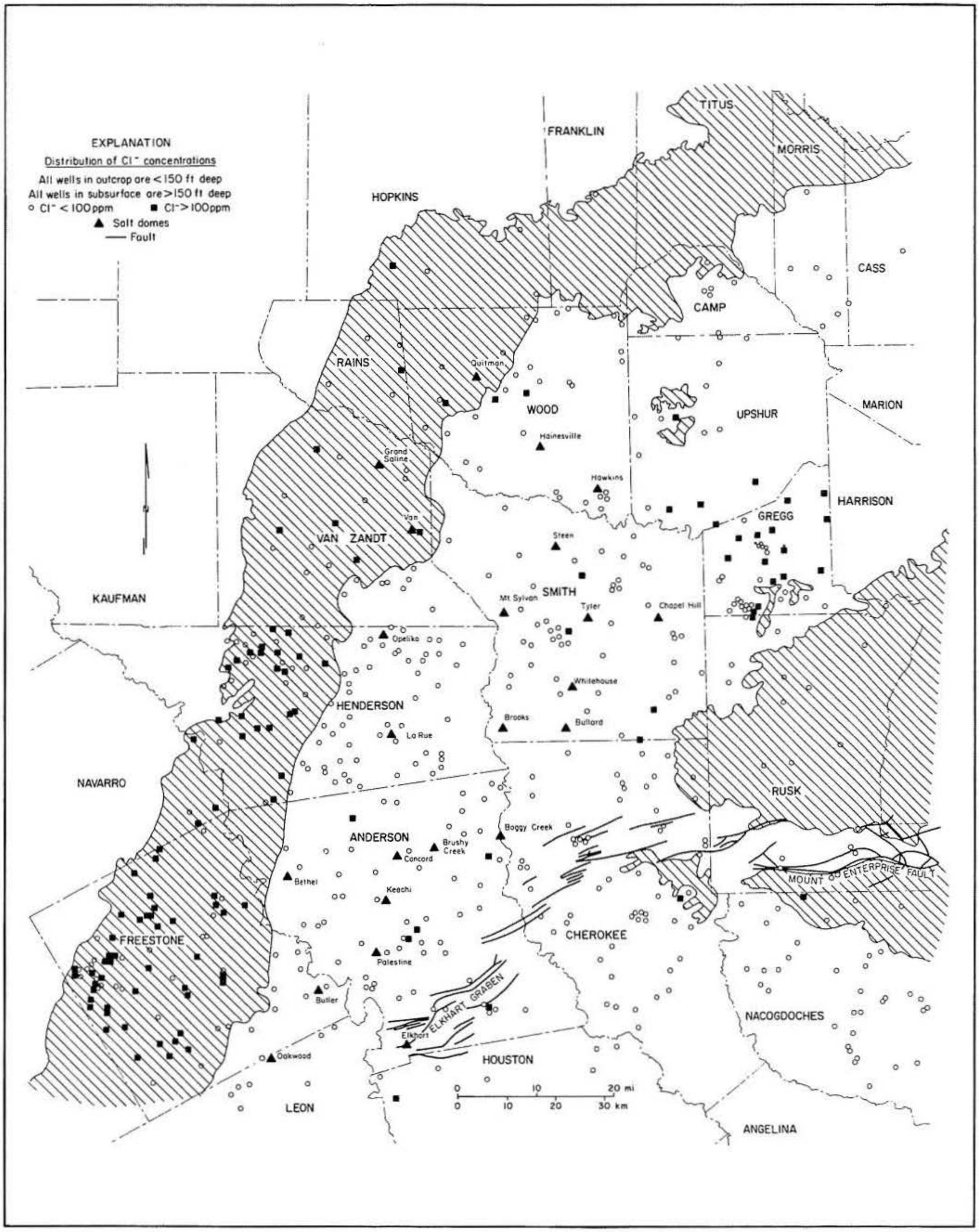

Figure 38. Map view of Cl⁻ concentrations, Wilcox-Carrizo aquifer. Data from oil field areas in the outcrop have been deleted. Note the high Cl⁻ concentrations in the outcrop and in Gregg County. Outcrop indicated by diagonal-line pattern.

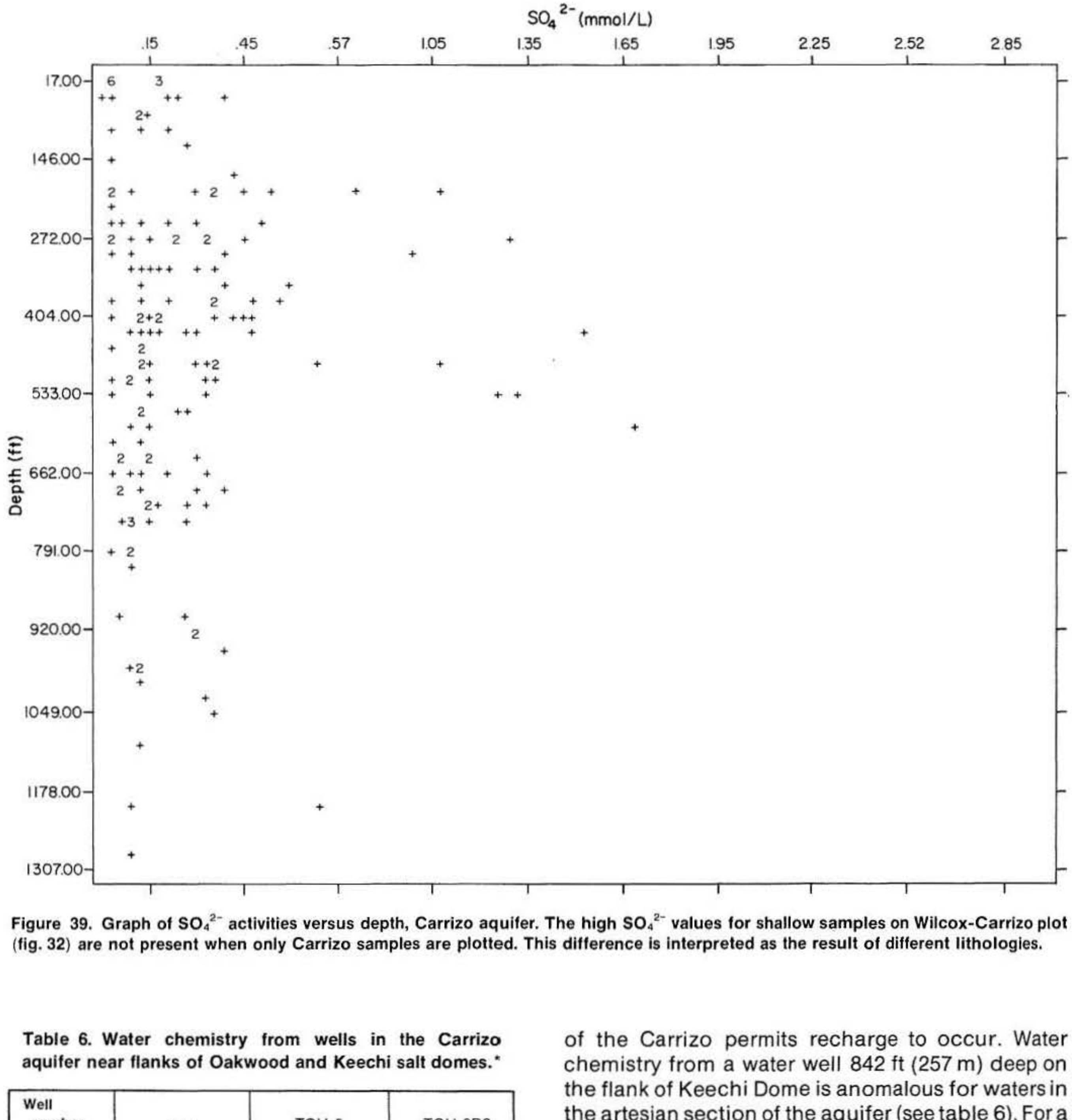

Figure 39. Graph of SO_4^{2-} activities versus depth, Carrizo aquifer. The high SO_4^{2-} values for shallow samples on Wilcox-Carrizo plot (fig. 32) are not present when only Carrizo samples are plotted. This difference is interpreted as the result of different lithologies.

Table 6. Water chemistry from wells in the Carrizo aquifer near flanks of Oakwood and Keechi salt domes.*

Well number	----	TOH-5	TOH-2D2
location	S.W. flank, Keechi Dome	N.E. flank, Oakwood Dome	S.E. flank, Oakwood Dome
Depth (ft)	842	474-600	515-575
pH	7.6	5.2	6.2
Ca^{2+}	6.7	18.3	28.0
Na^{+}	91.0	28.6	36.2
Mg^{2+}	1.3	5.6	9.6
K^{+}	2.1	7.6	9.7
Cl^{-}	16.4	44.0	29.2
SO_4^{2-}	5.7	82.0	158.0
HCO_3^{-}	120.0	121.0	64.3
SiO_2	63.0	17.0	13.0

*Concentrations in mg/L.

of the Carrizo permits recharge to occur. Water chemistry from a water well 842 ft (257 m) deep on the flank of Keechi Dome is anomalous for waters in the artesian section of the aquifer (see table 6). For a ground water in the artesian section of the Wilcox-Carrizo, this sample has anomalously low pH, sodium, and bicarbonate, and has anomalously high silica concentrations. Compare these values with the normal concentrations of these elements in the artesian section of the Wilcox-Carrizo aquifer. Ground water from the Carrizo aquifer on the flank of Oakwood Dome shows similar chemical characteristics of a recharge water--low pH and bicarbonate and high concentrations of calcium and sulfate. The high sulfate concentration may result from anhydrite cap rock dissolution (table 6). A

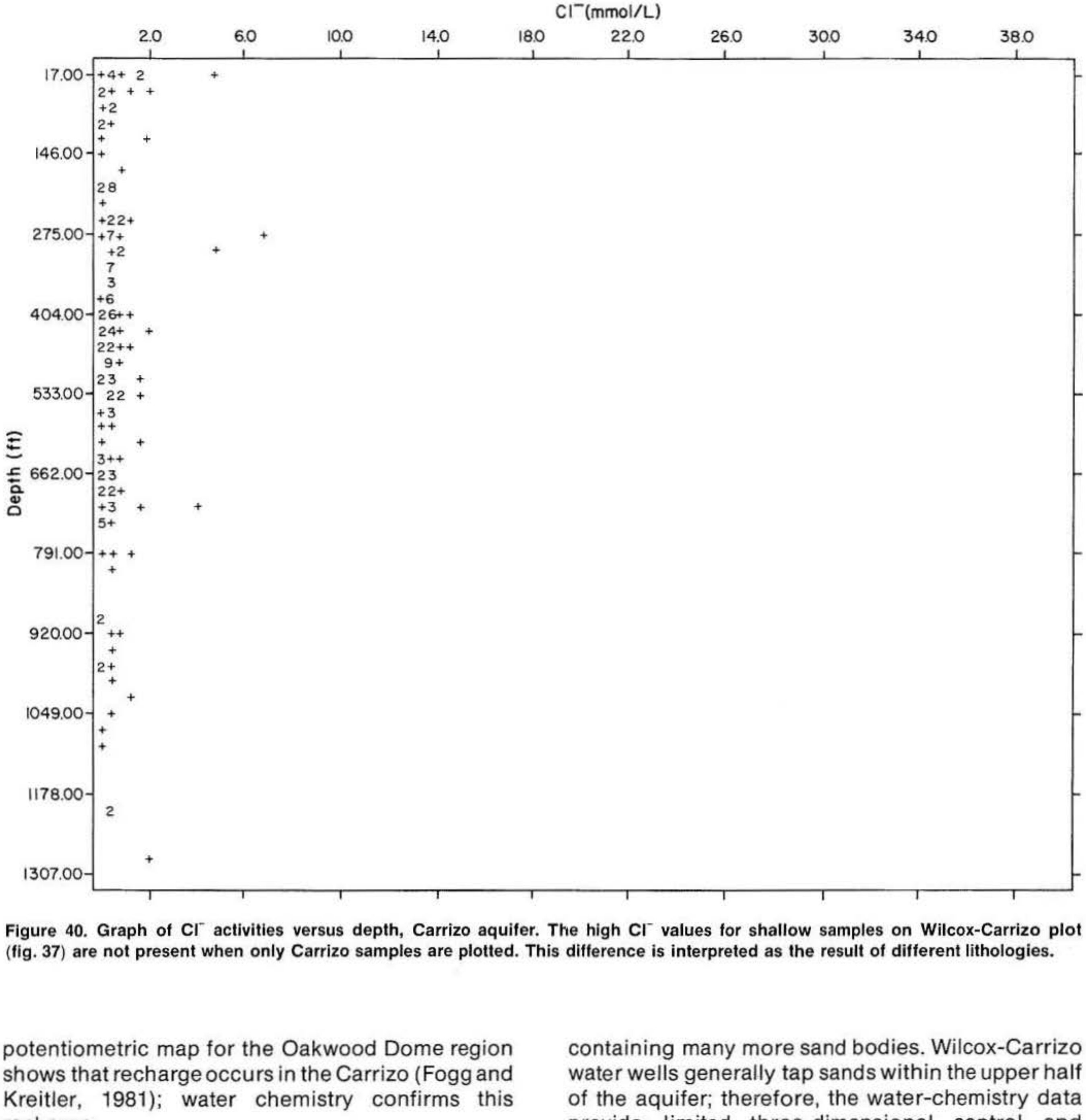

Figure 40. Graph of Cl^- activities versus depth, Carrizo aquifer. The high Cl^- values for shallow samples on Wilcox-Carrizo plot (fig. 37) are not present when only Carrizo samples are plotted. This difference is interpreted as the result of different lithologies.

potentiometric map for the Oakwood Dome region shows that recharge occurs in the Carrizo (Fogg and Kreitler, 1981); water chemistry confirms this recharge.

Low pH values also exist in the northern part of the basin (fig. 31), where the Reklaw aquitard is sandier and therefore probably allows higher rates of recharge.

TOTAL DISSOLVED SOLIDS

Analysis of water-chemistry data helps define important geochemical processes in an aquifer. However, a limitation of the water-chemistry data for the Wilcox-Carrizo is that they commonly represent only individual sand bodies within a thick sequence containing many more sand bodies. Wilcox-Carrizo water wells generally tap sands within the upper half of the aquifer; therefore, the water-chemistry data provide limited three-dimensional control and contribute little to our knowledge of hydrology of the deeper Wilcox-Carrizo in the East Texas Basin.

In an attempt to make a general assessment of the water chemistry in the deeper Wilcox-Carrizo aquifer, the regional distribution of total dissolved solids (TDS) was mapped using values interpreted from approximately 500 electrical resistivity logs. An advantage of this approach is that the logs usually represent most of the Wilcox-Carrizo section. Three specific problems were addressed: (1) fault control on water salinity, (2) facies control on water salinity, and (3) salinity in the deep Wilcox Group.

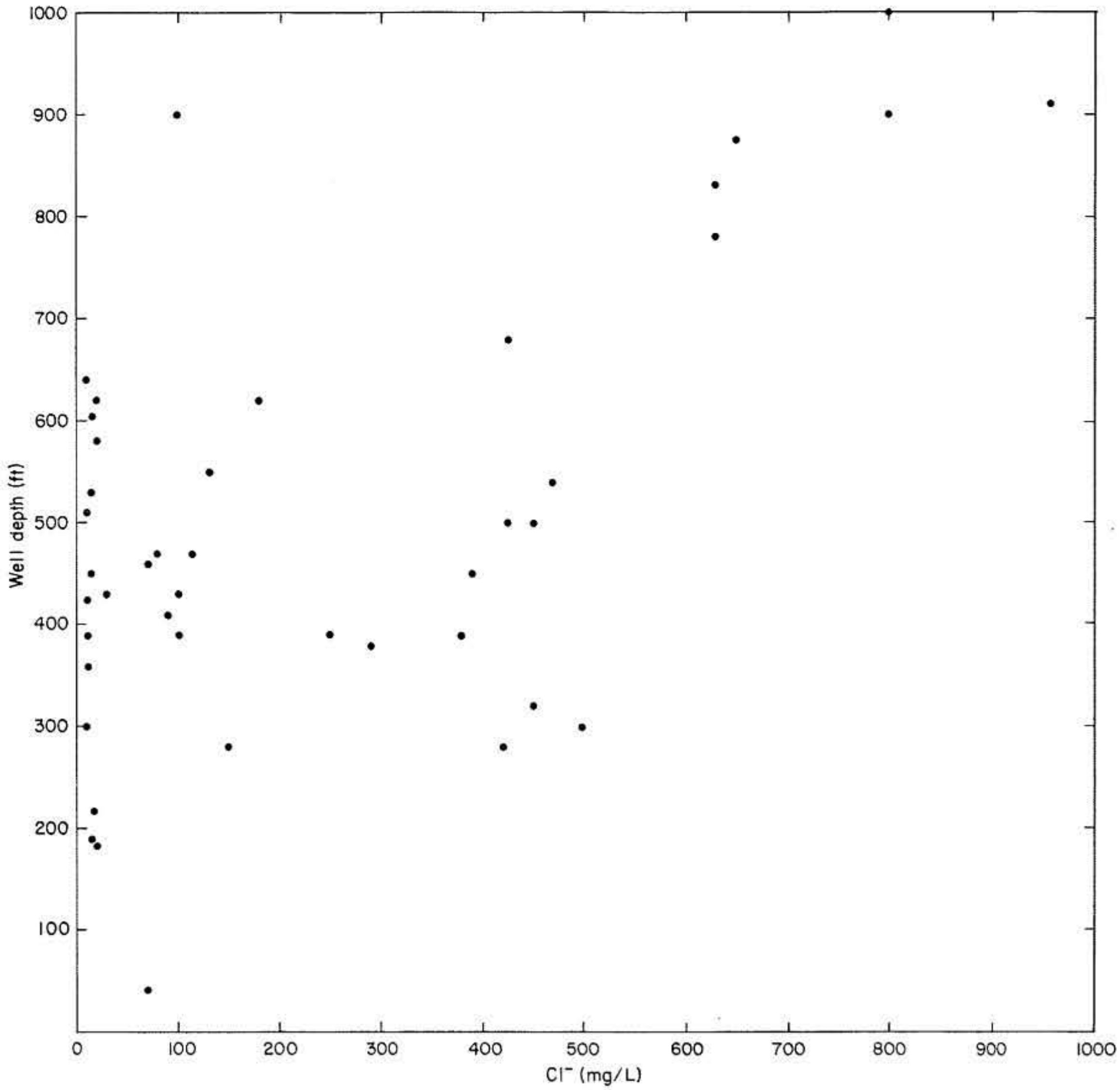

Figure 41. Graph of Cl^- concentrations versus depth, Gregg County, Texas. In contrast to those of figure 37, these Cl^- concentrations increase with depth. The Wilcox aquifer in Gregg County may be a discharge zone for saline waters from deeper in the basin.

Methods

The spontaneous potential (SP) and resistivity values displayed on borehole geophysical logs are partially dependent on electrical resistivity of formation fluid and are commonly used to estimate specific conductivity of formation fluid and, in turn, TDS. Methods for estimating TDS from either the SP or resistivity values are explained by Keys and MacCary (1971). The SP log records natural potentials developed between borehole fluid and the surrounding rock and fluid. If the chemical activities of the fluid in the borehole and of formation fluids are similar, the natural potentials will be weak and the SP will appear as a straight line. This is generally the case in the East Texas Eocene aquifers because they contain mostly fresh water, which contrasts insignificantly with the resistivity of the drilling muds. Thus, the SP could not be used to estimate TDS in Eocene units. Near the base of the Wilcox aquifer, levels of TDS in ground water are frequently high enough to cause noticeable deflections in the SP curve, and thus the SP was helpful as a general indicator of maximum values of TDS. Also, the SP method should be applied cautiously to fresh-water aquifers, since it assumes that the dominant salt in solution is sodium chloride (Alger, 1966; Keys and MacCary, 1971).

Estimates of TDS were made from the resistivity curve using a variation of the method of Turcan

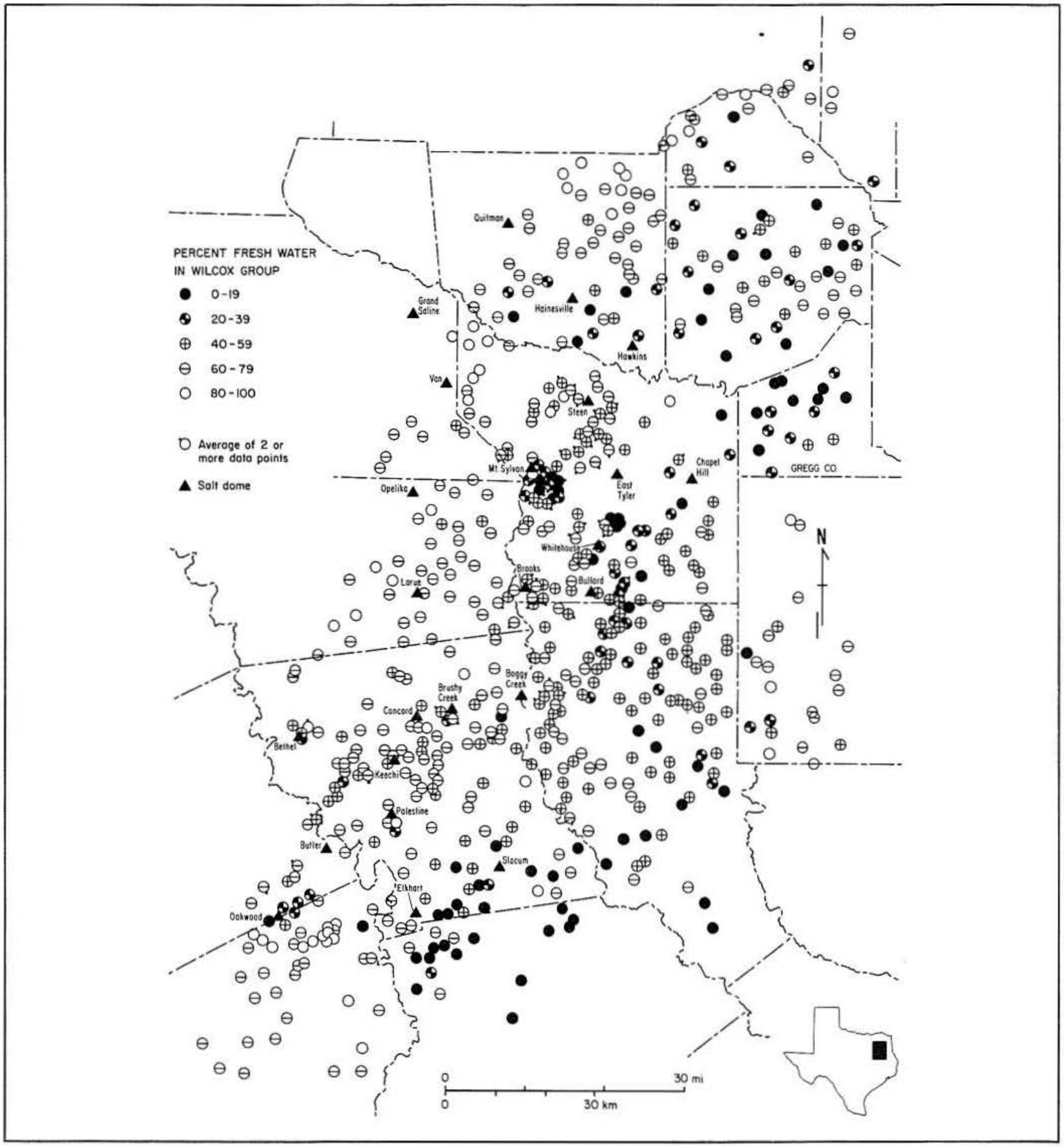

Figure 42. Map showing distribution of percent fresh water (TDS ≤ 1,000 mg/L) in Wilcox aquifer as determined from resistivity values on electric logs. Resistivity values greater than 20 ohm-meters are interpreted to have TDS values less than 1,000 mg/L. Fresh water was defined by resistivity values greater than 20 ohm-meters.

(1966), who applied the concept of a formation factor to calculate TDS values from resistivity logs. A detailed description of the technique used to estimate TDS values for the Eocene aquifers is presented in Fogg (in preparation).

A percent-thickness map of fresh water in the Wilcox Group (fig. 42) was constructed from approximately 500 resistivity logs using the premise that resistivity values of 20 ohm-meters or more indicate fresh water (less than 1,000 mg/L)

(Fogg, in preparation). The Carrizo Formation was not included because in each log examined, the Carrizo waters appeared to be fresh; similarly, the Queen City waters always appeared to be fresh. All water-chemistry determinations and geophysical logs in the Carrizo and Queen City aquifers in the East Texas Basin seem to indicate the presence of fresh water. Immediately south of the Elkhart Graben-Mount Enterprise fault system, these aquifer units dip more steeply into the subsurface, where they contain brackish water. A similar map was constructed by plotting only the thickness-percent values of 40 percent or less on a map showing the high-sand-percent pattern developed by Kaiser and others (1978) and the Elkhart Graben-Mount Enterprise fault zone (fig. 43). This map is useful for comparing TDS anomalies with geologic features.

Figures 42 and 43 indicate salinity variations but provide no information about concentrations of specific ions. Commonly, increased salinity implies increased chloride concentration; in the brackish salinity range, this relation is not well documented. The increase is probably related to monovalent ions, but not necessarily chloride. In the deeper artesian section of the Wilcox-Carrizo aquifer, where the dominant water type is sodium bicarbonate, brackish salinity values may be related to high sodium and bicarbonate values rather than to sodium and chloride. An example from three adjacent monitoring wells near Oakwood salt dome illustrates this point. The three wells with screens located at different depths have electrical resistivity values as well as complete chemical analyses (fig. 44). Measured TDS increases coincident with the TDS values interpreted from the electric logs, but the dramatic increase in TDS in the deepest well is caused by increases in sodium bicarbonate rather than increases in sodium chloride (fig. 44).

Results

The percent-fresh-water map of the Wilcox (fig. 42) shows relative changes in TDS values that have interesting hydrologic implications. South of the Elkhart Graben-Mount Enterprise fault system, the aquifer generally contains brackish water. Ground water in Gregg County is also brackish. The brackish water is limited to the muddier section of the Wilcox (fig. 43). Brackish ground waters, however, are not clustered around salt domes. An additional pattern observed during construction of these maps, but not evident on the maps, is that salinity increases with depth. All but a few electric logs indicate that the fresh water overlies the brackish zone (fig. 44).

Discussion

The high-TDS water downdip from the Elkhart Graben-Mount Enterprise fault system is definitely related to the fault system. The increase in salinity occurs only where faults have been identified in the Tertiary formations. Where fault displacement dies out to the west (Collins and others, 1980), low-TDS ground water extends farther into the subsurface than in the faulted area (fig. 42).

The zone of high-TDS water downdip from the Elkhart Graben-Mount Enterprise fault system may be the result of two different phenomena. The fault zone may alter permeabilities and transmissivities. Complete or partial offsets of discrete sand bodies would decrease transmissivities in this zone. Fault gouge or cementation along fault planes would reduce horizontal permeabilities. A fault can increase vertical permeability by disrupting and fracturing aquitards. Possible sources of any high-TDS water leaking up the faults are lower Wilcox sands and saline Mesozoic aquifers below the Midway Formation, both of which contain consistently high salinity values.

If the faults do not increase vertical permeabilities significantly, they may cause the observed downdip increase in TDS by limiting horizontal flow enough to prevent brackish and saline waters of deposition (connate) from being completely flushed. Such waters may have originated from transgressions over the Wilcox at least three times since it was deposited some 40 million years ago; transgressions occurred during Reklaw, Queen City (Hobday and others, 1979), and Weches times. The saline waters may also have originated from compaction of deep Wilcox sediments located downdip and south of the fault zone and from consequent updip migration of saline water out of the basin.

It can be argued that in dominantly fresh-water aquifer sands as permeable as those in the Wilcox, any saline water that invaded during the geologic past would have been flushed long ago, even near flow barriers such as faults. Existing data provide no way to verify whether the faults have prevented connate water from being completely flushed. Even if such waters have been completely flushed from sands, saline waters may be leaking from muds, which may still be incompletely flushed of the older waters because of the very low permeability of the muds. Calculations of the rate of ground-water movement using Darcy's law with estimated clay hydraulic conductivities of 10^{-4} and 10^{-6} ft/d (0.3×10^{-5} and 3.0×10^{-3} cm/d) (Freeze and Cherry, 1979) and hydraulic gradients (∇h) of 8.0×10^{-4} and 1.9×10^{-4} measured from wells located updip and downdip of the fault system, respectively, show that

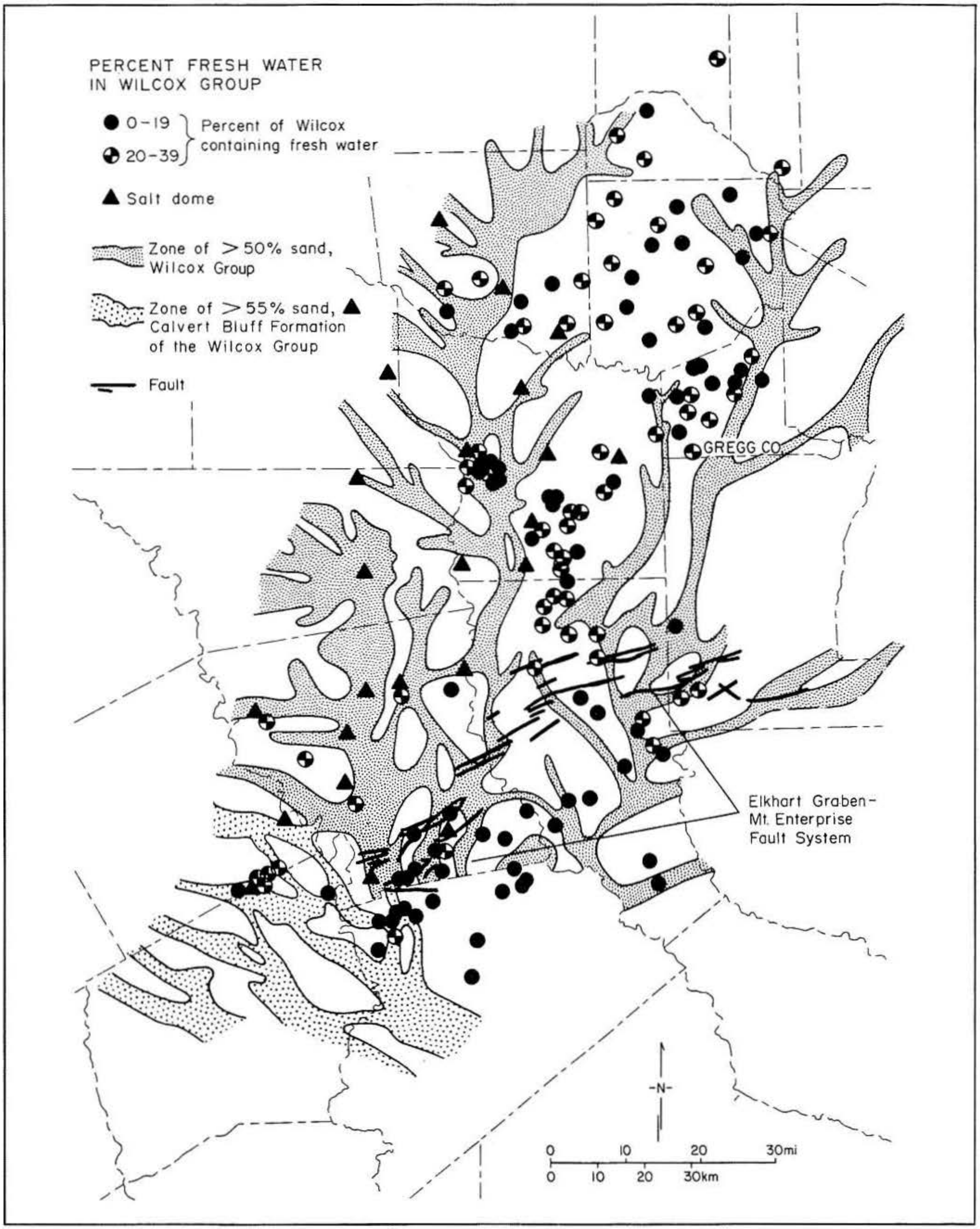

Figure 43. Map showing distribution of fresh-water (TDS ≤ 1,000 mg/L) percentages from figure 42 having values less than 40 percent, the trends of high sand percent from figure 7, and the Elkhart Graben-Mount Enterprise fault system. Anomalies in fresh-water percent are generally associated with muddy parts of the aquifer or with the fault system.

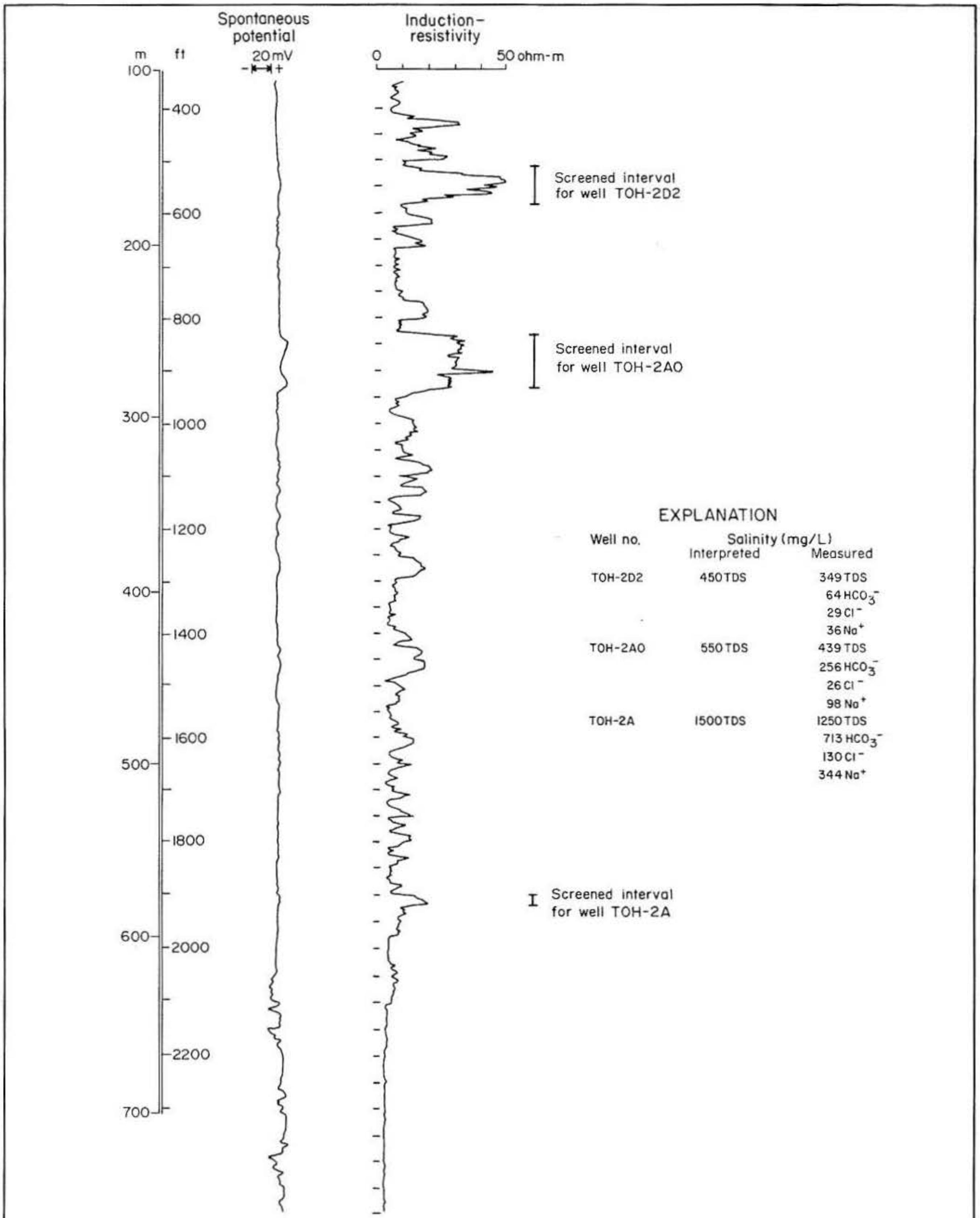

Figure 44. Induction-resistivity and spontaneous-potential curves for Wilcox aquifer near Oakwood Dome. Note general decrease in resistivity (and increase in interpreted salinity) with depth. Increase in salinity correlates better with increase in HCO_3 concentration than with increase in Cl^- concentration.

maximum and minimum rates of ground-water movement near the fault system are about 30 ft/10^6 yr (890 cm/10^6 yr) to 0.1 ft/10^6 yr (2 cm/10^6 yr). At these flow rates, it is feasible that saline water emplaced 40 million years ago during Reklaw, Queen City, or Weches deposition could still be present in the muds and could still be leaking into the sands. Over most of the basin, this saline water would probably have little effect on TDS in sands because of the dilution effect of abundant recharge. Near the fault zone, however, lateral fluxes may be sufficiently low to reduce the dilution effect and to raise TDS values. The measurements of hydraulic gradients used above, although they are from wells tapping sands, are also presumed to be representative of hydraulic heads in muds. This may not be true in areas where the muds are laterally extensive and flow in the muds is consequently vertical.

The brackish ground water in Gregg County (fig. 42) may also be related to leakage of saline waters from deeper formations, discussed previously in the section on chloride. Salinity data (fig. 42) agree with the chloride data (fig. 38).

High-TDS water in the muddy (interchannel) part of the Wilcox aquifer is evident from figure 43, where thicknesses of fresh water less than 40 percent are plotted with the sand channel systems from figure 7. North of the Elkhart Graben-Mount Enterprise fault zone, high-TDS water is most prevalent in the extensive low-sand-percent area extending from Cherokee to Upshur County. In fact, few high TDS values from wells in the high sand trends (fig. 43) occur except near the fault zone, Mount Sylvan Dome, and a few scattered locations near margins of sand trends. Possible sources of the high-TDS water are salt dome solution and, again, connate waters. Possible factors that prevented these waters from being completely flushed are (1) slow circulation in the interchannel sands because of their discontinuous nature and (2) slow leakage of water out of the muds. The latter factor may be especially important because of the relative abundance of mud facies in the interchannel areas.

The brackish ground water in the Wilcox aquifer typically lies beneath the low-TDS ground water (fig. 44). Near salt domes, lenses of brackish water may interfinger with fresh waters. These higher salinities may be caused by high sodium and bicarbonate concentrations rather than by increased sodium and chloride concentrations. This increase in sodium and bicarbonate content in the deep aquifer is evident in the chemical analyses from the three monitoring wells on the flank of Oakwood Dome. The bicarbonate concentration increases much more rapidly than does the chloride concentrat on (fig. 44). These high bicarbonate concentrations result from the combined reactions of coalification, calcite dissolution, and cation exchange.

Delineation of saline plumes from salt dome dissolution is complicated by other sources of salinity. Brackish waters may result from mixing of saline waters that leaked up along faults from deeper formations, from earlier formation waters slowly discharging into the permeable sands, or from long distances of transport that generated high sodium and high bicarbonate concentrations.

IMPLICATIONS FOR TRANSPORT OF GROUND-WATER CONTAMINANTS

The regional ground-water hydraulics and chemistry of meteoric aquifers in the East Texas Basin have direct implications for the transport of ground-water contaminants and for the evaluation of the suitability of a contaminant disposal site. Contaminants entering the ground-water system by means of the outcrops of either the Queen City or the Wilcox-Carrizo would have the greatest potential for resurfacing as ground-water discharge because of the closely spaced topographically controlled recharge and discharge areas in the outcrop areas. Contamination of any of the large recharge mounds in the Wilcox-Carrizo outcrop could potentially affect ground-water quality over a large area in both the outcrop and the artesian sections. Ground-water flow lines emanating from the large recharge mound in Van Zandt County extend over an area of several thousand square miles (fig. 14). Travel times from such a recharge area down into the artesian section, however, are probably on the order of 10^3 to 10^4 years (Kreitler and Wuerch, 1981).

Contaminants in the artesian section of the Wilcox-Carrizo would tend to move downward owing to the predominantly downward flow in the system. Nearly all the water wells tap the upper half of the Wilcox-Carrizo. The potential for upward flow apparently exists only near streams and, perhaps, in the Elkhart Graben-Mount Enterprise fault zone. In these areas, the potential for contamination of water wells or the biosphere is greatest. An assessment of potential impacts of contaminants in the artesian section should at least attempt to identify the sites of potential upward flow. Fortunately, these sites are relatively easy to recognize because they typically occur along the streams that have incised deepest into the stratigraphic column. The upward-flow hypothesis for a discharge site can then be tested by constructing well nests with screens at different depths.

Since salt domes are generally sites of recharge into the artesian section, potential for downward flow probably is increased near the domes. This, however, may be countered by upward flow along dome flanks from deeper aquifers. There is little evidence from water-chemistry data or electric log data to indicate that the domes are dissolving, which suggests that the domes are not in direct hydraulic communication with the meteoric aquifers. Salt dome hydrology is addressed in greater detail by Fogg and Kreitler (1981).

Transport of nonconservative ionic species in an aquifer is dependent on the geochemical environment of the aquifer. Because of chemical evolution, the ground water alters from an oxidizing acidic water in outcrop to a reducing basic water in the artesian part of the aquifer. Different ions are attenuated to varying degrees in these different environments. Many trace metals are more mobile in oxidizing environments. Henry and others (1982) observed decreasing concentrations of uranium, selenium, molybdenum, and arsenic as ground waters in the Oakville aquifer moved downdip and became more reducing. They attributed the decrease to either precipitation or adsorption of the metals. The same is true with radionuclides; they are less soluble in basic reducing ground waters (Bondietti, 1978; Relyea and others, 1978). Some radionuclides would be expected to be relatively immobile in the deep sections of the aquifer. The cation exchange capacity should be high throughout the aquifer. In the deeper parts of the aquifer, where coalification may be occurring, high concentrations of dissolved organics, as well as methane, may be present. These organics would be effective complexing agents for trace metals or radionuclides (Means and Hastings, 1979). Similarly, organic acids originating in the soil zone may be present in the shallow recharge water.

Information provided in this report does not provide absolute answers for ground-water contamination problems that may occur in the East Texas Basin. Such problems need to be addressed by site-specific studies, possibly involving test drilling and monitoring. A critical question of where to drill then arises. To select drill sites that will economically yield a maximum amount of relevant data, one must at least develop a conceptual model of the particular hydrogeologic system. The physical and chemical mechanisms outlined in this report can be used to conceive realistic conceptual models of Eocene aquifers in the East Texas Basin. Even if a given study area lacks hydraulic head data and water-chemistry data, a rational program of investigation could be devised on the basis of knowledge of the regional system and the local topography and geology.

ACKNOWLEDGMENTS

Funding for this research was provided by the U.S. Department of Energy under Contract No. DE-AC97-80ET46617. The authors are grateful to L. F. Brown, Jr., R. L. Bassett, W. F. Guyton, Sr., W. R. Kaiser, and R. T. Budnik, who critically reviewed the manuscript and provided helpful suggestions that improved the quality of this report. Sincere appreciation is also expressed to S. Cumella, E. Duncan, and C. Chomicky, who helped with the organization and mapping of data. Select chemical analyses were conducted at the Mineral Studies Laboratory, Bureau of Economic Geology, by Clara L. Ho and Steven W. Tweedy.

Typesetting was done by Phyllis J. Hopkins under the direction of Lucille C. Harrell. Drafting was done by John T. Ames, Thomas M. Byrd, Micheline R. Davis, Margaret L. Evans, Byron P. Holbert, Jeffrey Horowitz, and Judith Johnson under the direction of Dan F. Scranton, chief cartographer. Rebecca P. Lasley and Jean Trimble edited the report. Micheline R. Davis designed the cover and layout. Text illustration photography was by James A. Morgan.

REFERENCES

Alger, R. P., 1966, Interpretation of electric logs in fresh-water wells in unconsolidated formations: Society of Professional Well Log Analysts Seventh Annual Logging Symposium, Tulsa, Oklahoma, Transactions, p. CC1-CC25.

Anders, R. B., 1967, Ground-water resources of Sabine and San Augustine Counties, Texas: Texas Water Development Board Report 37, 115 p.

Back, William, 1966, Hydrochemical facies and ground-water flow patterns in northern part of Atlantic Coastal Plain: U.S. Geological Survey Professional Paper 498-A, 42 p.

Baker, B. B., Dillard, J. W., Souders, V. L., and Peckham, R. C. 1963a, Reconnaissance investigation of the ground-water resources of the Sabine River basin, Texas: Texas Water Commission Bulletin 6307, 57 p.

Baker, B. B., Peckham, R. C., Dillard, J. W., and Souders, V. L., 1963b, Reconnaissance investigation of the ground-water resources of the Neches River basin, Texas: Texas Water Commission Bulletin 6308, 67 p.

Barnes, V. E., 1965, Tyler sheet: University of Texas, Austin, Bureau of Economic Geology, Geologic Atlas of Texas, scale 1:250,000.

____ 1966, Texarkana sheet: University of Texas, Austin, Bureau of Economic Geology, Geologic Atlas of Texas, scale 1:250,000.

____ 1967, Sherman sheet: The University of Texas at Austin, Bureau of Economic Geology, Geologic Atlas of Texas, scale 1:250,000.

____ 1968, Palestine sheet: The University of Texas at Austin, Bureau of Economic Geology, Geologic Atlas of Texas, scale 1:250,000.

____ 1970, Waco sheet: The University of Texas at Austin, Bureau of Economic Geology, Geologic Atlas of Texas, scale 1:250,000.

____ 1972, Dallas sheet: The University of Texas at Austin, Bureau of Economic Geology, Geologic Atlas of Texas, scale 1:250,000.

Bondietti, E., 1978, The effect of redox potential on sorption of radionuclides to geologic media: Proceedings of the Task 4 Waste Isolation Safety Assessment Program, Battelle Pacific Northwest Laboratories, Second Contract Information Meeting, v. 1, EY-76-C-06-1830, p. 379-403.

Boulton, N. S., 1963, Analysis of data from non-equilibrium pumping tests allowing for delayed yield from storage: Proceedings of the Institute of Civil Engineering 26, p. 469-482.

Broom, M. E., 1968, Ground-water resources of Wood County, Texas: Texas Water Development Board Report 79, 84 p.

____ 1969, Ground-water resources of Gregg and Upshur Counties, Texas: Texas Water Development Board Report 101, 76 p.

Broom, M. E., Alexander, W. H., Jr., and Myers, B. N., 1965, Ground-water resources of Camp, Franklin, Morris, and Titus Counties, Texas: Texas Water Commission Bulletin 6517, 153 p.

Broom, M. E., and Myers, B. N., 1966, Ground-water resources of Harrison County, Texas: Texas Water Development Board Report 27, 73 p.

Collins, E. W., 1980, The Reklaw Formation of East Texas, *in* Perkins, B. F., and Hobday, D. K., eds., Middle Eocene coastal plain and nearshore deposits of East Texas, a field guide to the Queen City Formation and related papers: Society of Economic Paleontologists and Mineralogists, Gulf Coast Guidebook, p. 67-70.

Collins, E. W., Hobday, D. K., and Kreitler, C. W., 1980, Quaternary faulting in East Texas: The University of Texas at Austin, Bureau of Economic Geology Geological Circular 80-1, 20 p.

Davis, S. N., 1964, Silica in streams and ground water: American Journal of Science, v. 262, p. 870-891.

Dillard, J. W., 1963, Availability and quality of ground water in Smith County, Texas: Texas Water Commission Bulletin 6302, 35 p.

Dutton, S. P., 1980, Petrography and diagenesis of Wilcox sandstones, *in* Kreitler, C. W., Agagu, O. K., Basciano, J. M., Collins, E. W., Dix, O., Dutton, S. P., Fogg, G. E., Giles, A. B., Guevara, E. H., Harris, D. W., Hobday, D. K., McGowen, M. K., Pass, D., and Wood, D. H., Geology of the East Texas Basin -- a report on the progress of nuclear waste isolation feasibility studies (1979): The University of Texas at Austin, Bureau of Economic Geology Geological Circular 80-12, p. 83-87.

Fisher, W. L., 1964, Sedimentary patterns in Eocene cyclic deposits, northern Gulf Coast region: Kansas Geological Survey Bulletin 169, v. 1, p. 151-170.

____ 1965, Rock and mineral resources of East Texas: University of Texas, Austin, Bureau of Economic Geology Report of Investigations No. 54, 439 p.

Fisher, W. L., and McGowen, J. H., 1967, Depositional systems in the Wilcox Group of Texas and their relationship to the occurrence of oil and gas: Gulf Coast Association of Geological Societies Transactions, v. 17, p. 105-125.

Fogg, G. E., in preparation, Estimating ground-water quality using borehole-resistivity logs: The University of Texas at Austin, Bureau of Economic Geology.

Fogg, G. E., and Kreitler, C. W., 1981, Ground-water hydrology around salt domes in the East Texas Basin: a practical approach to the contaminant transport problem: Bulletin of the Association of Engineering Geologists, v. 18, no. 4, p. 387-411.

Foster, M. D., 1950, The origin of high sodium bicarbonate waters in the Atlantic and Gulf Coastal Plains: Geochimica et Cosmochimica Acta, v. 1, p. 33-48.

Freeze, R. A., and Cherry, J. A., 1979, Groundwater: New Jersey, Prentice-Hall, 604 p.

Garrels, R. M., and MacKenzie, F. T., 1967, Origin of the chemical composition of some springs and lakes, *in* Gould, R. F., ed., Equilibrium concepts in natural water systems: Washington, D.C., American Chemical Society Publications.

Guyton, W. F., and Associates, 1970, Ground-water conditions in Angelina and Nacogdoches Counties, Texas: Texas Water Development Board Report 110, 125 p.

_____ 1972, Ground-water conditions in Anderson, Cherokee, Freestone, and Henderson Counties, Texas: Texas Water Development Board Report 150, 250 p.

Henry, C. D., and Basciano, J. M., 1979, Environmental geology of the Wilcox Group lignite belt, East Texas: The University of Texas at Austin, Bureau of Economic Geology Report of Investigations No. 98, 28 p.

Henry, C. D., Basciano, J. M., and Duex, T. W., 1979, Hydrology and water quality of the Eocene Wilcox Group: significance for lignite development in East Texas: Gulf Coast Association of Geological Societies Transactions, v. 29, p. 127-135.

Henry, C. D., Galloway, W. E., Smith, G. E., Ho, C. L., Morton, J. P., and Gluck, J. K., 1982, Geochemistry of ground water in the Oakville sandstone, a major aquifer and uranium host of the Texas Coastal Plain: The University of Texas at Austin, Bureau of Economic Geology Report of Investigations No. 118, 63 p.

Hobday, D. K., Morton, R. A., and Collins, E. W., 1979, The Queen City Formation in the East Texas Embayment: a depositional record of riverine, tidal, and wave interaction: Gulf Coast Association of Geological Societies Transactions, v. 29, p. 136-146.

Kaiser, W. R., Johnston, J. E., and Bach, W. N., 1978, Sand-body geometry and the occurrence of lignite in the Eocene of Texas: The University of Texas at Austin, Bureau of Economic Geology Geological Circular 78-4, 19 p.

Keys, W. S., and MacCary, L. M., 1971, Application of borehole geophysics to water-resource investigations, *in* U.S. Geological Survey, Techniques of water-resources investigations: Chapter E1, Book 2, 124 p.

Kharaka, Y. K., and Barnes, I., 1973, SOLMNEQ: solution-mineral equilibrium computations: NTIS Technical Report PB214-899, 82 p.

Kreitler, C. W., Guevara, E., Granata, G., and McKalips, D., 1977, Hydrogeology of Gulf Coast aquifers, Houston-Galveston area: Gulf Coast Association of Geological Societies Transactions, v. 27, p. 72-89.

Kreitler, C. W., and Wuerch, H. V., 1981, Carbon-14 dating of ground water near Oakwood Dome, East Texas, *in* Kreitler, C. W., Collins, E. W., Davidson, E. D., Jr., Dix, O. R., Donaldson, G. A., Dutton, S. P., Fogg, G. E., Giles, A. B., Harris, D. W., Jackson, M. P. A., Lopez, C. M., McGowen, M. K., Muehlberger, W. R., Pennington, W. D., Seni, S. J., Wood, D. H., and Wuerch, H. V., 1981, Geology and geohydrology of the East Texas Basin: a report on the progress of nuclear waste isolation feasibility studies (1980): The University of Texas at Austin, Bureau of Economic Geology Geological Circular 81-7, p. 156-161.

Means, J. L., and Hastings, D. W., 1979, Status report on the importance of natural organic compounds in ground water as radionuclide-mobilization agents: Office of Nuclear Waste Isolation, Battelle Memorial Institute, 29 p.

Myers, B. N., 1969, Compilation of results of aquifer tests in Texas: Texas Water Development Board Report 98, 532 p.

Neuman, S. P., 1972, Theory of flow in unconfined aquifers considering delayed response of the water table: Water Resources Research, v. 8, p. 1031-1045.

Nichols, P. H., Peterson, G. E., and Wuestner, C. E., 1968, Summary of subsurface geology of northeast Texas: American Association of Petroleum Geologists Memoir 9, v. 2, p. 982-1004.

Nie, N. H., Hull, C. H., Jenkins, J. G., Steinbrennar, K., and Bent, D. H., 1975, SPSS: statistical package for the social sciences (2nd ed.): New York, McGraw-Hill, 675 p.

Peckham, R. C., 1965, Availability and quality of ground water in Leon County, Texas: Texas Water Commission Bulletin 6513, 43 p.

Peckham, R. C., Souders, V. L., Dillard, L. W., and Baker, B. B., 1963, Reconnaissance investigation of the ground-water resources of the Trinity River basin, Texas: Texas Water Commission Bulletin 6309, 109 p.

Piper, A. M., 1944, A graphic procedure in the geochemical interpretation of water analyses: American Geophysical Union Transactions, v. 25, p. 914-923.

Plummer, L. N., Jones, B. F., and Truesdell, A. H., 1976, WATEQF: a FORTRAN IV version of WATEQ, a computer program for calculating chemical equilibrium of natural waters: U.S. Geological Survey Water-Resources Investigations 76-13, 66 p.

Relyea, S. F., Ames, L. L., Serne, R. J., Fulton, R. W., and Washburne, C. D., 1978, Batch KD determinations with common minerals and representative ground waters: Proceedings of the Task 4 Waste Isolation Safety Assessment Program, Battelle Pacific Northwest Laboratories, Second Contract Information Meeting, v. 2, PNL-SA-7352, p. 259-330.

Seni, S. J., and Fogg, G. E., in preparation, Wilcox Group facies and syndepositional salt dome growth, southern East Texas Basin: The University of Texas at Austin, Bureau of Economic Geology.

Smith, C. G., Jr., 1976, Geohydrology of northeast Texas and Mississippi salt domes, *in* Martinez, L. D., Thorns, R. L., Kupfer, D. H., Smith, C. G., Jr., Kolb, C. R., Newchurch, E. J., Wilcox, R. E., Manning, T. A., Jr., Romberg, M., Lewis, A. L., and Rovik, L. E., An investigation of the utility of Gulf Coast salt domes for the storage or disposal of radioactive wastes: Louisiana State University, Institute for Environmental Studies, p. 237-282.

Stenzel, H. B., 1938, The geology of Leon County, Texas: University of Texas, Austin, Bureau of Economic Geology Publication 3818, 295 p.

Tarver, G. E., 1966, Ground-water resources of Houston County, Texas: Texas Water Development Board Report 18, 89 p.

Thornthwaite, C. W., 1948, An approach toward a rational classification of climate: Geographical Review, v. 38, p. 55-94.

Thorstenson, D. C., Fisher, D. W., and Croft, M. G., 1979, The geochemistry of the Fox Hills-Basal Hill Creek aquifer in southwestern North Dakota and northwestern South Dakota: Water Resources Research, v. 15, no. 6, p. 1479-1498.

Tóth, J., 1978, Gravity-induced cross-formational flow of formation fluids, Red Earth Region, Alberta, Canada: analysis, patterns, and evolution: Water Resources Research, v. 14, no. 5, p. 805-843.

Turcan, A. N., Jr., 1966, Calculation of water quality from electrical logs--theory and practice: Louisiana Geological Survey Water Resources Pamphlet 19, 23 p.

U.S. Geological Survey, 1975, Surface water supply of the United States, 1966-70, Part 8. Western Gulf of Mexico Basins, Volume 1: basins from Mermentau River to Colorado River: U.S. Geological Survey Water-Supply Paper 2122, 1144 p.

U.S. Government Printing Office, 1980, Census of population and housing advance report, Texas: Washington, D.C., publication PH80-v-45.

White, D. E., 1973, Ground-water resources of Rains and Van Zandt Counties, Texas: Texas Water Development Board Report 169, 80 p.

Wood, D. H., and Guevara, E. H., 1981, Regional structural cross sections and general stratigraphy, East Texas Basin: The University of Texas at Austin, Bureau of Economic Geology Cross Sections, 22 p.

APPENDIX A

TRENDS IN GROUND-WATER USE, EAST TEXAS BASIN

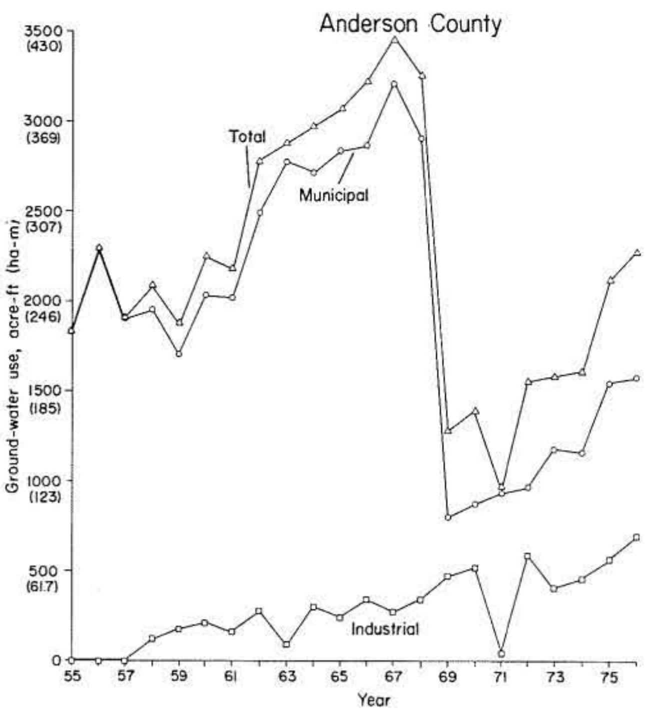

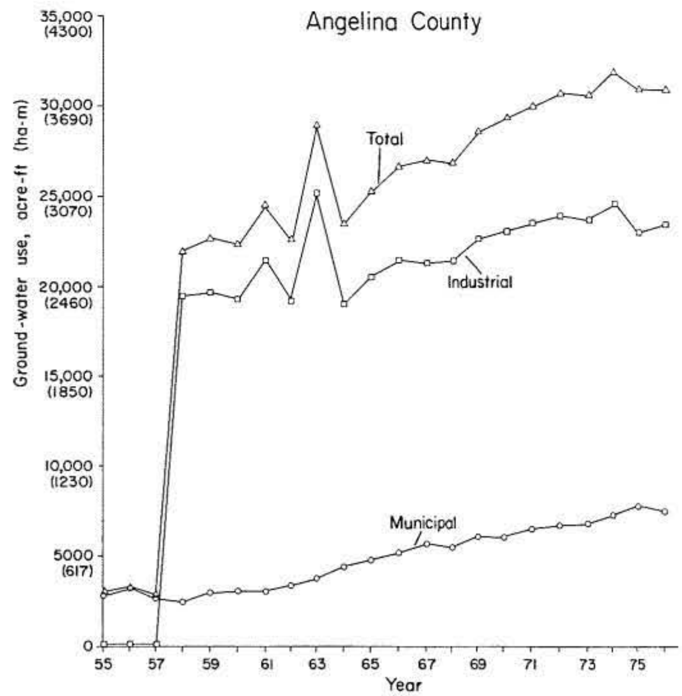

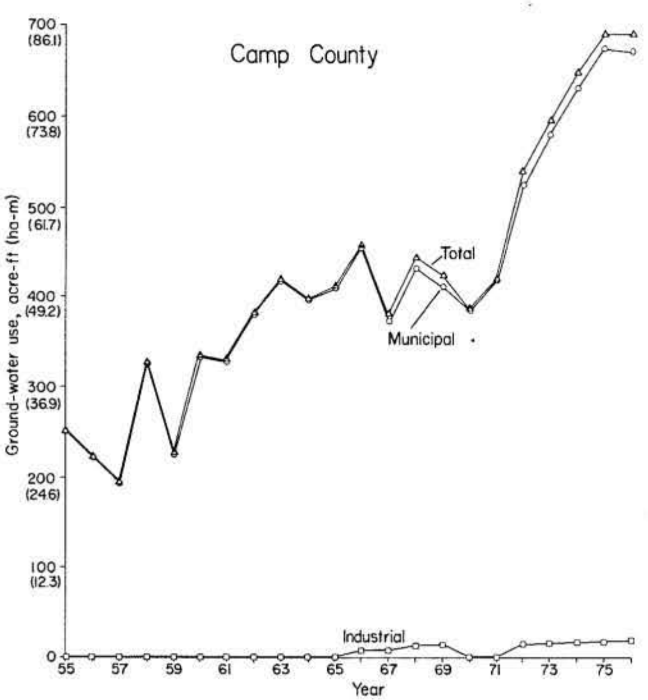

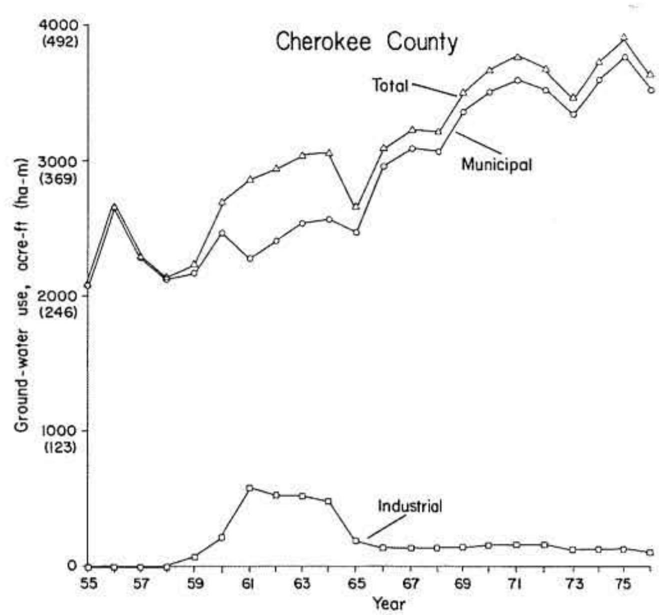

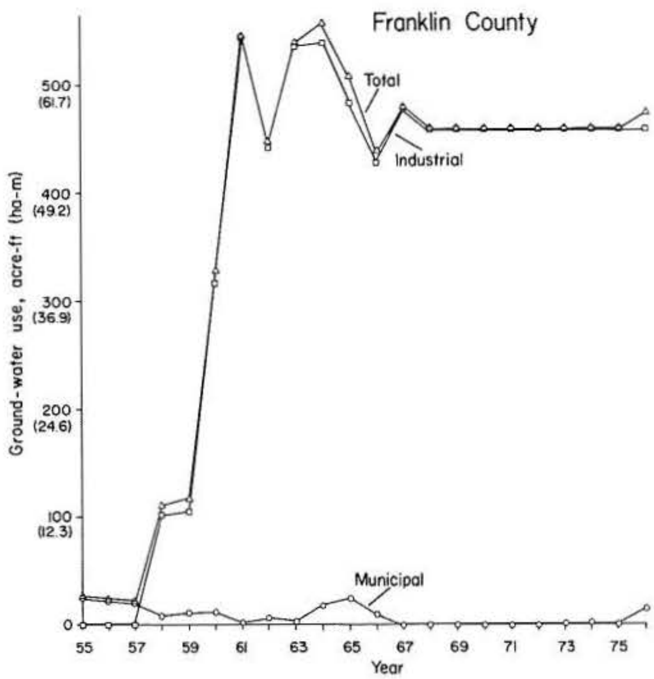
Franklin County
Total
Industrial
Municipal
Ground-water use, acre-ft (ha-m)
500 (61.7)
400 (49.2)
300 (36.9)
200 (24.6)
100 (12.3)
0
55 57 59 61 63 65 67 69 71 73 75
Year

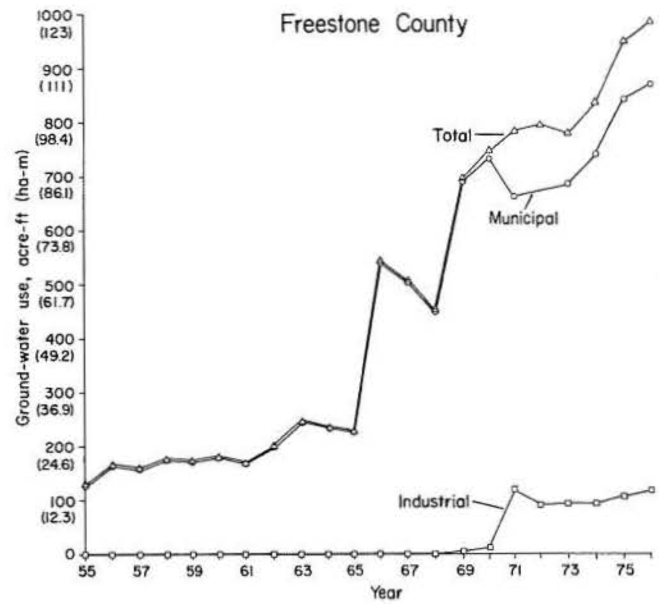
Freestone County
Total
Municipal
Industrial
Ground-water use, acre-ft (ha-m)
1000 (123)
900 (111)
800 (98.4)
700 (86.1)
600 (73.8)
500 (61.7)
400 (49.2)
300 (36.9)
200 (24.6)
100 (12.3)
0
55 57 59 61 63 65 67 69 71 73 75
Year

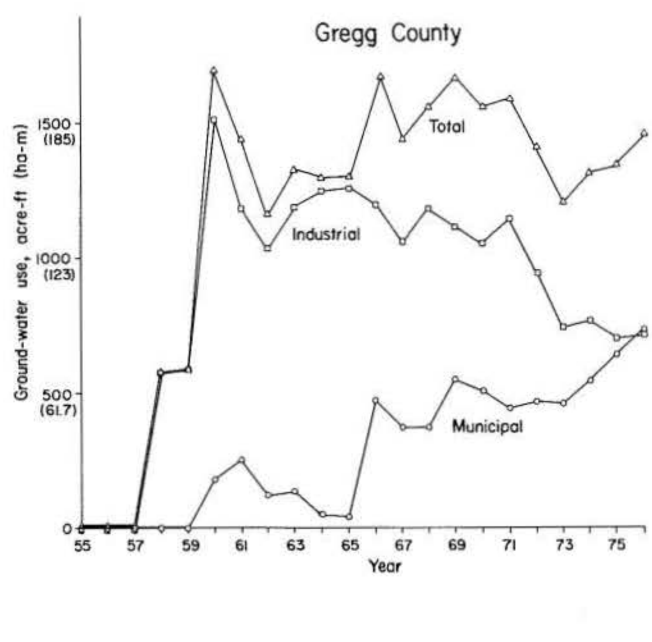
Gregg County
Total
Industrial
Municipal
Ground-water use, acre-ft (ha-m)
1500 (185)
1000 (123)
500 (61.7)
0
55 57 59 61 63 65 67 69 71 73 75
Year

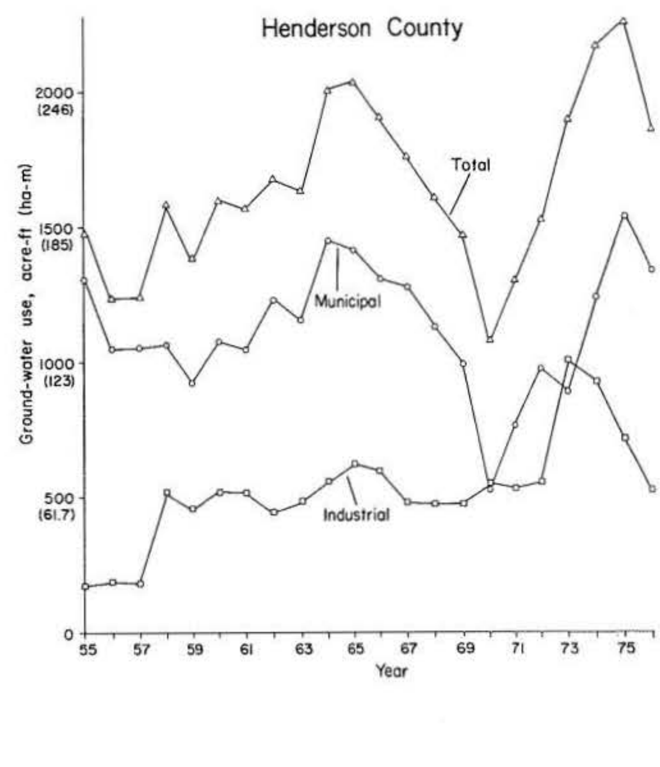
Henderson County
Total
Municipal
Industrial
Ground-water use, acre-ft (ha-m)
2000 (246)
1500 (185)
1000 (123)
500 (61.7)
0
55 57 59 61 63 65 67 69 71 73 75
Year

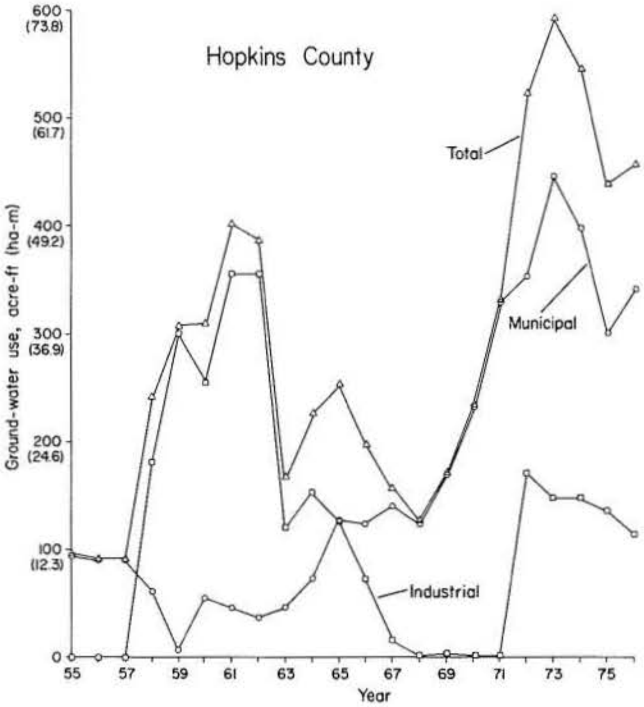
Hopkins County
Ground-water use, acre-ft (ha-m)
600 (73.8)
500 (61.7)
400 (49.2)
300 (36.9)
200 (24.6)
100 (12.3)
0
Total
Municipal
Industrial
55 57 59 61 63 65 67 69 71 73 75
Year

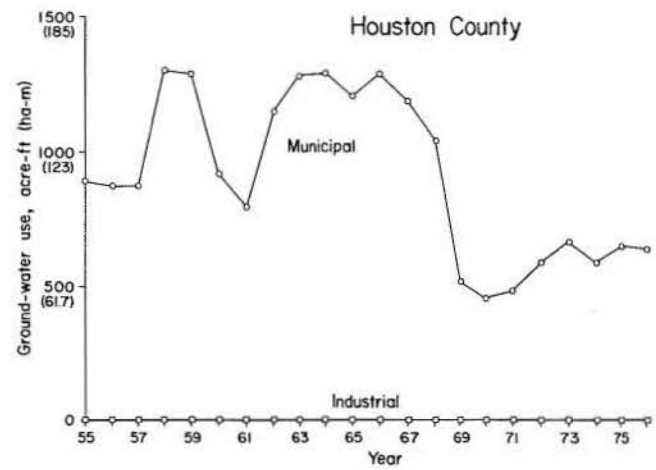
Houston County
Ground-water use, acre-ft (ha-m)
1500 (185)
1000 (123)
500 (61.7)
0
Municipal
Industrial
55 57 59 61 63 65 67 69 71 73 75
Year

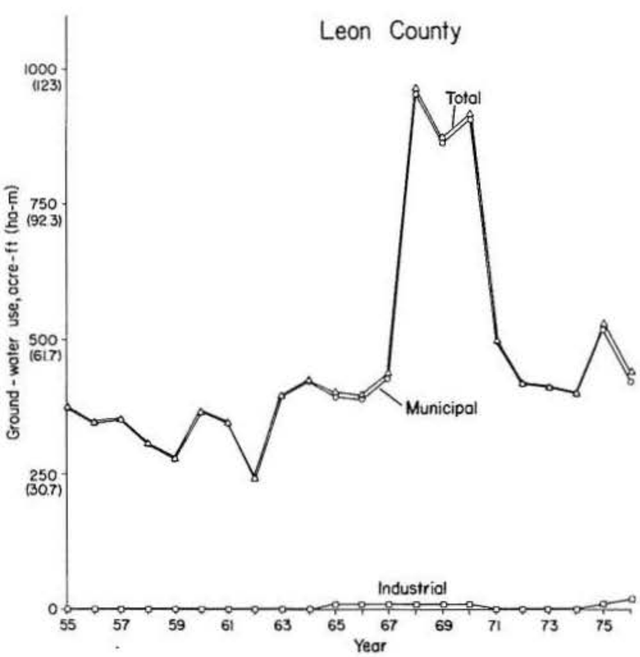
Leon County
Ground-water use, acre-ft (ha-m)
1000 (123)
750 (92.3)
500 (61.7)
250 (30.7)
0
Total
Municipal
Industrial
55 57 59 61 63 65 67 69 71 73 75
Year

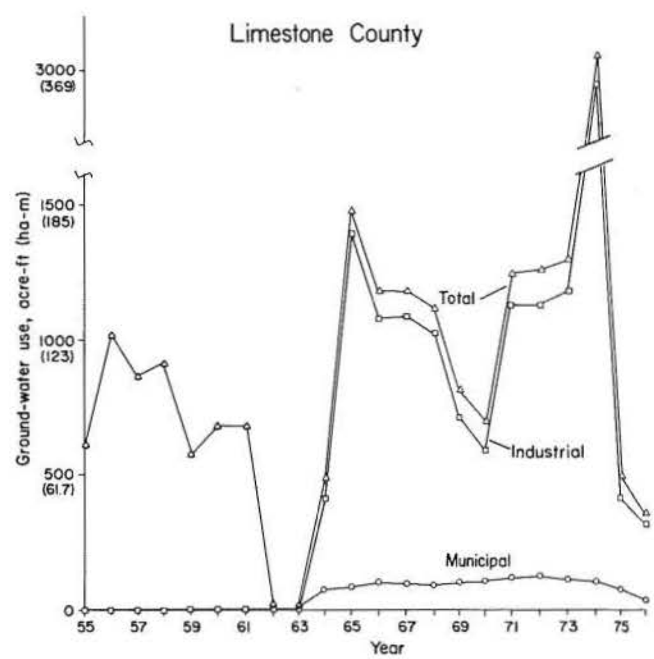
Limestone County
Ground-water use, acre-ft (ha-m)
3000 (369)
1500 (185)
1000 (123)
500 (61.7)
0
Total
Industrial
Municipal
55 57 59 61 63 65 67 69 71 73 75
Year

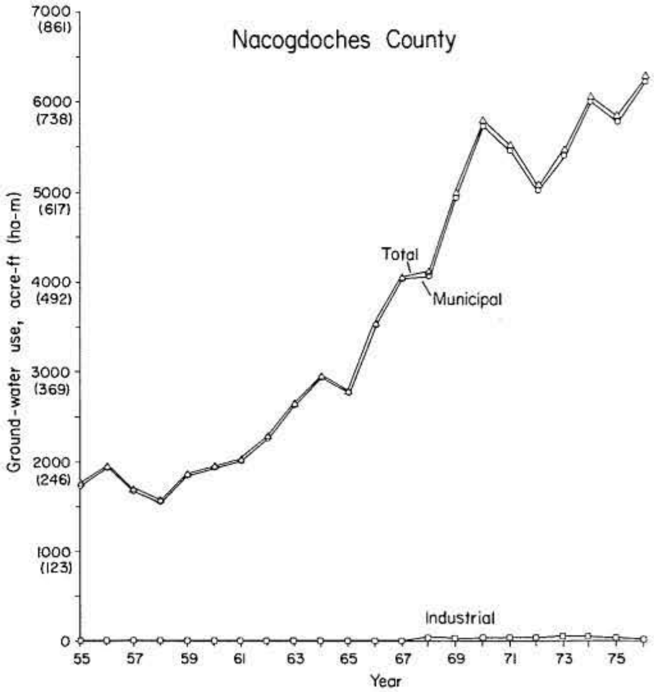
Nacogdoches County
Ground-water use, acre-ft (ha-m)
7000 (861)
6000 (738)
5000 (617)
4000 (492)
3000 (369)
2000 (246)
1000 (123)
0
Total
Municipal
Industrial
55 57 59 61 63 65 67 69 71 73 75
Year

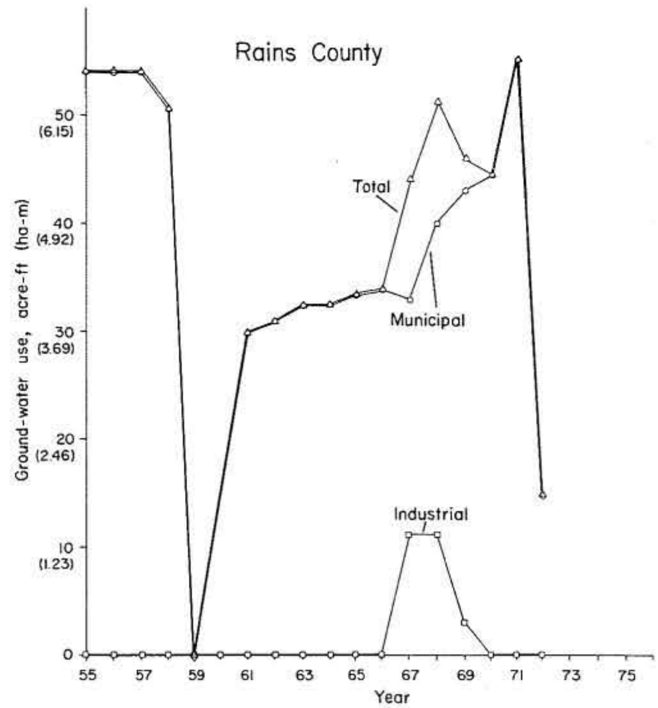
Rains County
Ground-water use, acre-ft (ha-m)
50 (6.15)
40 (4.92)
30 (3.69)
20 (2.46)
10 (1.23)
0
Total
Municipal
Industrial
55 57 59 61 63 65 67 69 71 73 75
Year

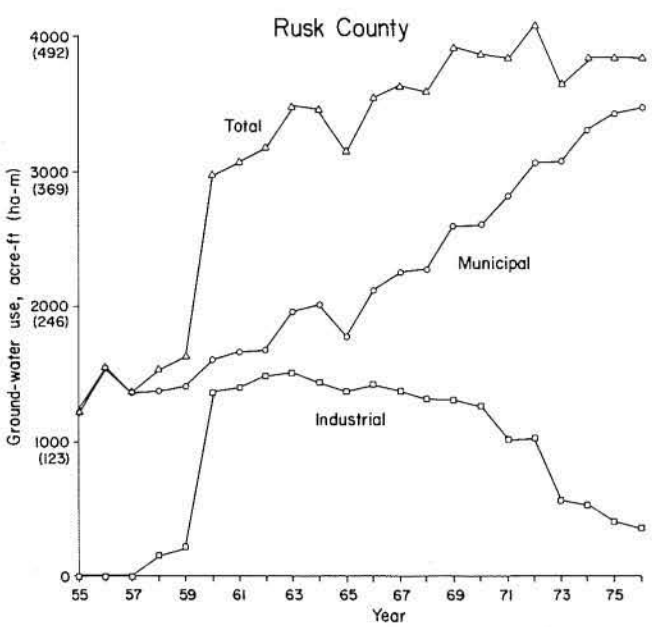
Rusk County
Ground-water use, acre-ft (ha-m)
4000 (492)
3000 (369)
2000 (246)
1000 (123)
0
Total
Municipal
Industrial
55 57 59 61 63 65 67 69 71 73 75
Year

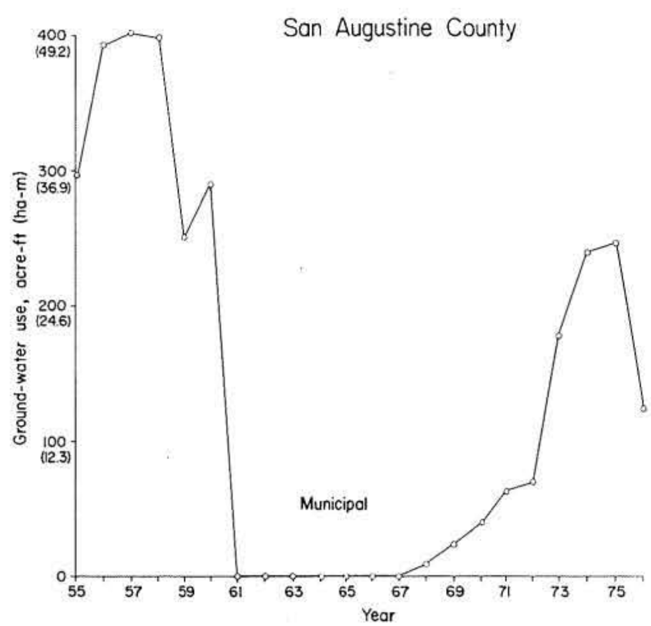
San Augustine County
Ground-water use, acre-ft (ha-m)
400 (49.2)
300 (36.9)
200 (24.6)
100 (12.3)
0
Municipal
55 57 59 61 63 65 67 69 71 73 75
Year

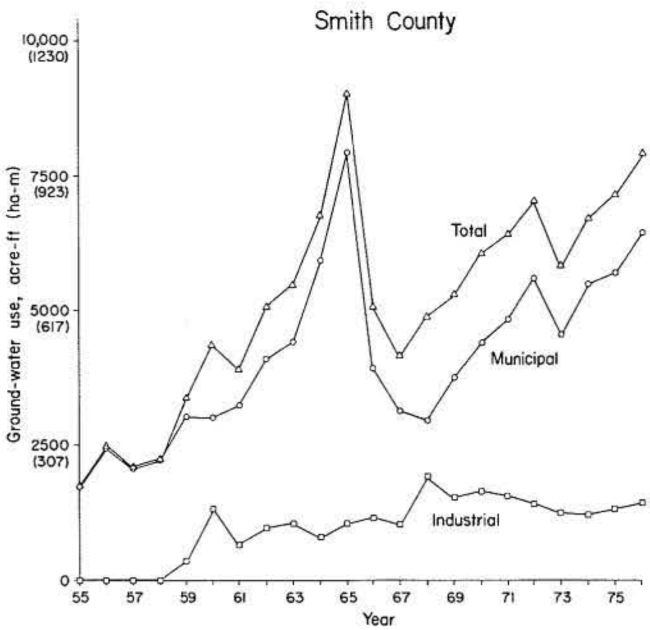

Smith County
10,000
(1230)
7500
(923)
5000
(617)
2500
(307)
0
Ground-water use, acre-ft (ha-m)
Total
Municipal
Industrial
55
57
59
61
63
65
67
69
71
73
75
Year

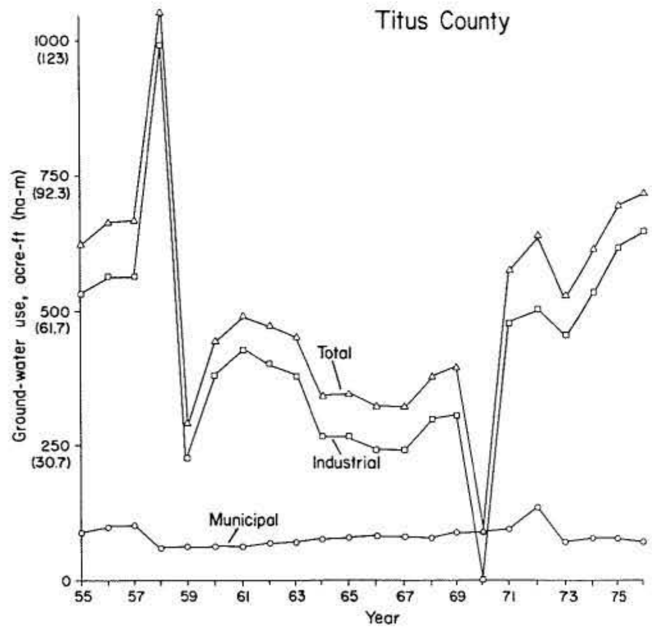

Titus County
1000
(123)
750
(92.3)
500
(61.7)
250
(30.7)
0
Ground-water use, acre-ft (ha-m)
Total
Industrial
Municipal
55
57
59
61
63
65
67
69
71
73
75
Year

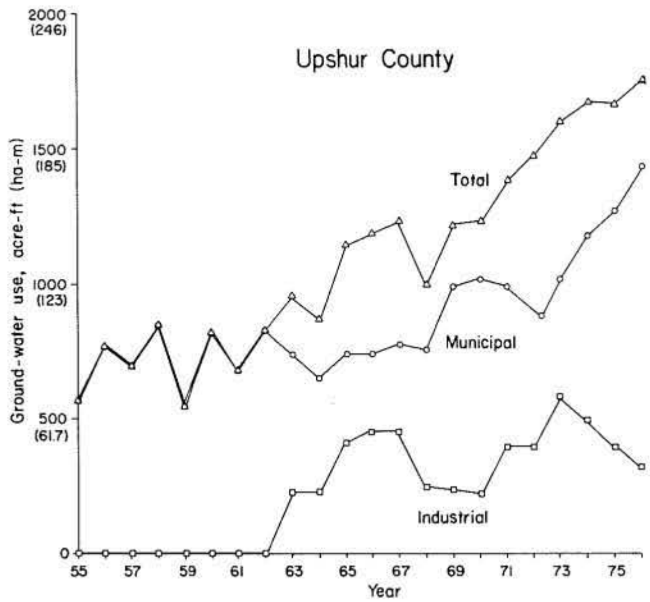

Upshur County
2000
(246)
1500
(185)
1000
(123)
500
(61.7)
0
Ground-water use, acre-ft (ha-m)
Total
Municipal
Industrial
55
57
59
61
63
65
67
69
71
73
75
Year

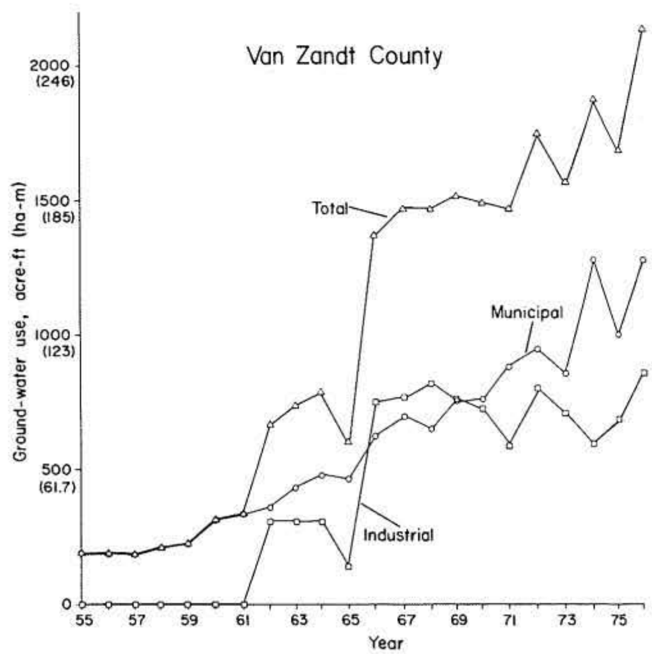

Van Zandt County
2000
(246)
1500
(185)
1000
(123)
500
(61.7)
0
Ground-water use, acre-ft (ha-m)
Total
Municipal
Industrial
55
57
59
61
63
65
67
69
71
73
75
Year

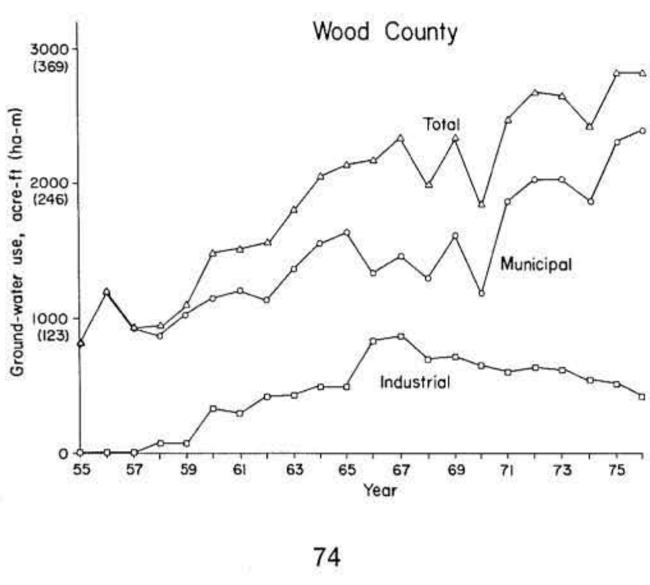

Wood County
3000
(369)
2000
(246)
1000
(123)
0
Ground-water use, acre-ft (ha-m)
Total
Municipal
Industrial
55
57
59
61
63
65
67
69
71
73
75
Year

APPENDIX B

BASIC AXIOMS OF PRESSURE-VERSUS-DEPTH INTERPRETATION

The pressure-versus-depth (P-D) relationship can be used to determine whether fluid movement is directed upward, downward, or horizontally. For example, consider the hypothetical soil-column experiments in figures B-1a, b, and c in which fresh water flows downward, upward, and horizontally through the sand-packed column, in each case under an imposed hydraulic gradient of 2 units. Pressures at any point in the column can be calculated in terms of fresh water from the values of head (h) and elevation (e) at that point. From these pressures, the P-D plot shown in figure B-1d can be constructed. Each experiment yields a different slope (m) for the P-D lines: When flow is downward (fig. B-1a), $m < 1$ (and > 0); when flow is upward (fig. B-1b), $m > 1$; and when flow is perfectly horizontal (fig. B-1c), $m = 1$. The same would be true for any other magnitude of head drop imposed on the column. Furthermore, additional experiments in which the column is tipped at various angles from vertical would always conclude that $m < 1$ when flow has a downward component and $m > 1$ when flow has an upward component. As direction of flow moves closer to horizontal, the value of m moves closer to 1.

The term "hydrostatic" is often used to describe systems in which $m = 1$. Hydrostatic conditions can occur either when flow is horizontal, as in figure B-1d, or when no flow is occurring. In most ground-water systems, the latter case is extremely rare and can usually be ruled out altogether. Significant vertical flow may in some cases occur at very small vertical hydraulic gradients ($m \approx 1$) owing to high vertical hydraulic conductivity. For a more detailed discussion of interpretation of P-D relationships, consult Tóth (1978).